NASA TN D-941

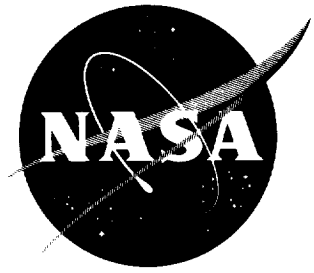

TECHNICAL NOTE

D-941

A TRANSONIC INVESTIGATION OF CHANGING INDENTATION DESIGN MACH NUMBER ON THE AERODYNAMIC CHARACTERISTICS OF A 45° SWEPTBACK-WING–BODY COMBINATION DESIGNED FOR HIGH PERFORMANCE

By Donald L. Loving

Langley Research Center
Langley Air Force Base, Va.

NATIONAL AERONAUTICS AND SPACE ADMINISTRATION
WASHINGTON October 1961

NATIONAL AERONAUTICS AND SPACE ADMINISTRATION

TECHNICAL NOTE D-941

A TRANSONIC INVESTIGATION OF CHANGING INDENTATION DESIGN MACH NUMBER ON THE AERODYNAMIC CHARACTERISTICS OF A 45° SWEPTBACK-WING—BODY COMBINATION DESIGNED FOR HIGH PERFORMANCE*

By Donald L. Loving

SUMMARY

The effects of changing indentation design Mach number on the aerodynamic characteristics of a 45° sweptback-wing—body combination designed for high performance have been investigated at Mach numbers from 0.80 to 1.13 in the Langley 8-foot transonic tunnel and at a Mach number of 1.43 in the Langley 8-foot transonic pressure tunnel. The Reynolds number of the investigation covered the range from approximately 2.5×10^6 to approximately 3.0×10^6 based on the mean aerodynamic chord of the wing. The 45° sweptback wing with camber and a thickened root was tested at 0° angle of incidence on an unindented body and on bodies indented for Mach numbers M of 1.0, 1.2, and 1.4. Transonic and supersonic area rules were used in the design of the indented bodies. Theoretical zero-lift wave drag was calculated for these wing-body combinations. A -2° angle of incidence of the wing, and M = 1.4 revised body indentation, and fixed transition also were investigated.

Experimental values of zero-lift wave drag for the indented-body combinations followed closely the area-rule concept in that the lowest zero-lift wave-drag coefficient was obtained at or near the Mach number for which the body of the combination was designed. Theoretical values of zero-lift wave drag were considered to be in good agreement with the experimental results. At a given supersonic Mach number the highest values of maximum lift-drag ratio for the various combinations also were obtained at or near the Mach number for which the body of the combination was designed. At Mach numbers of 1.0, 1.2, and 1.43, the maximum lift-drag ratios were 15.3, 13.0, and 9.2, respectively. The use of an angle of incidence of -2° for the wing in combination with the M = 1.2 body increased the zero-lift wave drag and decreased the maximum lift-drag ratio. All configurations maintained stable characteristics up to the highest lift coefficient of the investigation ($C_L \approx 0.5$).

*Supersedes recently declassified NACA RM L55J07, 1956.

INTRODUCTION

A suitable wing-body combination which will exhibit high values of maximum lift-drag ratio at high subsonic speeds and lowest possible drag at supersonic speeds at moderate lift conditions is of prime importance in the design of airplanes capable of high subsonic cruise and supersonic bursts. Many detailed studies have been undertaken with the purpose of providing basic information for the design of such a high-performance wing-body combination. The use of body indentation according to the transonic area rule of reference 1 has resulted in large reductions in wave drag especially at a Mach number of 1.0. A concept was developed in reference 2 which also qualitatively interrelated the zero-lift wave drag of wing-body combinations at moderate supersonic speeds with axial distributions of cross-sectional areas. Theoretical and experimental studies of the application of the supersonic area rule to the reduction of drag of unswept wings have been presented in such references as 3, 4, and 5.

The object of the present investigation was to determine the effect of changing the indentation design Mach number (that is, shaping the bodies for several different Mach numbers) on the aerodynamic characteristics of a sweptback-wing—body combination designed to exhibit the type of high performance desired for high subsonic cruise and supersonic bursts. An unindented body and a series of indented bodies designed for Mach numbers of 1.0, 1.2, and 1.4 were used. A 45° sweptback wing was especially designed for this investigation to have high-performance characteristics when used in combination with the various bodies and also to have good pitching-moment and structural characteristics. This wing was tested primarily at an angle of incidence of 0°.

Other parts of the test program included the use of the wing at an angle of incidence of -2° in combination with the body indented for a Mach number of 1.2, a Mach number 1.4 revised body indentation, and fixed transition on all configurations.

SYMBOLS

a	mean-line designation, fraction of chord from leading edge over which design load is uniform
b	wing span
c	wing chord measured parallel to plane of symmetry
$\bar{c}$	mean aerodynamic chord measured parallel to plane of symmetry, $\frac{2}{S}\int_0^{b/2} c^2 dy$

M	Mach number
q	free-stream dynamic pressure, $\frac{1}{2}\rho V^2$
S	total wing area
V	velocity in undisturbed stream
x	body station, distance from nose of body
α	angle of attack of body center line
i_W	angle of incidence of wing relative to body center line
ρ	mass density in undisturbed stream
C_L	lift coefficient, Lift/qS
C_{L_α}	lift-curve slope, averaged over a lift-coefficient range from -0.05 to 0.3
C_D	drag coefficient, Drag/qS
$C_{D_{\alpha=0}}$	drag coefficient at $\alpha = 0^o$
C_{D_o}	zero-lift drag coefficient, Zero-lift drag/qS
$C_{D_{o_M}}$	zero-lift drag coefficient at a given Mach number
ΔC_{D_o}	zero-lift wave-drag coefficient, $C_{D_{o_M}} - C_{D_{o_{M=0.8}}}$
$\delta\Delta C_{D_o}$	incremental zero-lift wave-drag coefficient, $\left(\Delta C_{D_{o_{\text{fixed transition}}}} - \Delta C_{D_{o_{\text{natural transition}}}}\right)$
$C_{D_{min}}$	minimum drag coefficient, Minimum drag/qS
$(L/D)_{max}$	maximum lift-drag ratio
C_m	pitching-moment coefficient about 25 percent chord of mean aerodynamic chord, Pitching moment/qS$\bar{c}$

$\partial C_m/\partial C_L$ pitching-moment-curve slope, averaged over a lift-coefficient range from -0.05 to 0.3

θ roll angle of axis of tilt of Mach planes around the center line of the various configurations, zero when Mach planes cut in vertical direction

DESIGN OF WING-BODY COMBINATIONS

Details of the wing-body combinations investigated are shown in figure 1. The wing has 45° sweepback of the 0.25-chord line, an aspect ratio of 4, and a taper ratio of 0.15, and is cambered for a design lift coefficient of 0.2. At the root a streamwise NACA 64A206, a = 0 airfoil section was used. Streamwise NACA 64A203, a = 0.8 (modified) airfoil sections were used from 50-percent semispan to the tip as shown in figure 1. Straight-line elements were used in fairing the wing sections from the root to 50-percent semispan. The ordinates of the wing sections are listed in table I. The wing, constructed of steel, was mounted in a midwing position on a sting-supported body for all test configurations.

L 1 6 9 8

Wing

The wing of the combinations has been designed to have low drag associated with lift at subsonic and moderate supersonic speeds, low wave drag when used with an indented body for a range of transonic and moderate supersonic speeds, relatively good pitching-moment characteristics, and good structural characteristics.

The quarter-chord line was swept back in order to have low drag associated with lift and also to have high effectiveness of indentation by insuring that the leading edge would be swept behind Mach lines at moderate supersonic speeds. In a previous investigation (ref. 2), a 60° sweptback wing was designed on the same basic assumptions. This 60° sweptback wing, however, exhibited extremely unfavorable pitching-moment characteristics which, to date, have not been alleviated sufficiently to make it a practical airplane component. The sweepback of the present wing, therefore, was limited to 45° to assure more favorable pitching-moment characteristics. It has been indicated in reference 2 that, for obtaining smooth area distributions and reductions in wave drag at supersonic speeds, the body for the best wing-body compromise should be indented and the wing thickness ratio should be decreased from the root outboard. Consequently, the thickness ratio of the present wing varies from 6 percent at the root to 3 percent from the midsemispan to

the tip. This taper in thickness also permits better structural design of the wing. Other studies of the effect of thickness ratio have been presented in references 6 and 7. The taper ratio of 0.15 was selected to reduce the severity of pitch-up tendency at lifting conditions (see ref. 8) and also to improve the structural characteristics of the wing. An aspect ratio of 4 was considered a suitable compromise for obtaining high lift-drag ratios and high-performance characteristics at transonic speeds. Generally, camber has been shown to improve subsonic and supersonic performance. (See refs. 9, 10, and 11.) The entire chords in the present wing were cambered since it has been found that this method is highly effective in improving the lift-drag ratio. A mean line of $a = 0$ was used at the root so that the camber near the leading edge when used in combination with an indented body could take better advantage of the upflow around the body. It was believed that the leading edge of the wing could be lined up better with the streamlines in the upflow than for a symmetrical airfoil section. In this manner, the strength of the compression shock on the lower surface at the leading edge of the wing would be weaker, a peak pressure on the upper surface at the leading edge with its accompanying adverse pressure gradient would be less evident, and laminar flow in the boundary layer on the upper surface would be extended in a chordwise direction - all tending to produce a lower drag at moderate lifting conditions. A mean line of $a = 0.8$ (modified) was used for the outboard sections in order to maintain a more uniform distribution of load both spanwise and chordwise.

As has been stated previously, the wing was tested primarily at an angle of incidence of 0°. In one instance, however, the wing was tested at an angle of incidence of -2° in combination with an indented body. An improvement in the drag characteristics of a similar wing-body configuration has been reported in reference 11. For these configurations, when the wing was at an angle of attack of 0°, the body was inclined at an angle of attack of 2°. In the present investigation it was assumed that the inboard stations of the cambered wing would operate in an increased upflow around the body compared with the configurations with an angle of incidence of 0°, and it was believed that these inboard sections would develop an additional lift without a penalty in drag. It was anticipated, also, that a slight increase in lift would be realized from the body itself. In this manner, higher values of $(L/D)_{max}$ were expected for the configurations with an angle of incidence of -2° than were obtained from the configurations with an angle of incidence of 0°.

Body

The unindented, original-body shape used as a basis of comparison for the indented configurations is the same as the body used in reference 2. This body was obtained by cutting off the rear 21.2 percent of a Sears-Haack body. (See ref. 12.) For the present tests this body

was made 35.3 inches long by extending the tail end of the original body 3.6 inches rearward by using Sears-Haack body ordinates. The ordinates for this 35.3-inch body, referred to as the basic body, and the 31.7-inch original body, are shown in table II. The ratio of basic-body maximum frontal area to total wing planform area was 0.040, which places the model in the category of present-day bombers.

The outer portion of the body was made of detachable, wood impregnated plastic so that any type of body shape in the region of the wing could be investigated. In order to provide sufficient body cross section to allow for 100-percent compensation of the average area of the wing for Mach plane cuts at $M = 1.2$, the maximum diameter of the basic body was increased from 3.212 to 3.296 inches. This unindented, slightly larger diameter body, referred to as the modified body, was indented axially symmetrical to obtain relatively smooth area distributions at Mach numbers of 1.0, 1.2, and 1.4. The contour for the $M = 1.0$ body was 95 percent of the full indentation specified by the transonic area rule. This limitation was imposed by the basic structure of the test model. It is believed that the difference in results for a 95-percent and a 100-percent $M = 1.0$ indentation would be small. This body will be referred to simply as the $M = 1.0$ body. As is stated in reference 13 for radially symmetrical modifications, the area used for the approximate optimum indentation for any particular supersonic Mach number is obtained by averaging the frontal projection of wing areas cut by Mach planes at all angles of roll θ of the Mach planes with respect to the configuration. For symmetrical models, only the average areas between 0° and 90° have to be considered. For the present investigation, areas for 0°, 45°, and 90° were averaged by giving a weight of 1 to the 0° and 90° cuts and a weight of 2 to the 45° cut. Indentations for Mach numbers of 1.2 and 1.4 compensated for the wing areas in full. The resulting area distributions for the respective design Mach numbers were the same as the normal cross-sectional area distribution of the modified body. The indentations used removed about 20 percent of the volume of the basic body shape. Representative axial distributions of cross-sectional area for these configurations are shown in figures 2, 3, 4, and 5 for roll angles θ of 0°, 45°, and 90° at Mach numbers of 1.0, 1.2, and 1.4.

Another $M = 1.4$ indentation was developed which will be referred to as the $M = 1.4$ revised body. This indentation was developed from a body that was shaped slightly different from the modified body, as shown in figure 6, so that the effect of a type of partial $M = 1.4$ indentation in combination with the 45° sweptback wing could be investigated. In particular, it was desired to determine whether the partial indentation would improve the wave drag over a wide speed range, that is, at off-design Mach numbers, and at the same time maintain the improvement in drag obtained by the regular indentation at its design Mach number. The $M = 1.4$ revised indentation was approximately 85 percent as deep as the regular $M = 1.4$ body indentation. Ordinates for all the body

contours are given in table II. Errors between these design ordinates and those obtained from measurements of the completed models were not greater than 1 percent and in most cases were much less.

APPARATUS, MEASUREMENTS, AND ACCURACY

The investigation was conducted in the Langley 8-foot transonic tunnel and the Langley 8-foot transonic pressure tunnel. In the former facility, the slotted-test-section Mach number can be varied continuously from about 0.2 to 1.14. All data presented from this tunnel are essentially free of the effects of wall-reflected disturbances, except where noted for a Mach number of 1.13. In the latter facility, nozzle blocks were placed in the slots of the test section to produce a test section in which the Mach number is 1.43. The design of these nozzle blocks has been described in reference 14. The models mounted on an internal strain-gage balance were sting supported in the usual manner in the tunnels.

Lift, drag, and pitching moment were determined by means of the internal strain-gage balance. The pitching moments were taken about the 0.25 chord of the mean aerodynamic chord. The coefficients of these forces and moments are estimated to be accurate within the following limits: for C_L, ± 0.01; for C_{D_o}, ± 0.0005; and for C_m, ± 0.002. These limits include the effect of possible errors in the measurements of angle of attack. The force and moment results also have been adjusted to the condition of stream static pressure on the base of the body.

Model angle of attack was measured by means of a fixed-pendulum strain-gage unit mounted in the nose of the body. Angles of attack are estimated to be accurate within $\pm 0.10^\circ$. An attempt was made to maintain the models aerodynamically smooth throughout the investigation. Photographs of the wing mounted on the basic body are presented as figure 7.

Transition was fixed across the span of the wing at 10 percent of the chord. It consisted of a roughness strip approximately 0.10 inch wide which was made by sprinkling carborundum grains on an adhesive agent sprayed on the wing. The grain size, density, and application of the strip were carefully controlled. Transition was fixed around the body at 10 percent of the body length in the same manner used for the wing. For all the wing-body combinations tested at Mach numbers from 0.80 to 1.43, a medium density (30 grains per inch) of No. 120 carborundum grain was used in the transition strip. Photographs of the wing mounted on an indented body with transition fixed on both wing and body are presented as figure 8.

TESTS

The following tests were made for a Mach number range from 0.80 to 1.13 in the Langley 8-foot transonic tunnel, and the average Reynolds number varied from 2.56×10^6 to 2.90×10^6 based on a mean-aerodynamic-chord length of 8.42 inches:

Configuration	Wing angle of incidence, i_W, deg	Angle of attack, α, deg	Transition
Original body		0	Natural
Basic body		0 to 12	Natural
Modified body		0	Natural
Wing with basic body . . .	0	-2 to approx. 6	Natural
Wing with modified body . .	0	0	Natural
Wing with M = 1.0 body . .	0	-2 to approx. 6	Natural
Wing with M = 1.2 body . .	0	-2 to approx. 6	Natural
Wing with M = 1.4 body . .	0	-2 to approx. 6	Natural
Wing with M = 1.4 revised body	0	-2 to approx. 6	Natural
Wing with M = 1.2 body . .	-2	0 to approx. 8	Natural
Wing with basic body . . .	0	-2 to approx. 6	Fixed
Wing with M = 1.0 body . .	0	-2 to approx. 6	Fixed
Wing with M = 1.2 body . .	0	-2 to approx. 6	Fixed
Wing with M = 1.4 body . .	0	-2 to approx. 6	Fixed

The following tests were made at a Mach number of 1.43 in the Langley 8-foot transonic pressure tunnel, and the average Reynolds number was 2.83×10^6 based on a mean-aerodynamic-chord length of 8.42 inches:

Configuration	Wing angle of incidence, i_W, deg	Angle of attack, α, deg	Transition
Basic body		0 to 12	Natural
Wing with basic body . . .	0	-2 to 10	Natural
Wing with M = 1.0 body . .	0	-2 to approx. 11	Natural
Wing with M = 1.2 body . .	0	-2 to approx. 11	Natural
Wing with M = 1.4 body . .	0	-2 to approx. 10	Natural
Wing with basic body . . .	0	-2 to approx. 11	Fixed
Wing with M = 1.0 body . .	0	-2 to approx. 11	Fixed
Wing with M = 1.2 body . .	0	-2 to approx. 11	Fixed
Wing with M = 1.4 body . .	0	-2 to approx. 10	Fixed
Wing with M = 1.4 revised body	0	-2 to approx. 11	Fixed

RESULTS AND DISCUSSION

Bodies

Basic aerodynamic data.- The variations of lift, drag, and pitching-moment coefficients with angle of attack for the basic body for the various test Mach numbers are presented in figure 9. The coefficients are based on a wing area of 1.408 square feet.

Drag characteristics.- The variation with Mach number of the drag coefficient based on wing area at zero angle of attack for the three bodies tested (original, basic, and modified) is presented in figure 10. Between Mach numbers of 1.13 and 1.43, the curves are interpolated, since test data were not obtained in this range. These data indicate that the lowest level of drag coefficient at all Mach numbers was obtained for the basic body. This was expected since this body had the highest fineness ratio (11.0) of those tested. Very little difference between the drag coefficients for all the bodies was observed up to a Mach number of 1.03. This difference was of the order of a drag coefficient of 0.0002 which is within the accuracy of test measurements.

Of interest at $M = 1.13$ is the difference in drag coefficient between the original and basic bodies. This difference (approximately 0.0006) indicates that the drag coefficient for the basic and modified bodies is lower than should be expected on the basis of the drag coefficients at $M = 1.0$ and 1.03. A study of the tunnel-boundary-reflection interference for these two bodies indicated that wave reflections were impinging on the afterbody of the basic and modified bodies at a Mach number of 1.13. This was a direct result of increasing the length of the bodies from the original body length of 31.70 inches to the basic and modified body length of 35.30 inches.

Systematic Series of Wing-Body Combinations

Basic aerodynamic data.- The variations with lift coefficient of angle of attack, drag coefficient, and pitching-moment coefficient for the wing-body configurations investigated at Mach numbers from 0.80 to 1.43 are presented in figures 11 and 12. The coefficients are based on a wing area of 1.408 square feet. The symbol at the intersection of the zero lines on these figures is for the purpose of Mach number identification.

Drag characteristics.- The wing was investigated in combination with the basic and modified bodies at an angle of attack of 0°. In figure 13, it is shown that the modified body combination has a slightly higher drag coefficient level (approximately 0.0003) as a result of its slightly lower

fineness ratio. The drag coefficients at $M = 1.13$ have been adjusted upward by 0.0006 to allow for the tunnel-boundary-reflection interference discussed previously. The zero-lift wave drag of the two combinations is essentially the same over the Mach number range for which data are available. Curves between Mach numbers of 1.13 and 1.43 are interpolated since test points were not taken in this range.

The variation with Mach number of drag coefficient at lift coefficients of 0, 0.2, and 0.4 for the combinations of the wing with the basic body and bodies indented for Mach numbers of 1.0, 1.2, and 1.4 is presented in figure 14. The data have not been adjusted for tunnel-boundary-reflection interference. These drag coefficient results indicate that the subsonic level of zero-lift drag coefficient for the basic body combination was 0.009; body indentation was effective in reducing the zero-lift drag coefficients at Mach numbers above 0.95; and these reductions in zero-lift drag, obtained by indenting the body for the various design Mach numbers, were maintained at lift coefficients at least up to 0.4 throughout the test Mach number range.

L
1
6
9
8

In figure 15, all the zero-lift drag coefficient data for the wing-body combinations tested have been adjusted upward by an increment in zero-lift drag coefficient of 0.0006 for tunnel boundary interference at $M = 1.13$. Also included in figure 15 are the zero-lift drag coefficients which would have been obtained for the basic body combination if the size of the basic body had been decreased by a first-approximation method to have the same volume as that of the indented bodies. In this method the skin friction of the body was reduced in proportion to the square root of the volume ratio. The wave drag of the body was reduced in proportion to the square of the volume ratio. The increment in drag between the adjusted and unadjusted drag of the body was subtracted from the drag of the wing-body combination to obtain the drag coefficient which probably would have occurred if the basic body of the combination had the same volume as the indented bodies. These data will be used as the basis for the analysis of the zero-lift drag and wave-drag characteristics in the remainder of this report. The variation with Mach number of the minimum drag coefficient for the various combinations, as shown in figure 16, is very similar to the zero-lift drag coefficient variation. A value of 0.008 for the subsonic minimum drag coefficient was obtained for the basic wing-body combination at a lift coefficient of 0.075 compared with a value of 0.009 for the zero-lift drag coefficient. When the indentation design Mach number was changed, the subsonic value of $C_{D_{min}}$ increased approximately 0.0008.

The experimental values of zero-lift wave-drag coefficient shown in figure 17 were obtained from the difference between the zero-lift drag at any particular higher Mach number and the zero-lift drag at a Mach number of 0.80 where the drag is due primarily to skin friction. These values follow closely the area-rule concept in that the lowest wave drag

for the various combinations was obtained at or near the particular Mach number for which the body of the combination was designed. The same trend is exhibited by the theoretical values of zero-lift wave-drag coefficient (indicated by the symbols) calculated for the various combinations by the method of reference 3. These theoretical wave-drag computations did not evaluate the effect of camber of the test wing. The theoretical values, however, are considered to be in good agreement with the experimental results. The use of indentation in combination with the wing accounted for reductions in zero-lift wave drag ranging from 0.0058 at a Mach number of 1.0 to 0.0028 at a Mach number of 1.43 when compared with the basic body combination with the body volume adjusted to have the same volume as the indented bodies. The percentage wave-drag reductions of the difference in zero-lift wave drag between the basic combination adjusted for volume and the basic body alone are in the range from 75 percent at $M = 1.0$ to 43 percent at $M = 1.43$.

The maximum lift-drag ratio values shown in figure 18 for the basic body combination compare favorably with those reported for a 60° sweptback wing-body combination (ref. 2) also designed for obtaining high values of $(L/D)_{max}$ and low wave-drag characteristics at transonic and supersonic speeds.

At a given supersonic speed the highest values of maximum lift-drag ratio occurred at the Mach number for which the body indentations were designed. These values of $(L/D)_{max}$ ranged from 15.3 at $M = 1.0$ to 9.2 at $M = 1.43$. The percentage increase in $(L/D)_{max}$ for the different indentations was in the range from 35 percent at $M = 1.0$ to 8.2 percent at $M = 1.43$. Even though data points were not taken between 1.13 and 1.43, it is believed that the interpolation of the curve between these two points would not be a straight line but would be similar to that shown in figure 18. It is reasonable, therefore, to expect that $(L/D)_{max}$ would have a value of approximately 13 at $M = 1.2$ which amounts to a 20-percent increase over the value for the basic body combination. These improvements in $(L/D)_{max}$ were due primarily to decreases in wave drag. The relative increase would have been slightly less if the size of the basic body had been decreased to have the same volume as that of the indented bodies. A complete airplane with empennage, external stores, and protuberances will have maximum values of lift-drag ratio somewhat below those measured for the wing-body combination.

The lift coefficients at which $(L/D)_{max}$ occurred for the various combinations varied from approximately 0.23 at $M = 0.80$ to about 0.3 at $M = 1.03$ and then to a value of the order of 0.23 at $M = 1.43$. This variation indicates that $(L/D)_{max}$ was obtained at very nearly the wing design lift coefficient.

A calculation of the skin-friction-drag coefficient by the method of Van Driest (ref. 15) gives a value of 0.0096 for completely turbulent flow at $M = 0.8$ for the basic body combination. When this value is compared with the experimentally obtained $C_{D_{min}}$ value of 0.008 for the same basic body combinations at $M = 0.8$ with natural transition, it appears that at least partial laminar flow existed in the low lift range for this configuration. The fact that the values of $(L/D)_{max}$ are of the order of 20 at subsonic speeds also suggests the possibility of the existence of some laminar flow over the wing and body.

These considerations of the possible existence of laminar flow on the configurations investigated with natural transition may lead to the conclusion that the drag values for natural transition herein may not be directly applicable to actual airplane configurations similar to those tested. Less extensive laminar boundary and in most cases fully turbulent flow exists on actual airplanes. In this connection, however, it should be remembered that at the higher Reynolds numbers encountered in flight the skin-friction-drag coefficient for the actual airplane may approach the values for natural transition obtained during the model tests in the wind tunnel. The reduction in skin-friction drag associated with the increase in Reynolds number that occurs in going from wind-tunnel test to flight is in the right direction to make the drag results of the present report approximately what would be expected at flight conditions.

Lift characteristics.- The lift-curve slope as shown in figure 19 for the basic, $M = 1.0$, $M = 1.2$, and $M = 1.4$ body combinations was averaged for a lift-coefficient range of approximately -0.05 to 0.3. At Mach numbers from 0.90 to 0.96 use of the various indentations reduced the average lift-curve slope of the basic body by about 10 percent. At supersonic speeds the slope was increased approximately 8 percent by the indentations. In general, the most significant effect of changing indentation design Mach number on the average lift-curve slopes was a decrease in the slopes of the indented combinations at $M = 1.0$ as the design Mach number was increased.

Pitching-moment characteristics.- An examination of the variation with lift coefficient of the pitching-moment coefficients for all configurations tested at all Mach numbers from 0.80 to 1.43, in figures 11(m) to 11(p), indicates that the combinations were stable up to the highest lift coefficients of the investigation (of the order of 0.5). On the basis of past experience with sweptback wings, it may be expected for the wing of the present test that a region of reduced stability will be encountered at higher lift coefficients up to high subsonic speeds. It is believed, however, that design features of the present wing reduce the probability of severe pitch-up. For the basic-body combination, the aerodynamic center, as may be computed from figure 20, moved rapidly rearward from 40 percent of the mean aerodynamic chord at $M = 0.90$

to 51 percent of the mean aerodynamic chord at $M = 0.96$. At Mach numbers from 0.80 to 1.08, the aerodynamic centers for the indented combinations were farther forward than those for the basic wing-body combination as shown by the variation of $\partial C_m/\partial C_L$ with Mach number in figure 20. Between Mach numbers of 0.80 and 0.98, the aerodynamic centers moved rearward with increase in indentation design Mach number but did not equal or exceed the rearward travel for the basic wing-body combination. At supersonic speeds the aerodynamic centers, in general, approached the same locations as for the basic wing-body combination.

Angle of Incidence of -2°

Drag characteristics.- The variation of drag characteristics with Mach number for lift coefficients of 0, 0.2, and 0.4, as affected by a change in wing angle of incidence from 0° to -2° in combination with the body indented for a Mach number of 1.2, is shown in figure 21. These data indicate that the anticipated improvements in performance were not obtained. The change in angle of incidence had an adverse effect on the performance characteristics of the combination throughout the transonic Mach number range. This adverse effect produced an increase in minimum-drag coefficient (fig. 22) and zero-lift wave-drag coefficient (fig. 23) and a decrease in the values of maximum lift-drag ratio (fig. 24).

Lift characteristics.- Changing the angle of incidence from 0° to -2° for the wing on the body indented for a Mach number of 1.2 resulted in a decrease in average lift-curve slope of about 4 percent (as shown in fig. 25) throughout the Mach number range for which data were available.

Pitching-moment characteristics.- As indicated in figure 26, neither the stability characteristics nor the aerodynamic centers of the wing-body combinations were seriously affected by changing wing incidence angle from 0° to -2°.

M = 1.4 Revised Body

The drag-coefficient results for the wing in combination with the $M = 1.4$ and $M = 1.4$ revised bodies for lift coefficients of 0, 0.2, and 0.4 are shown in figure 27. The effect of the revision to the $M = 1.4$ body on the minimum drag coefficient, as shown in figure 28, was small. The wave drag at off-design Mach numbers was not noticeably improved. In the Mach number range ($M = 0.80$ to 1.13) for which comparable data are available, it is indicated in figure 29 that the revision to the $M = 1.4$ indentation resulted in a small increase in wave drag at supersonic speeds comparable to the increase in cross-sectional area between the $M = 1.4$ and $M = 1.4$ revised bodies without adversely affecting the wave drag at or near $M = 1.0$. The maximum cross-sectional

area of the M = 1.4 revised body combination would be 5 percent greater than for the regular M = 1.4 combination. (See fig. 6.) In the absence of comparable data at M = 1.43, transition-fixed data may be used to show that at a Mach number of 1.43 the conclusions would be the same as at a Mach number of 1.13. The effects of the M = 1.4 revised body were small on the maximum lift-drag ratio, the lift-curve slope, and the pitching-moment-curve slope shown in figures 30, 31, and 32, respectively.

Transition

L
1
6
9
8

In the present investigation, it was desired to determine whether turbulence at supersonic speeds, as produced by a fixed transition strip, would change the effect of indentation on the wave-drag characteristics of the sweptback-wing—body combinations tested.

Drag characteristics.- The drag coefficients of the various wing-body combinations tested with and without transition are shown as a function of Mach number in figure 33 for lift coefficients of 0, 0.2, and 0.4. The effect of fixed transition on the zero-lift wave-drag coefficients of the various wing-body combinations is shown in figure 34 for Mach numbers from 0.8 to 1.43. Except for the data at a Mach number of 1.43, the results indicate that the changes due to fixed transition were small and, in general, were of the order of accuracy of the data. At a Mach number of 1.43, however, the transition strip appeared to exert a more or less noticeable influence on the incremental zero-lift wave drag.

As shown in figure 34, adding transition to the basic body combination reduced the incremental zero-lift wave drag about 0.0015, whereas for the M = 1.2 body combination it increased the incremental zero-lift wave drag by about the same amount, 0.0015. The effects for the M = 1.0 and M = 1.4 body combinations were within the accuracy of the data. There is no apparent reason why the effect of transition on the basic body combination was different from that on the M = 1.2 body combination.

In reference 16 it is indicated that unindented models and models indented for a Mach number of 1.41 for an elliptical wing and tested with natural transition did not show the drag reduction predicted by theory. During the same investigation (ref. 16), in order to separate the potential and viscous effects, transition-fixed tests were made. These transition-fixed results showed that the experimental reduction in wave drag brought about by the indentation agreed with that predicted by theory. In the present investigation, there is no consistent improvement in the agreement of experiment with theory between the models tested.

Lift and pitching-moment characteristics.- The effect on the lift-curve slope and pitching-moment-curve slope of fixing transition was small throughout the test Mach number range, as shown in figures 35 and 36.

CONCLUSIONS

The following conclusions have been made as a result of an investigation to determine the effects of changing indentation design Mach number at transonic and moderate supersonic speeds on the aerodynamic characteristics of a wing-body combination designed for high performance:

Systematic Series of Wing-Body Combinations

1. The experimental zero-lift wave-drag coefficient values followed closely the area-rule concept in that the lowest zero-lift wave-drag coefficient was obtained at or near the Mach number for which the body of the combination was designed.

2. Theoretical values of zero-lift wave-drag coefficient for all the wing-body combinations were considered to be in good agreement with the experimental results.

3. At a given supersonic Mach number, the highest values of maximum lift-drag ratio for the various combinations were obtained at or near the specific Mach number for which the body of the combination was tested. This was due primarily to decreases in the wave drag. At Mach numbers of 1.0, 1.2, and 1.4, the maximum lift-drag ratios were 15.3, 13, and 9.2, respectively.

4. In general, the most significant effect of changing indentation design Mach number on the lift-curve slopes occurred at a Mach number of 1.0 where the lift-curve slopes of the indented combinations decreased as the indentation design Mach number increased.

5. All wing-body combinations exhibited linear stability characteristics up to the highest lift coefficient of the investigation ($C_L \approx 0.5$).

-2° Angle of Incidence

1. Changing the wing angle of incidence from 0° to -2° resulted in an adverse effect on the performance characteristics for the wing in combination with the body indented for a Mach number of 1.2 throughout the transonic Mach number range. The effect of the change in wing angle of incidence on the lift and moment characteristics was small; primarily, the lift-curve slope was decreased slightly.

M = 1.4 Revised Body

1. At supersonic speeds, a small increase in zero-lift wave drag comparable to the increase in cross-sectional area between the M = 1.4 and M = 1.4 revised bodies was obtained without an adverse effect on the zero-lift wave drag at a Mach number of 1.0.

Transition

1. Consistent effects of fixing transition on the zero-lift wave-drag characteristics through the Mach number range could not be obtained.

Langley Research Center,
National Aeronautics and Space Administration,
Langley Field, Va., September 28, 1955.

REFERENCES

1. Whitcomb, Richard T.: A Study of the Zero-Lift Drag-Rise Characteristics of Wing-Body Combinations Near the Speed of Sound. NACA Rep. 1273, 1956. (Supersedes NACA RM L52H08.)

2. Whitcomb, Richard T., and Sevier, John R., Jr.: A Supersonic Area Rule and an Application to the Design of a Wing-Body Combination With High Lift-Drag Ratios. NASA TR R-72, 1960. (Supersedes NACA RM L53H31a.)

3. Holdaway, George H.: Comparison of Theoretical and Experimental Zero-Lift Drag-Rise Characteristics of Wing-Body-Tail Combinations Near the Speed of Sound. NACA RM A53H17, 1953.

4. Holdaway, George H.: An Experimental Investigation of Reduction in Transonic Drag Rise at Zero Lift by the Addition of Volume to the Fuselage of a Wing-Body-Tail Configuration and a Comparison With Theory. NACA RM A54F22, 1954.

5. Hoffman, Sherwood, Wolff, Austin L., and Faget, Maxime A.: Flight Investigation of the Supersonic Area Rule for a Straight Wing-Body Configuration at Mach Numbers Between 0.8 and 1.5. NACA RM L55C09, 1955.

6. Bielat, Ralph P., Harrison, Daniel E., and Coppolino, Domenic A.: An Investigation at Transonic Speeds of the Effects of Thickness Ratio and of Thickened Root Sections on the Aerodynamic Characteristics of Wings With 47° Sweepback, Aspect Ratio 3.5, and Taper Ratio 0.2 in the Slotted Test Section of the Langley 8-Foot High-Speed Tunnel. NACA RM L51I04a, 1951.

7. Carmel, Melvin M.: Transonic Wind-Tunnel Investigation of the Effects of Aspect Ratio, Spanwise Variations in Section Thickness Ratio, and a Body Indentation on the Aerodynamic Characteristics of a 45° Sweptback Wing-Body Combination. NACA RM L52L26b, 1953.

8. Morgan, Francis G., Jr., and Carmel, Melvin M.: Transonic Wind-Tunnel Investigation of the Effects of Taper Ratio, Body Indentation, Fixed Transition, and Afterbody Shape on the Aerodynamic Characteristics of a 45° Sweptback Wing-Body Combination. NACA RM L54A15, 1954.

9. Harrison, Daniel E.: A Transonic Wind-Tunnel Investigation of the Characteristics of a Twisted and Cambered 45° Sweptback Wing-Fuselage Configuration. NACA RM L52K18, 1952.

10. Harrison, Daniel E.: The Influence of a Change in Body Shape on the Effects of Twist and Camber As Determined by a Transonic Wind-Tunnel Investigation of a 45° Sweptback Wing-Fuselage Configuration. NACA RM L53B03, 1953.

11. Cooper, J. Lawrence: A Transonic Wind-Tunnel Investigation of the Effects of Twist and Camber With and Without Incidence, Twist, and Body Indentation on the Aerodynamic Characteristics of a 45° Sweptback Wing-Body Configuration. NACA RM L54B15, 1954.

12. Sears, William R.: On Projectiles of Minimum Wave Drag. Quarterly Appl. Math., vol. IV, no. 4, Jan. 1947, pp. 361-366.

13. Jones, Robert T.: Theory of Wing-Body Drag at Supersonic Speeds. NACA Rep. 1284, 1956. (Supersedes NACA RM A53H18a.)

14. Matthews, Clarence W.: An Investigation of the Adaptation of a Transonic Slotted Tunnel to Supersonic Operation by Enclosing the Slots With Fairings. NACA RM L55H15, 1955.

15. Van Driest, E. R.: Turbulent Boundary Layer in Compressible Fluids. Jour. Aero. Sci., vol. 18, no. 3, Mar. 1951, pp. 145-160, 216.

16. Lomax, Harvard, and Heaslet, Max. A.: A Special Method for Finding Body Distortions That Reduce the Wave Drag of Wing and Body Combinations at Supersonic Speeds. NACA Rep. 1282, 1956. (Supersedes NACA RM A55B16.)

TABLE I

AIRFOIL ORDINATES

Chord station, percent chord	Ordinate, percent chord											
	Root-chord station (c = 12.382 in.)		11.86-percent-semispan station (c = 11.134 in.)		23.72-percent-semispan station (c = 9.886 in.)		35.58-percent-semispan station (c = 8.639 in.)		47.44-percent-semispan station (c = 7.391 in.)		50-percent-semispan to tip stations (c = 7.120 in. at midsemispan; c = 1.857 in. at tip)	
	Upper surface	Lower surface	Upper surface	Lower surface	Upper surface	Lower surface	Upper surface	Lower surface	Upper surface	Lower surface	Upper surface	Lower surface
0	0	0	0	0	0	0	0	0	0	0	0	0
.25	.47	-.25	.43	-.23	.38	-.21	.32	-.19	.24	-.15	.21	-.13
.5	.62	-.36	.57	-.33	.52	-.30	.44	-.25	.35	-.21	.31	-.18
.75	.75	-.43	.69	-.40	.62	-.35	.53	-.30	.42	-.24	.38	-.21
1.25	.96	-.53	.89	-.48	.80	-.43	.68	-.36	.56	-.28	.49	-.25
2.5	1.37	-.67	1.28	-.62	1.15	-.55	1.00	-.45	.81	-.34	.72	-.30
5	1.95	-.85	1.82	-.77	1.65	-.68	1.44	-.54	1.18	-.39	1.07	-.34
10	2.76	-1.08	2.58	-.97	2.36	-.84	2.06	-.66	1.73	-.44	1.56	-.36
15	3.31	-1.25	3.11	-1.12	2.84	-.95	2.50	-.73	2.12	-.45	1.92	-.36
20	3.71	-1.41	3.48	-1.25	3.20	-1.04	2.84	-.79	2.43	-.46	2.20	-.35
30	4.15	-1.64	3.92	-1.44	3.62	-1.18	3.24	-.86	2.84	-.44	2.60	-.30
40	4.23	-1.77	4.01	-1.54	3.73	-1.24	3.38	-.87	3.02	-.37	2.78	-.22
50	3.93	-1.72	3.75	-1.47	3.52	-1.16	3.23	-.76	2.95	-.24	2.74	-.08
60	3.36	-1.52	3.23	-1.28	3.07	-.97	2.87	-.58	2.70	-.06	2.52	.08
70	2.60	-1.22	2.53	-1.00	2.44	-.72	2.33	-.37	2.26	.11	2.14	.22
80	1.73	-.84	1.71	-.67	1.68	-.46	1.64	-.17	1.60	.20	1.57	.30
90	.85	-.45	.84	-.35	.84	-.23	.83	-.09	.82	.11	.82	.17
100	.01	-.01	.01	-.01	.01	-.01	.01	-.01	.01	-.01	.01	-.01

TABLE II

BODY ORDINATES

Forebody	
Body station, in.	Radius, in.
0	0
.5	.165
1.0	.282
1.5	.378
2.0	.460
2.5	.540
3.0	.612
3.5	.680
4.0	.743
4.5	.806
5.0	.862
5.5	.917
6.0	.969
6.5	1.015
7.0	1.062
7.5	1.106
8.0	1.150
8.5	1.187
9.0	1.222
9.5	1.257
10.0	1.290
10.5	1.320
11.0	1.350

Afterbody							
Body station, in.	Radius, in., for —						
	Original body	Basic body	Modified body	M = 1.0 body	M = 1.2 body	M = 1.4 body	M = 1.4 revised body
11.5	1.376	1.376	1.376	1.376	1.376	1.376	1.376
12.0	1.404	1.404	1.404	1.404	1.404	1.399	1.403
12.5	1.430	1.430	1.430	1.430	1.427	1.408	1.416
13.0	1.452	1.452	1.454	1.453	1.440	1.403	1.414
13.5	1.476	1.476	1.477	1.471	1.440	1.388	1.399
14.0	1.493	1.493	1.499	1.472	1.433	1.366	1.380
14.5	1.512	1.512	1.520	1.461	1.416	1.340	1.358
15.0	1.526	1.526	1.540	1.441	1.390	1.309	1.333
15.5	1.540	1.540	1.558	1.416	1.359	1.278	1.307
16.0	1.552	1.552	1.575	1.385	1.323	1.253	1.290
16.5	1.565	1.565	1.590	1.353	1.283	1.233	1.276
17.0	1.575	1.575	1.604	1.317	1.242	1.217	1.268
17.5	1.585	1.585	1.615	1.277	1.203	1.203	1.264
18.0	1.590	1.590	1.626	1.242	1.173	1.195	1.262
18.5	1.598	1.598	1.634	1.213	1.149	1.192	1.263
19.0	1.602	1.602	1.642	1.185	1.133	1.198	1.265
19.5	1.606	1.606	1.646	1.163	1.126	1.212	1.272
20.0	1.606	1.606	1.648	1.147	1.133	1.239	1.284
20.5	1.604	1.604	1.647	1.137	1.150	1.270	1.307
21.0	1.602	1.602	1.643	1.135	1.175	1.298	1.327
21.5	1.600	1.600	1.637	1.143	1.202	1.325	1.345
22.0	1.594	1.594	1.629	1.158	1.236	1.343	1.358
22.5	1.587	1.587	1.619	1.177	1.263	1.357	1.365
23.0	1.578	1.578	1.608	1.201	1.306	1.366	1.370
23.5	1.570	1.570	1.596	1.232	1.341	1.372	1.372
24.0	1.560	1.560	1.581	1.269	1.363	1.373	1.373
24.5	1.547	1.547	1.565	1.306	1.375	1.374	1.374
25.0	1.532	1.532	1.547	1.337	1.380	1.373	1.373
25.5	1.517	1.517	1.529	1.361	1.380	1.372	1.372
26.0	1.501	1.501	1.508	1.373	1.376	1.368	1.368
26.5	1.480	1.480	1.486	1.375	1.370	1.362	1.362
27.0	1.460	1.460	1.465	1.374	1.362	1.352	1.352
27.5	1.438	1.438	1.439	1.369	1.349	1.339	1.339
28.0	1.414	1.414	1.414	1.359	1.335	1.325	1.325
28.5	1.387	1.387	1.387	1.346	1.318	1.308	1.308
29.0	1.360	1.360	1.360	1.332	1.300	1.290	1.290
29.5	1.330	1.330	1.330	1.316	1.280	1.269	1.269
30.0	1.300	1.300	1.300	1.296	1.255	1.245	1.245
31.0	1.231	1.231	1.231	1.231	1.201	1.194	1.194
31.7	1.182	1.182	1.182	1.182	1.158	1.153	1.153
32.0		1.158	1.158	1.158	1.138	1.134	1.134
33.0		1.076	1.076	1.076	1.065	1.064	1.064
34.0		.984	.984	.984	.980	.980	.980
35.0		.878	.878	.878	.878	.878	.878
35.3		.844	.844	.844	.844	.844	.844

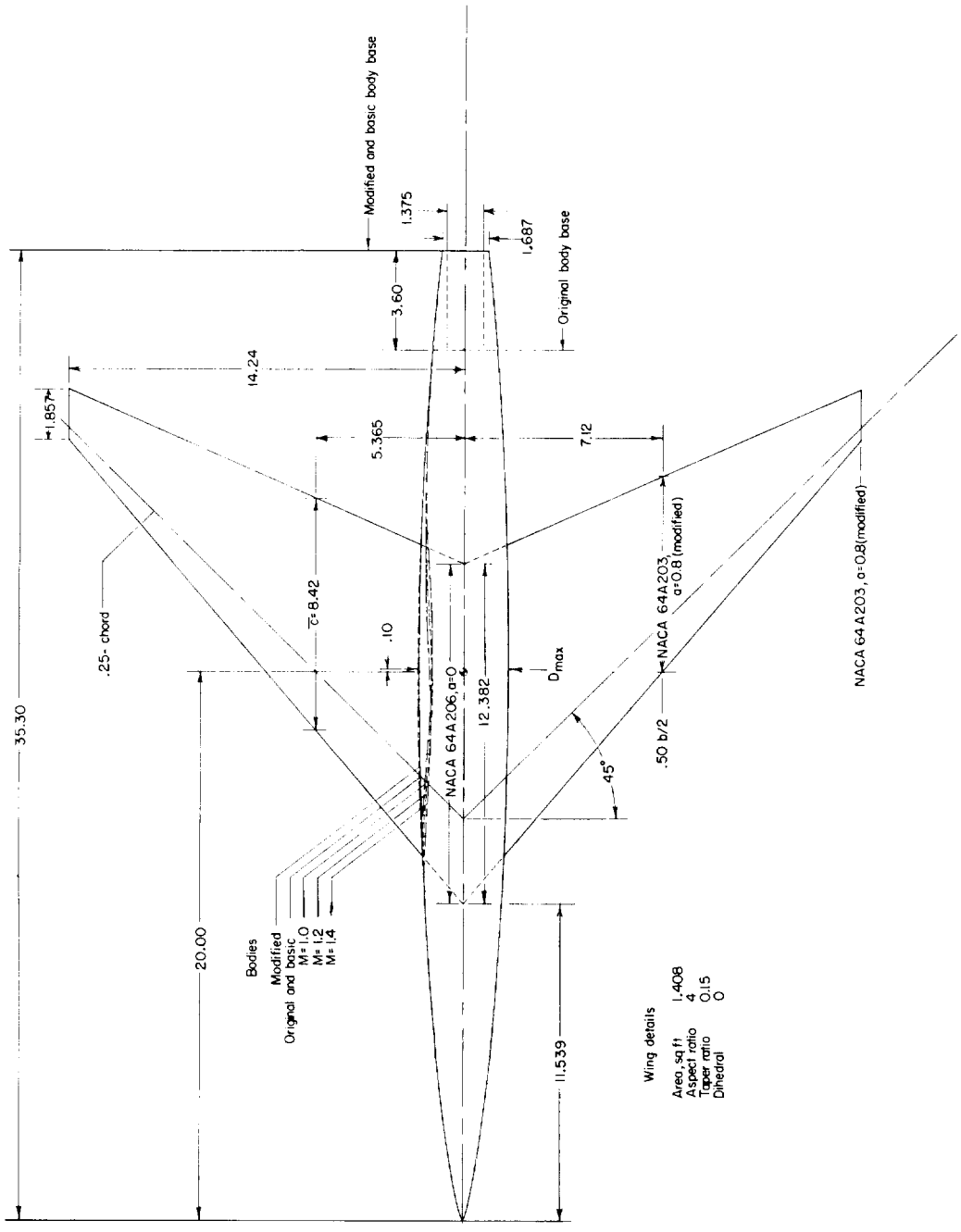

Figure 1.- Details of wing-body combinations investigated. All dimensions are in inches.

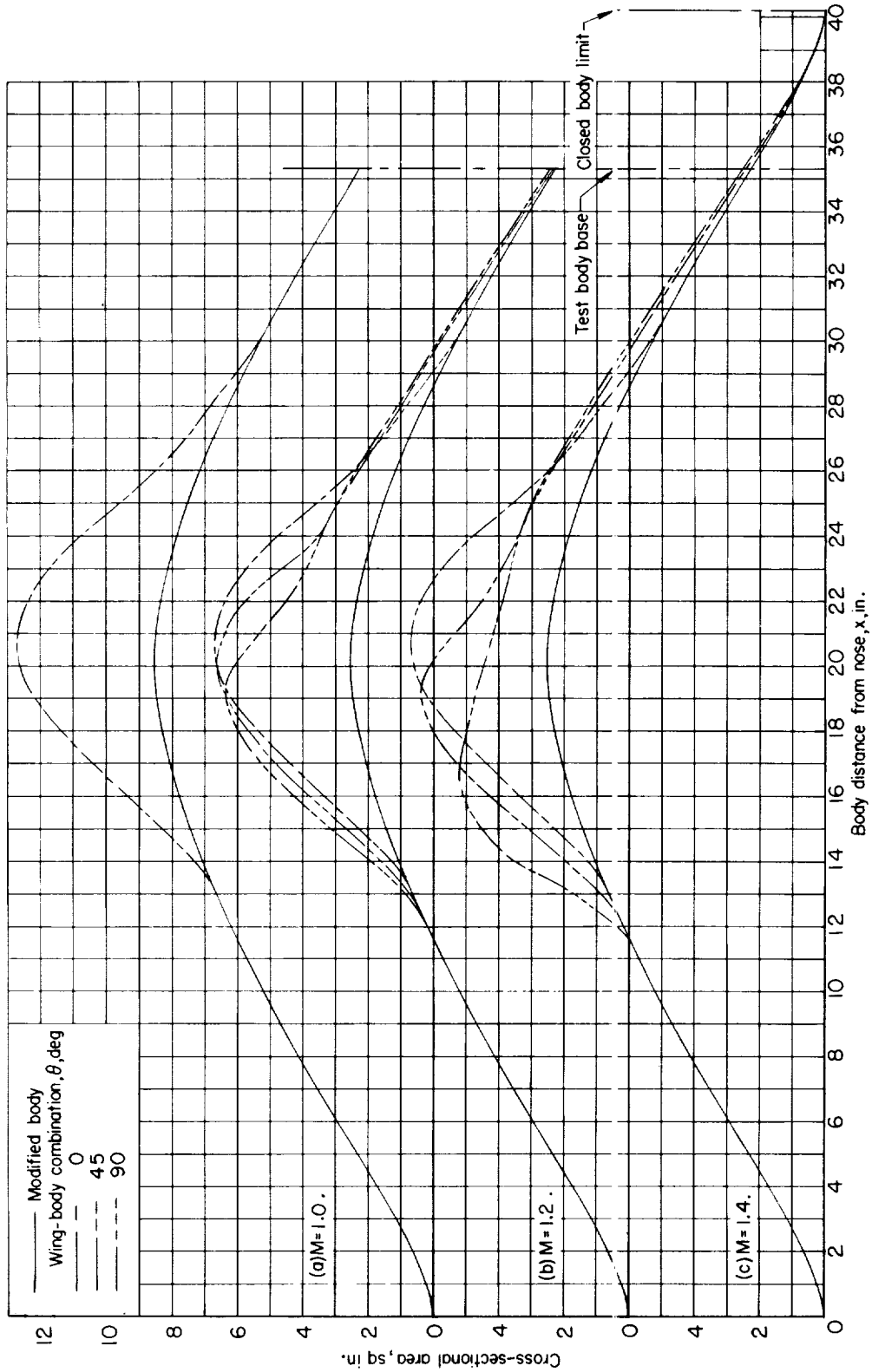

Figure 2.- Representative axial distributions of cross-sectional area for 45° sweptback wing in combination with modified body at M = 1.0, 1.2, and 1.4.

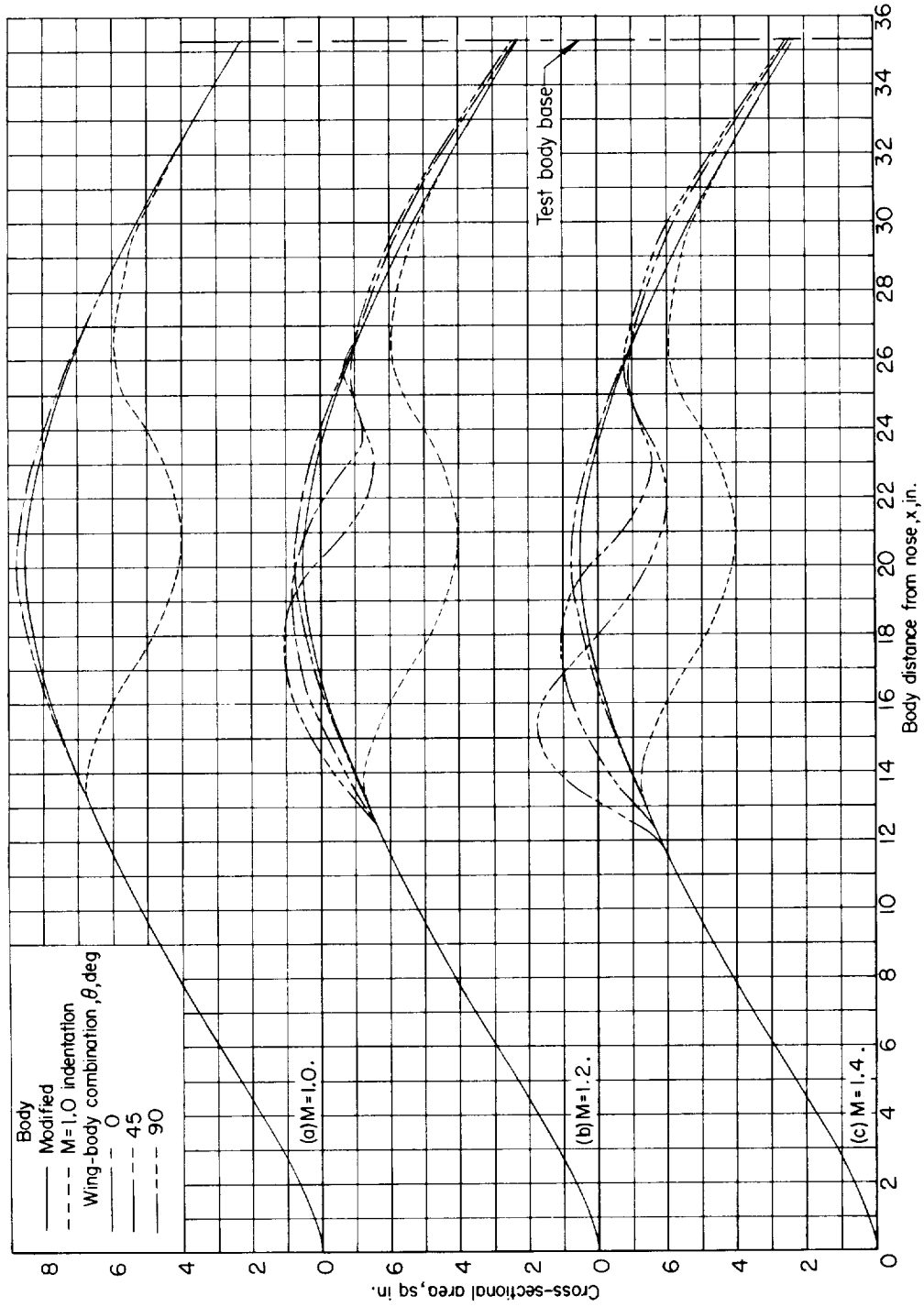

Figure 3.- Representative axial distributions of cross-sectional area for 45° sweptback wing in combination with the body indented for M = 1.0 at M = 1.0, 1.2, and 1.4.

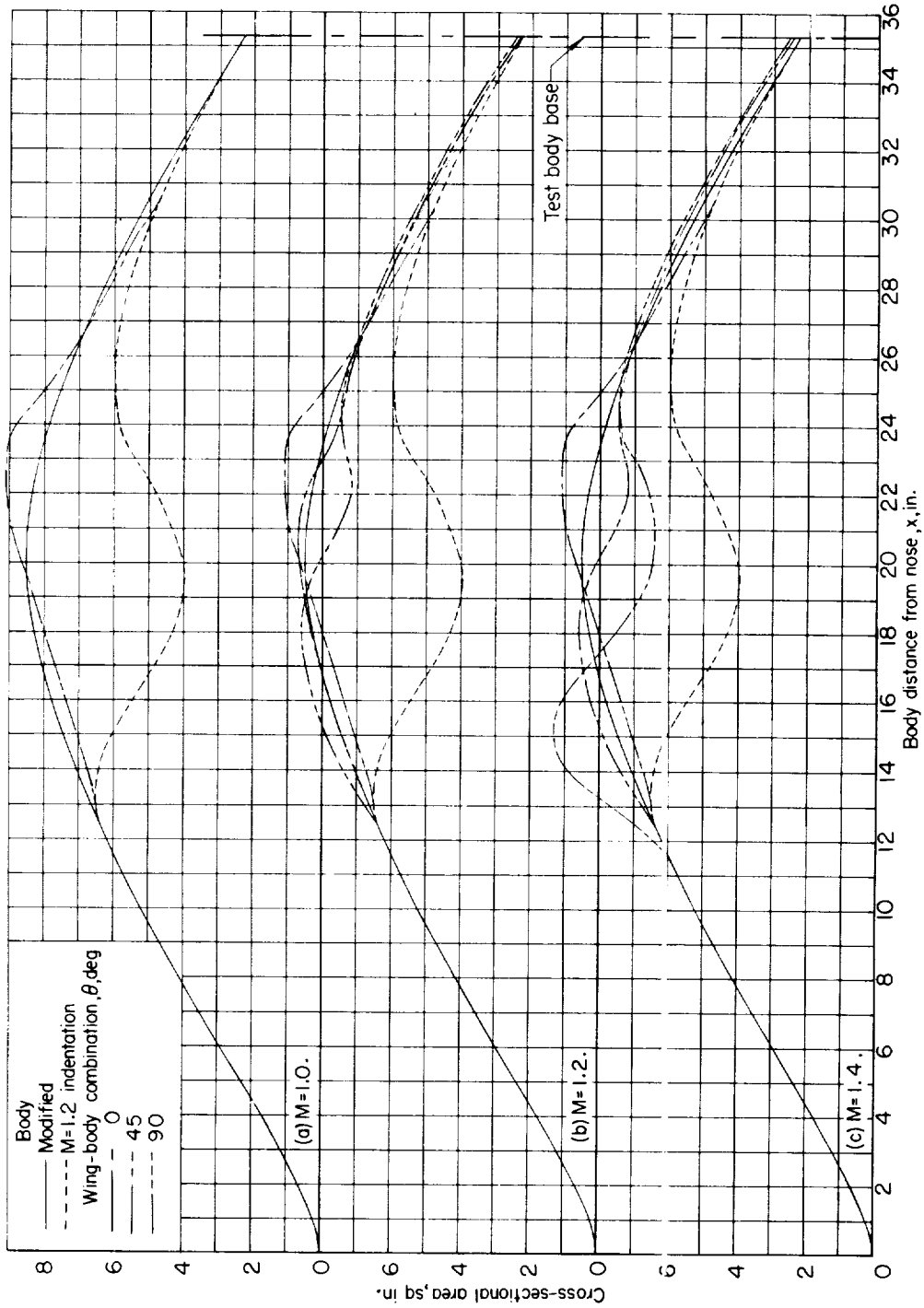

Figure 4.- Representative axial distributions of cross-sectional area for 45° sweptback wing in combination with the body indented for M = 1.2 at M = 1.0, 1.2, and 1.4.

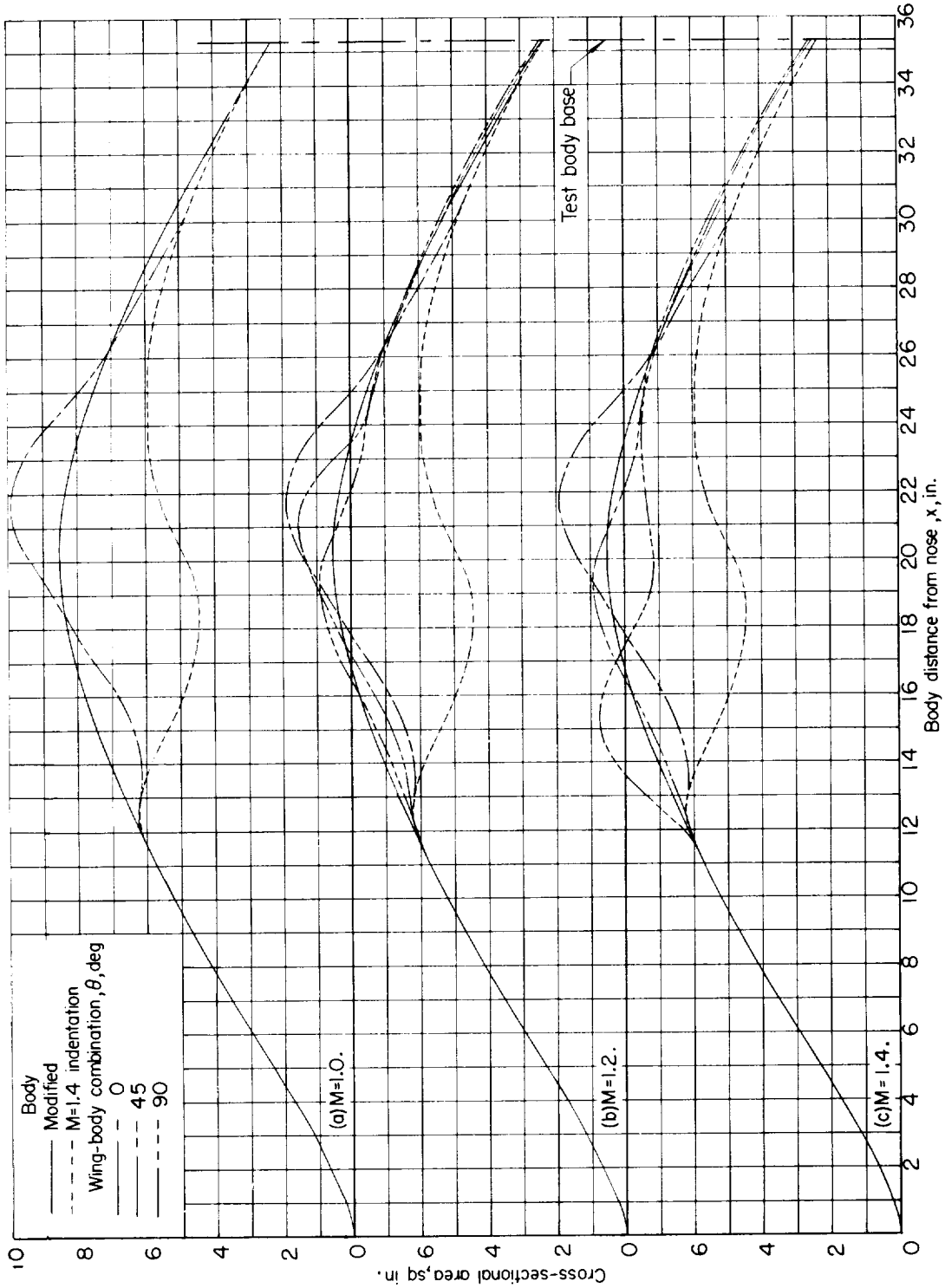

Figure 5.- Representative axial distributions of cross-sectional area for 45° sweptback wing in combination with the body indented for M = 1.4 at M = 1.0, 1.2, and 1.4.

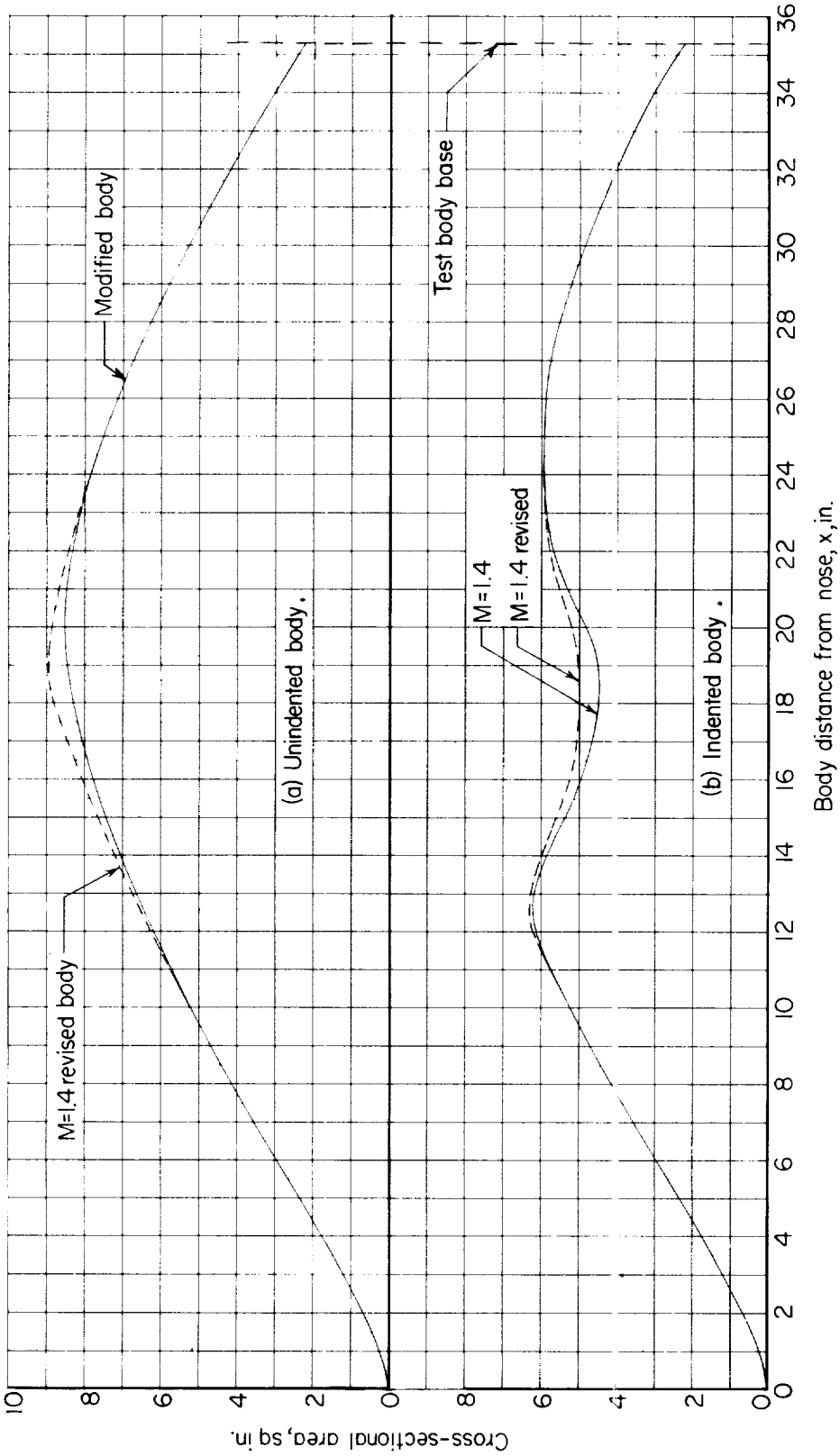

Figure 6.- Representative axial distributions of cross-sectional area for modified and revised bodies, and M = 1.4 and M = 1.4 revised indented bodies at M = 1.0.

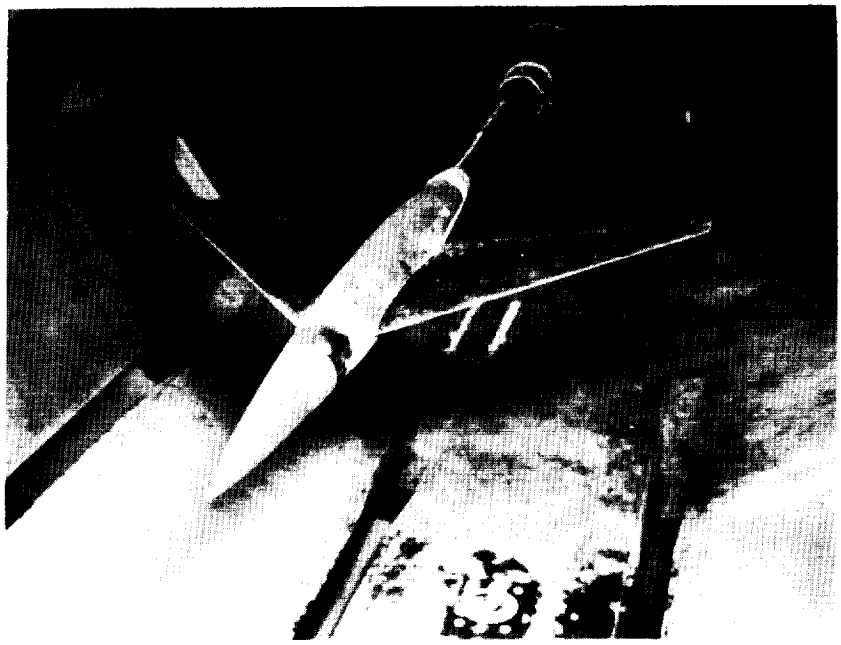

(a) Front quarter. L-86288

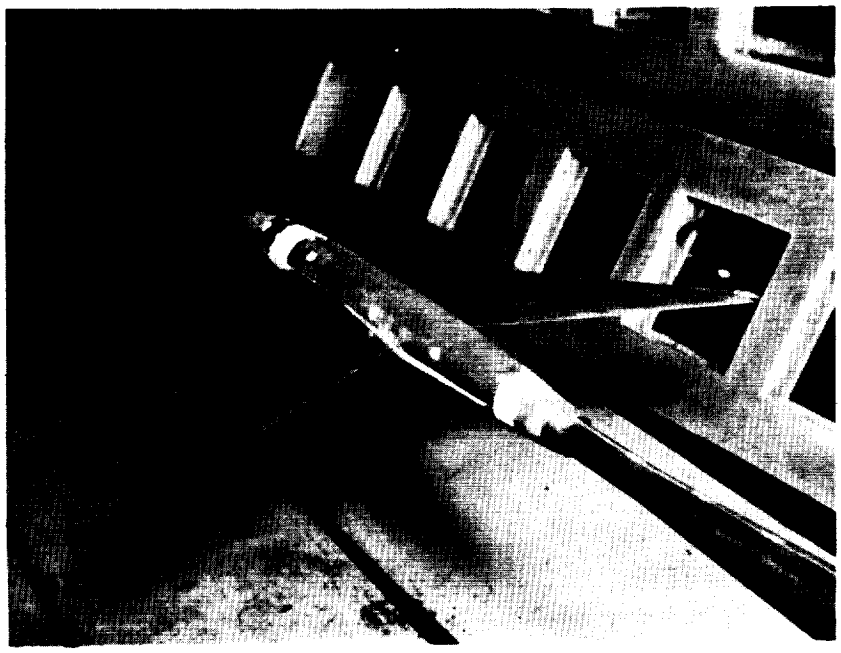

(b) Rear quarter. L-86287

Figure 7.- Photographs of the 45° sweptback wing in combination with the basic body mounted in the Langley 8-foot transonic tunnel.

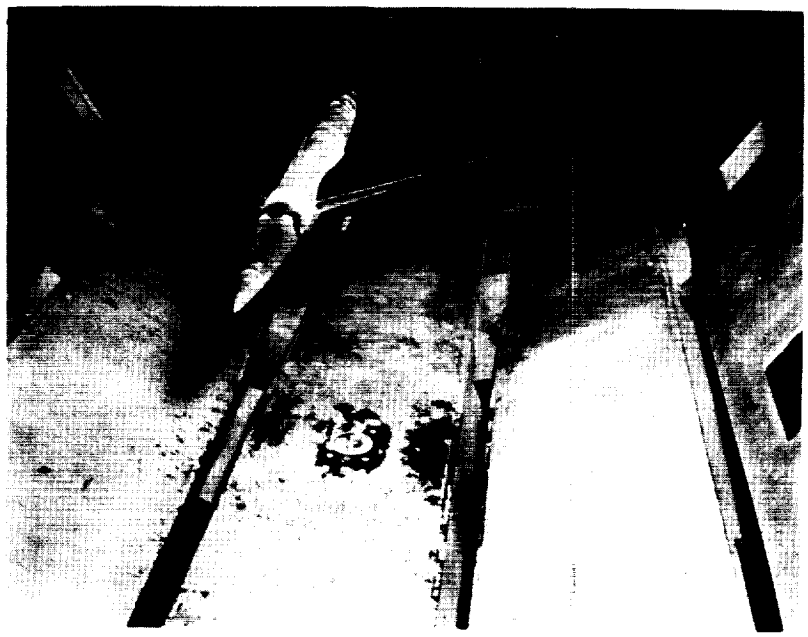

(a) Front quarter. L-86572

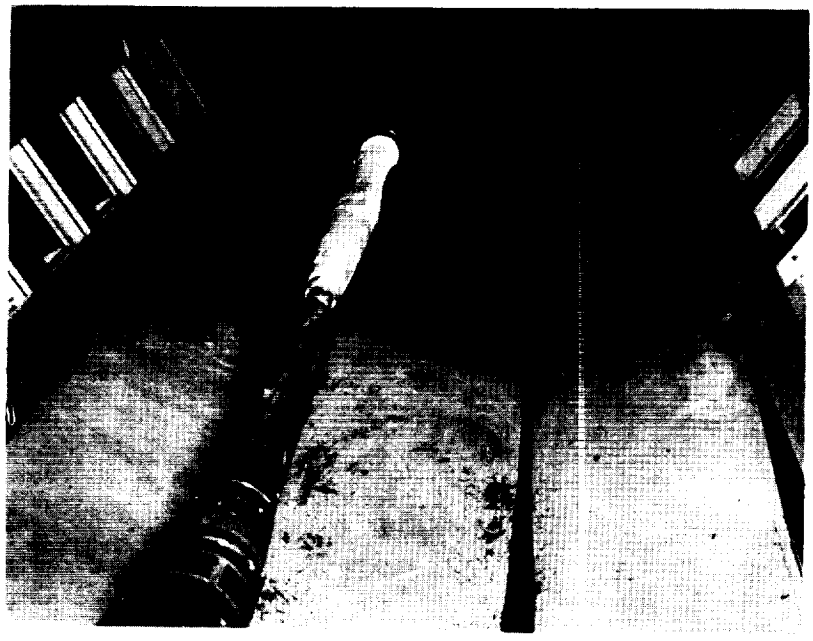

(b) Rear quarter. L-86573

Figure 8.- Photographs of the 45° sweptback wing in combination with an indented body with transition fixed on both wing and body. Model is mounted in the Langley 8-foot transonic tunnel.

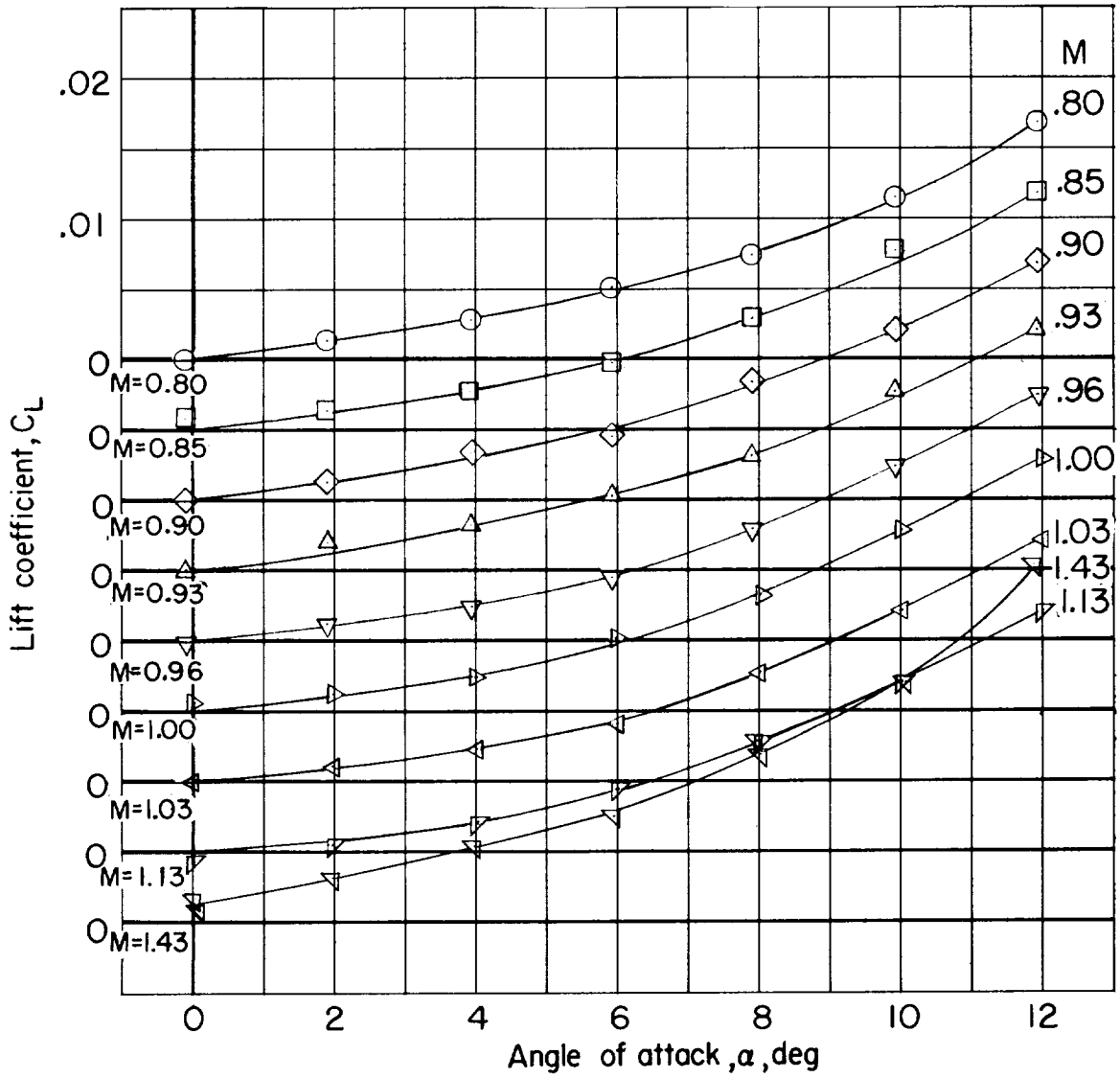

(a) C_L against α.

Figure 9.- Basic aerodynamic characteristics of the basic body.

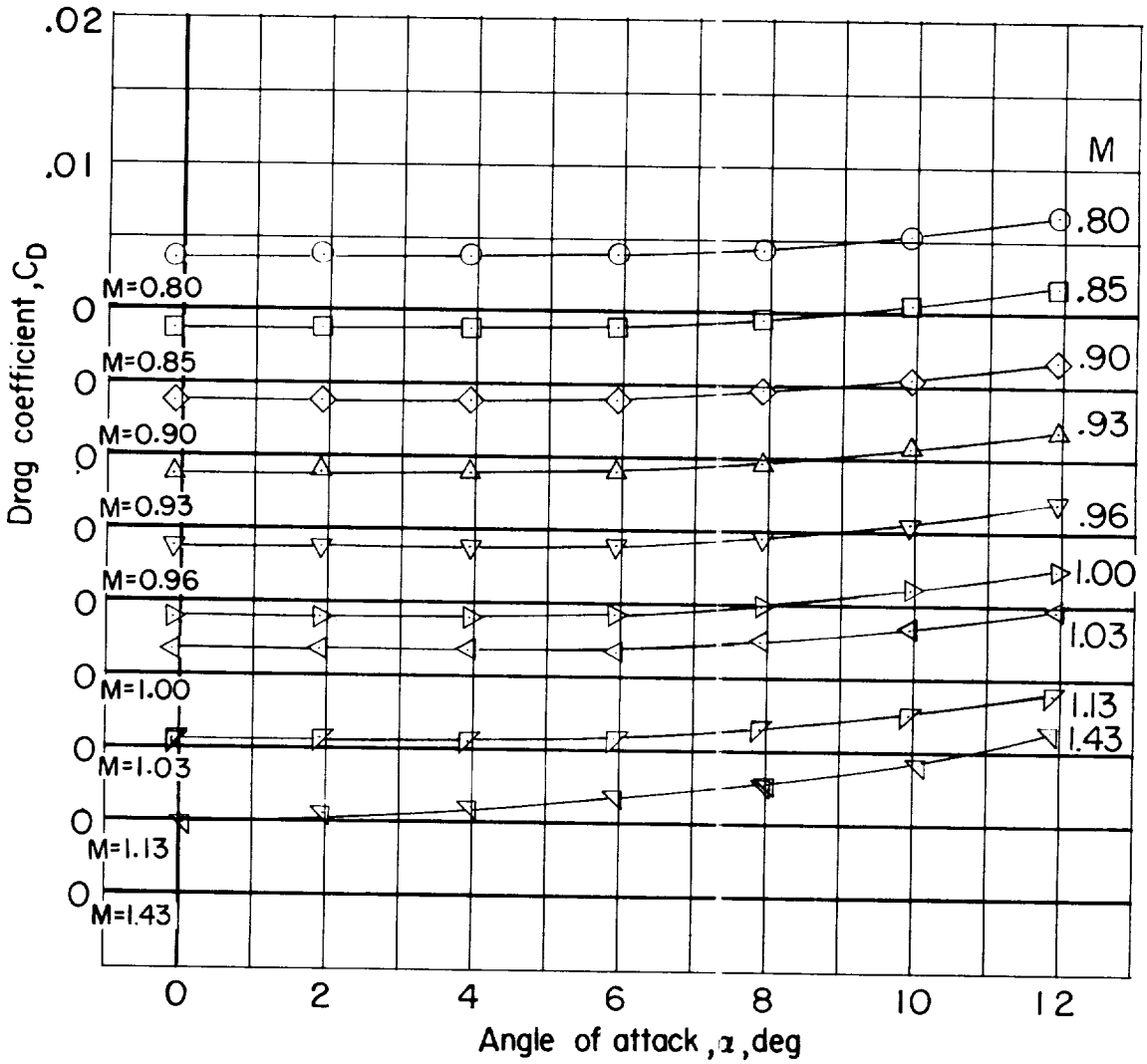

(b) C_D against α.

Figure 9.- Continued.

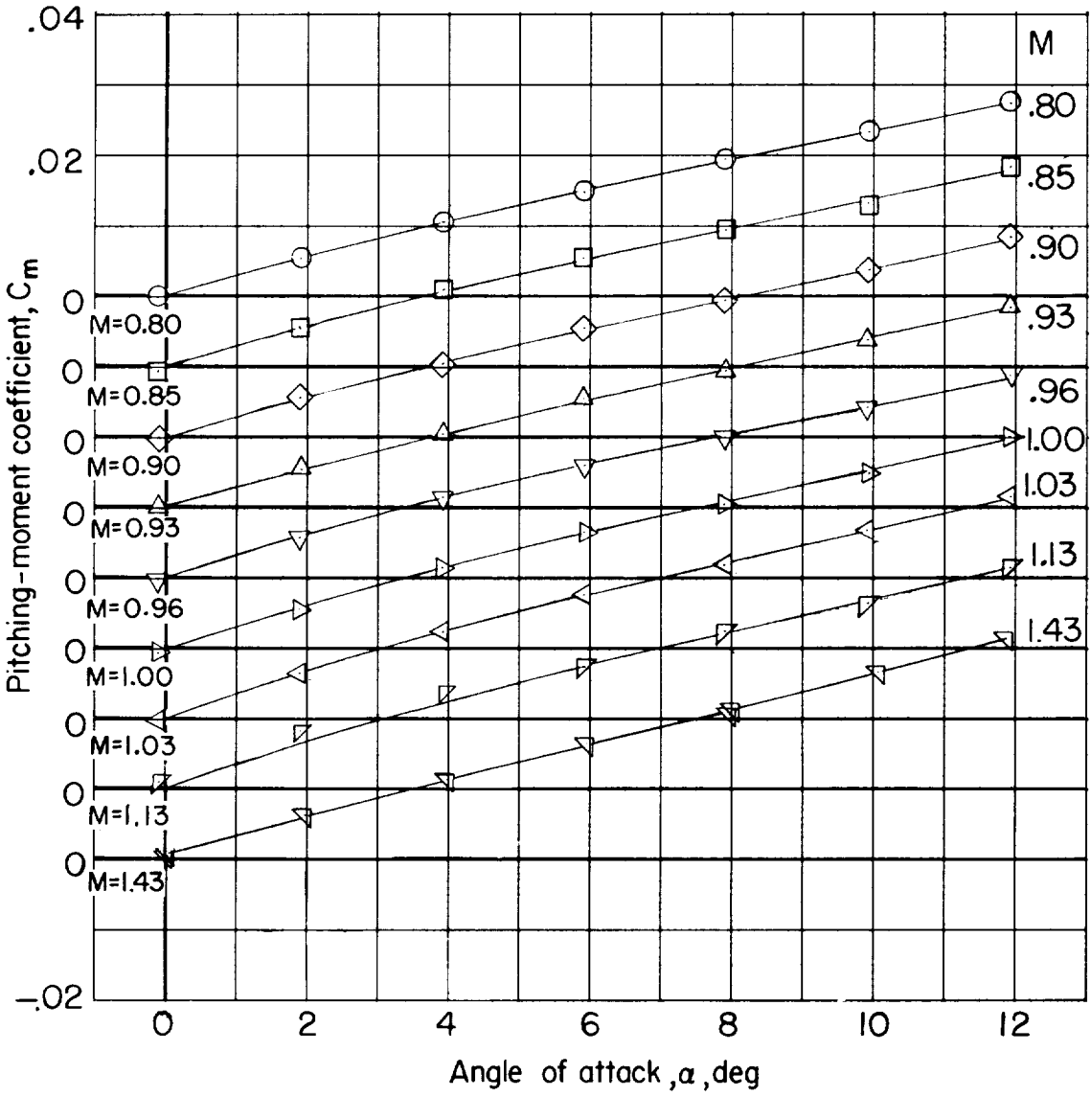

(c) C_m against α.

Figure 9.- Concluded.

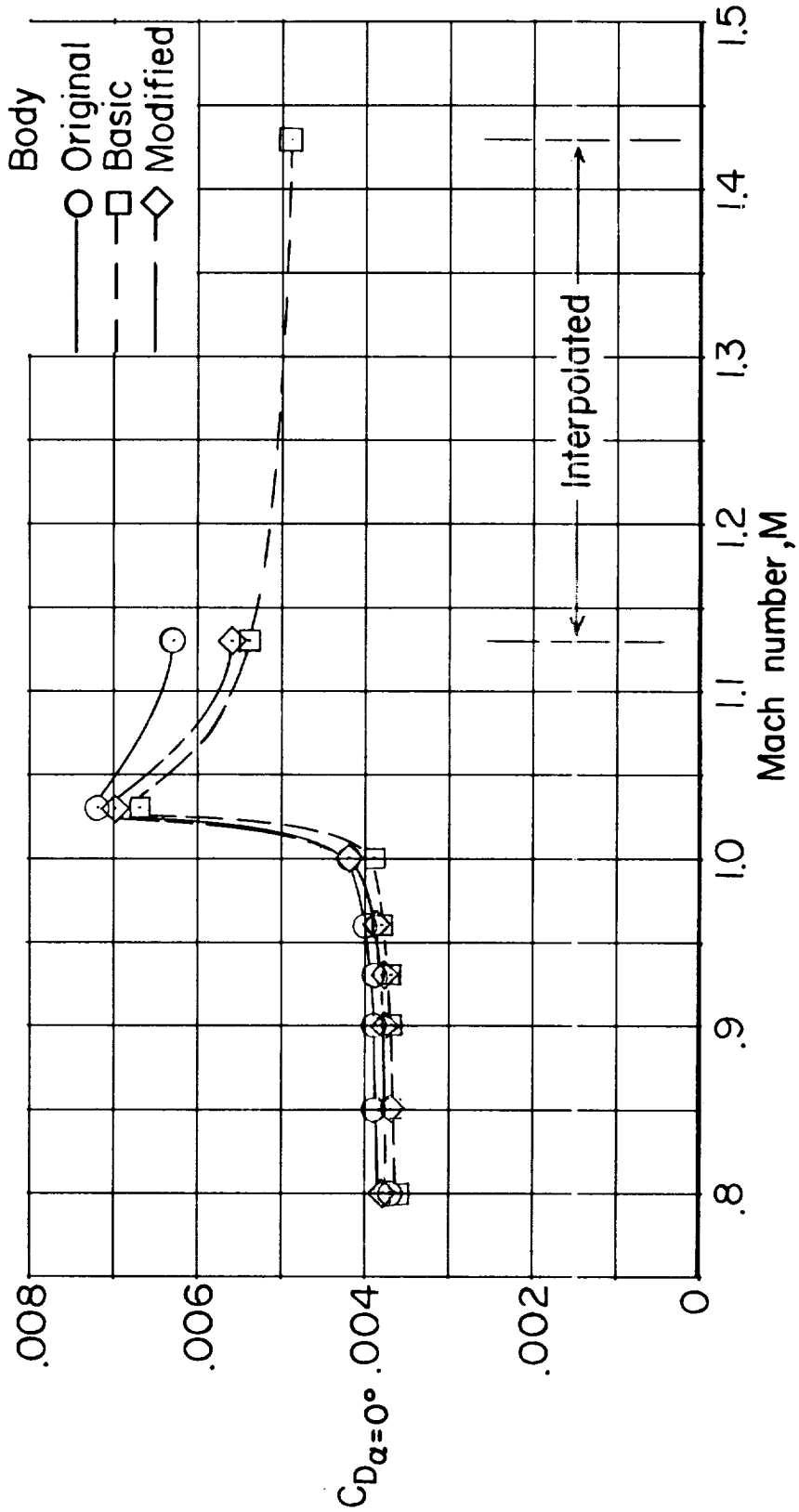

Figure 10.- Drag characteristics of original, basic, and modified bodies. $\alpha = 0^\circ$.

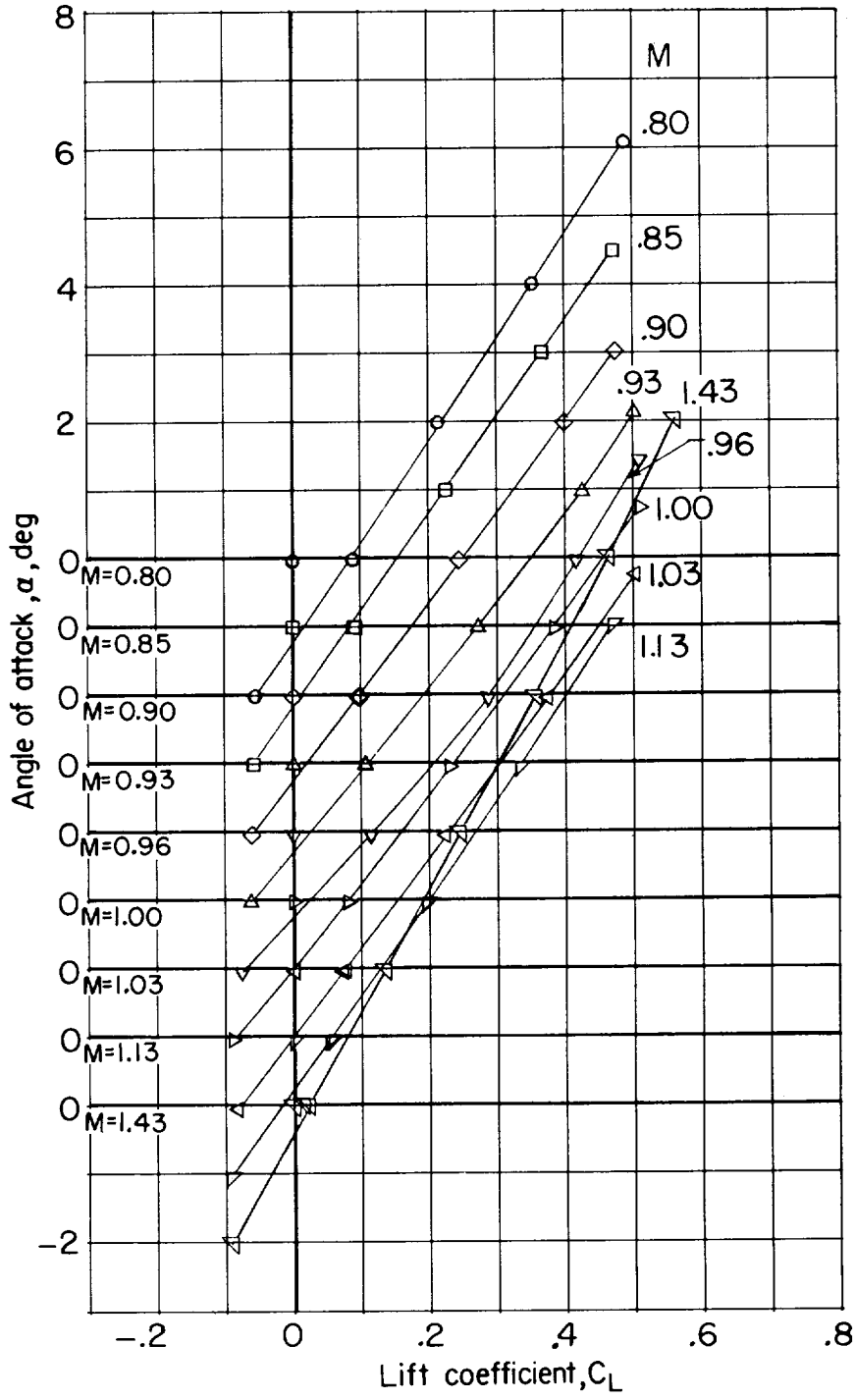

(a) α against C_L for basic wing-body combination. $i_W = 0^\circ$.

Figure 11.- Basic aerodynamic characteristics of the various wing-body combinations with transition natural.

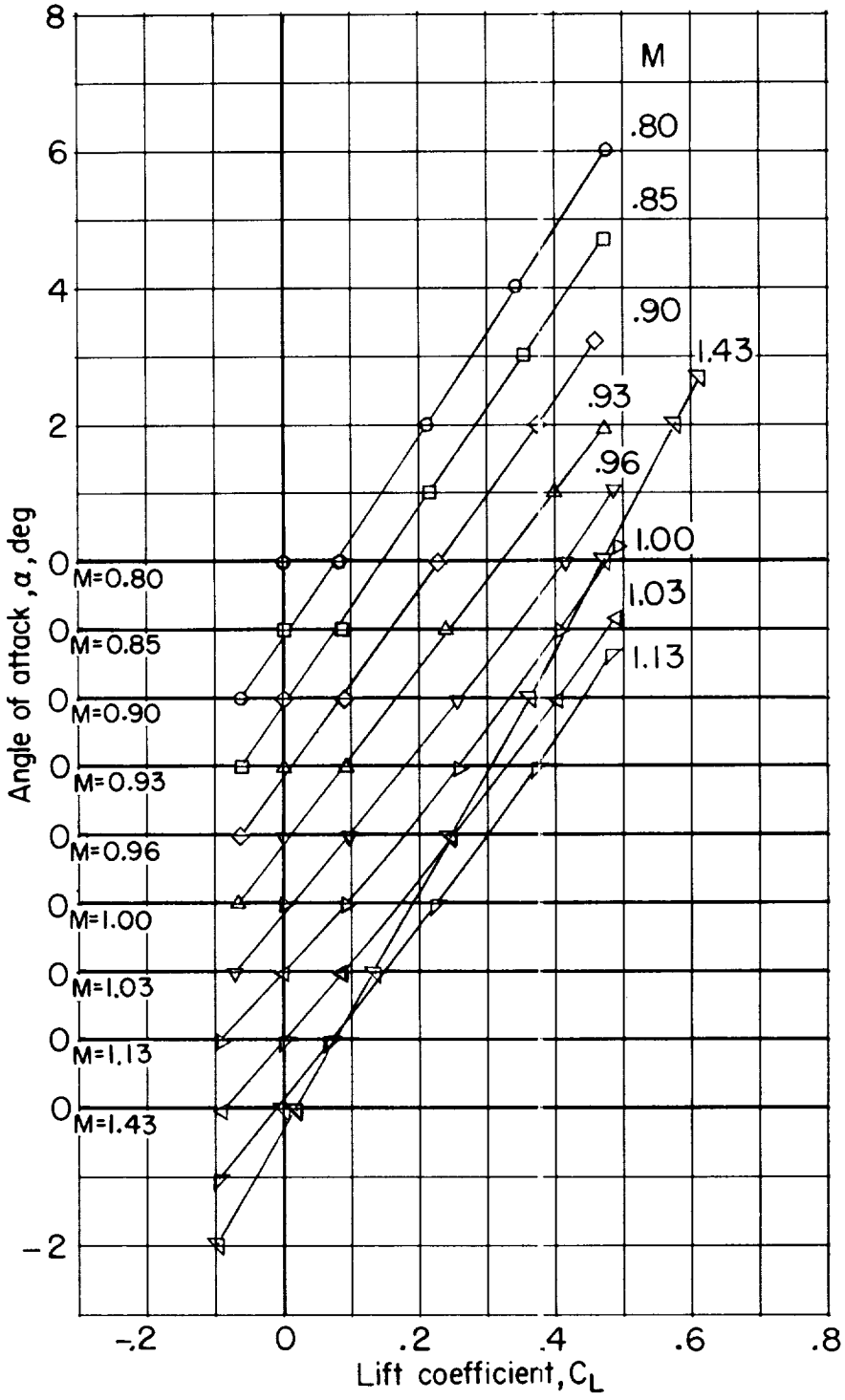

(b) α against C_L for M = 1.0 wing-body combination. $i_W = 0^\circ$.

Figure 11.- Continued.

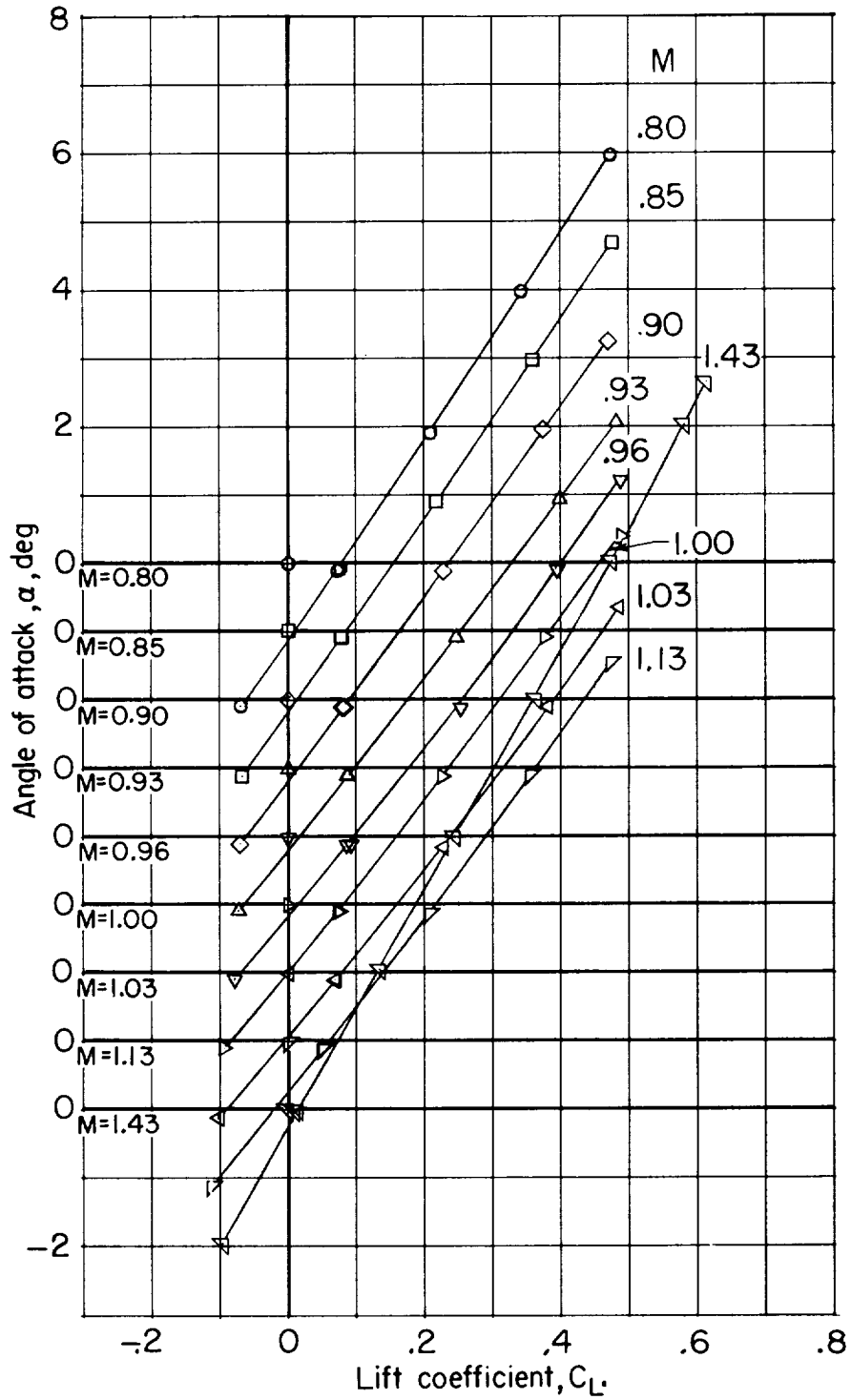

(c) α against C_L for M = 1.2 wing-body combination. $i_W = 0^o$.

Figure 11.- Continued.

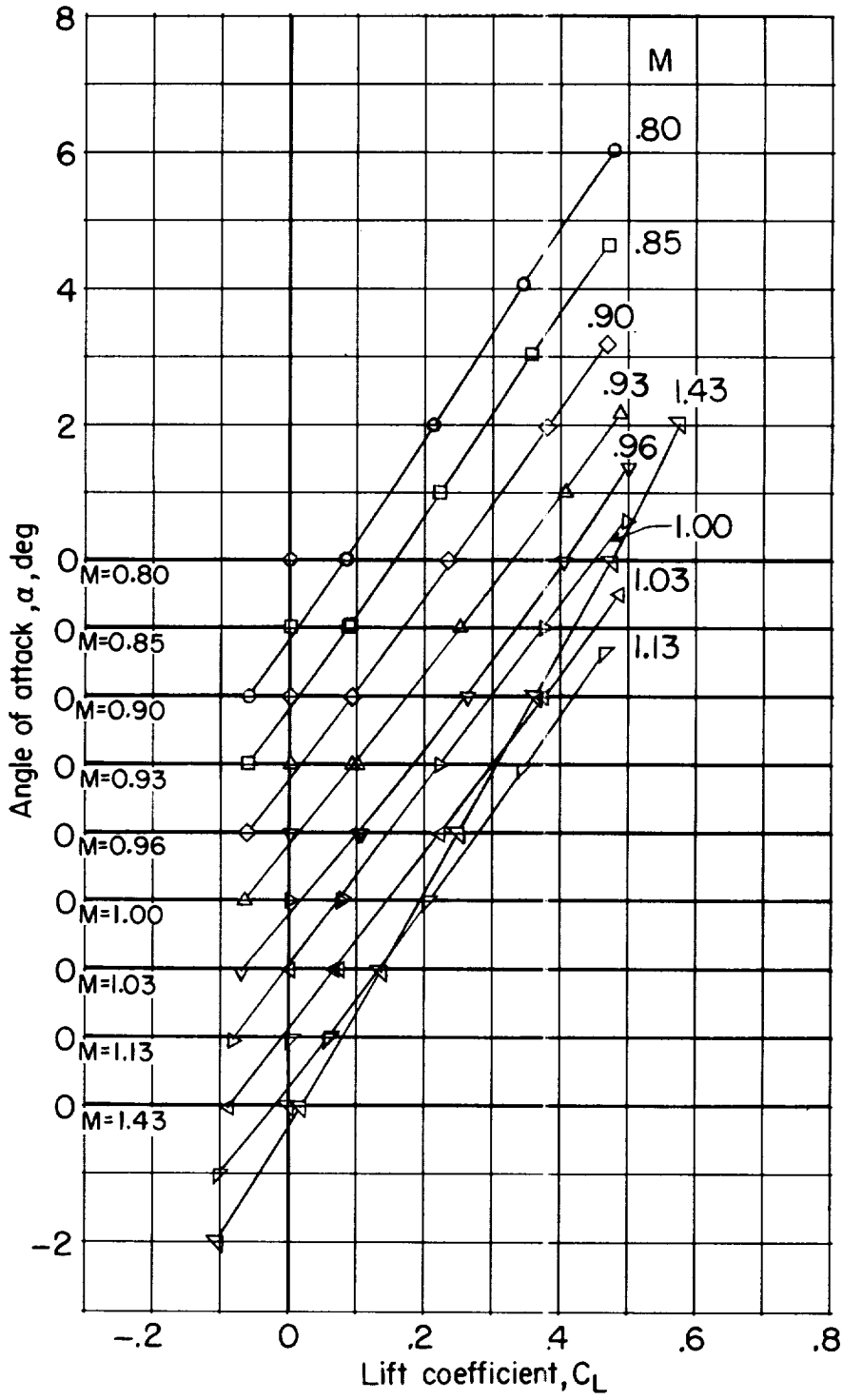

(d) α against C_L for $M = 1.4$ wing-body combination. $i_W = 0^\circ$.

Figure 11.- Continued.

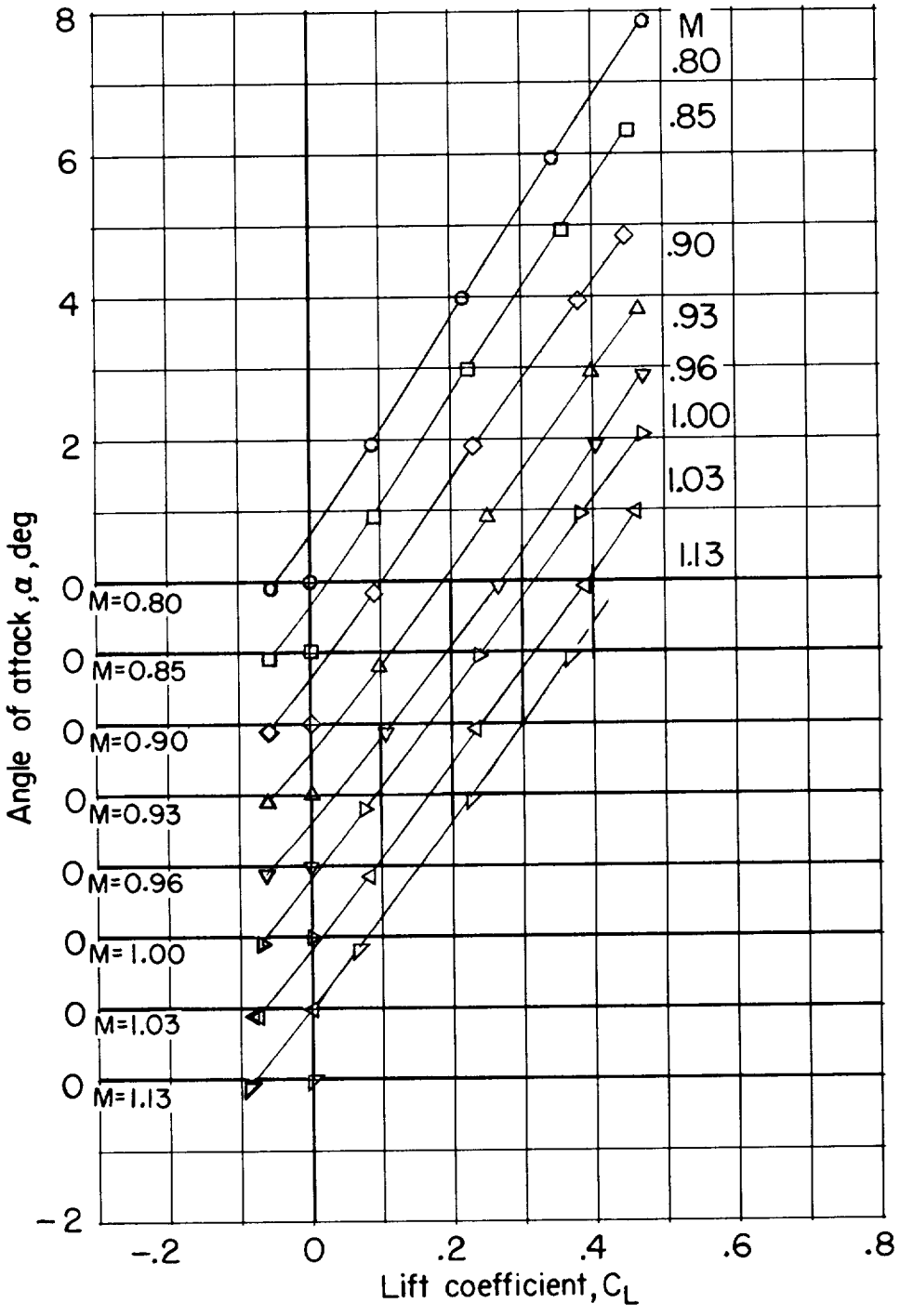

(e) α against C_L for M = 1.2 wing-body combination. $i_W = -2^o$. Dashed line indicates extrapolation of data.

Figure 11.- Continued.

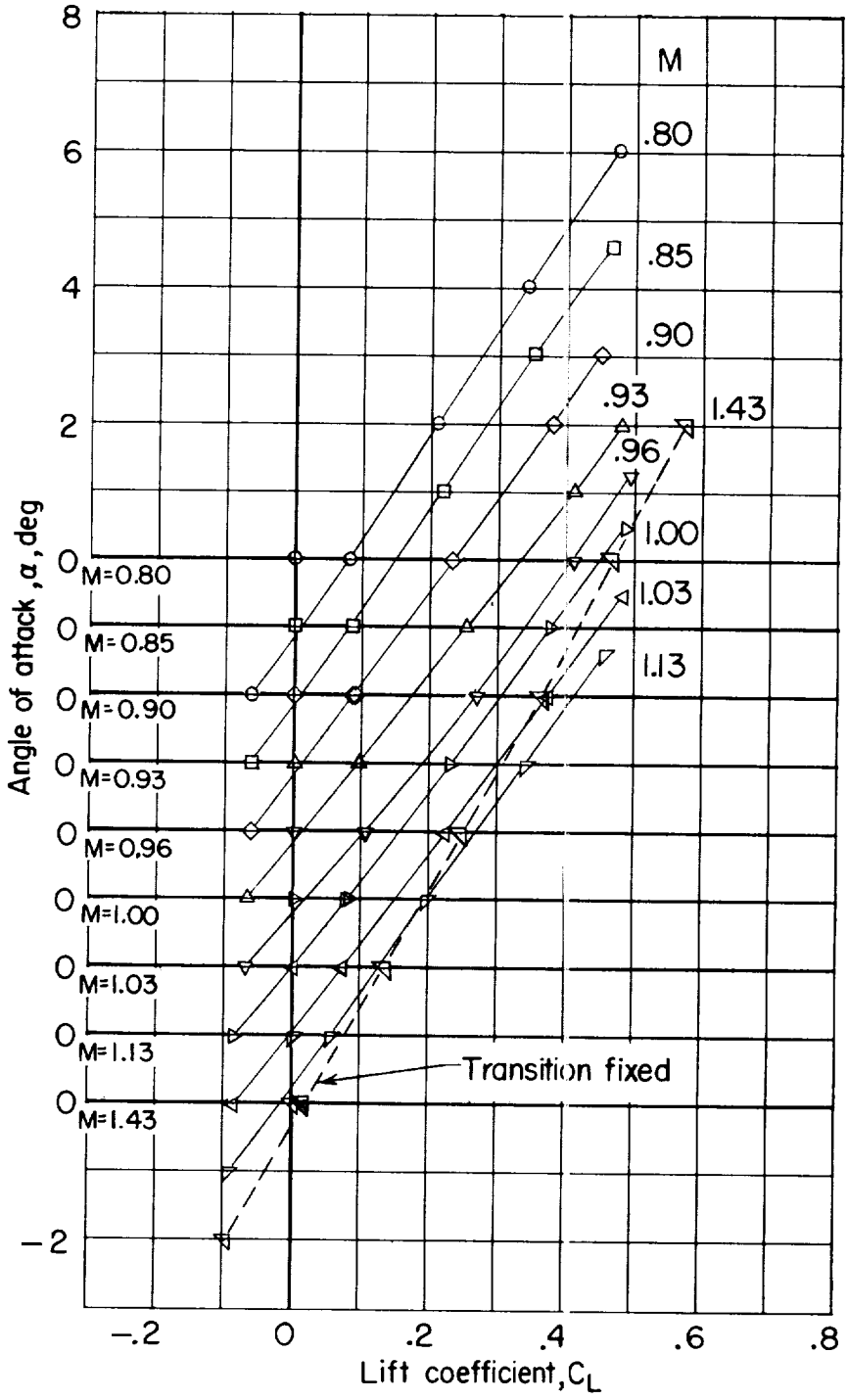

(f) α against C_L for M = 1.4 revised wing-body combination. $i_W = 0^o$.

Figure 11.- Continued.

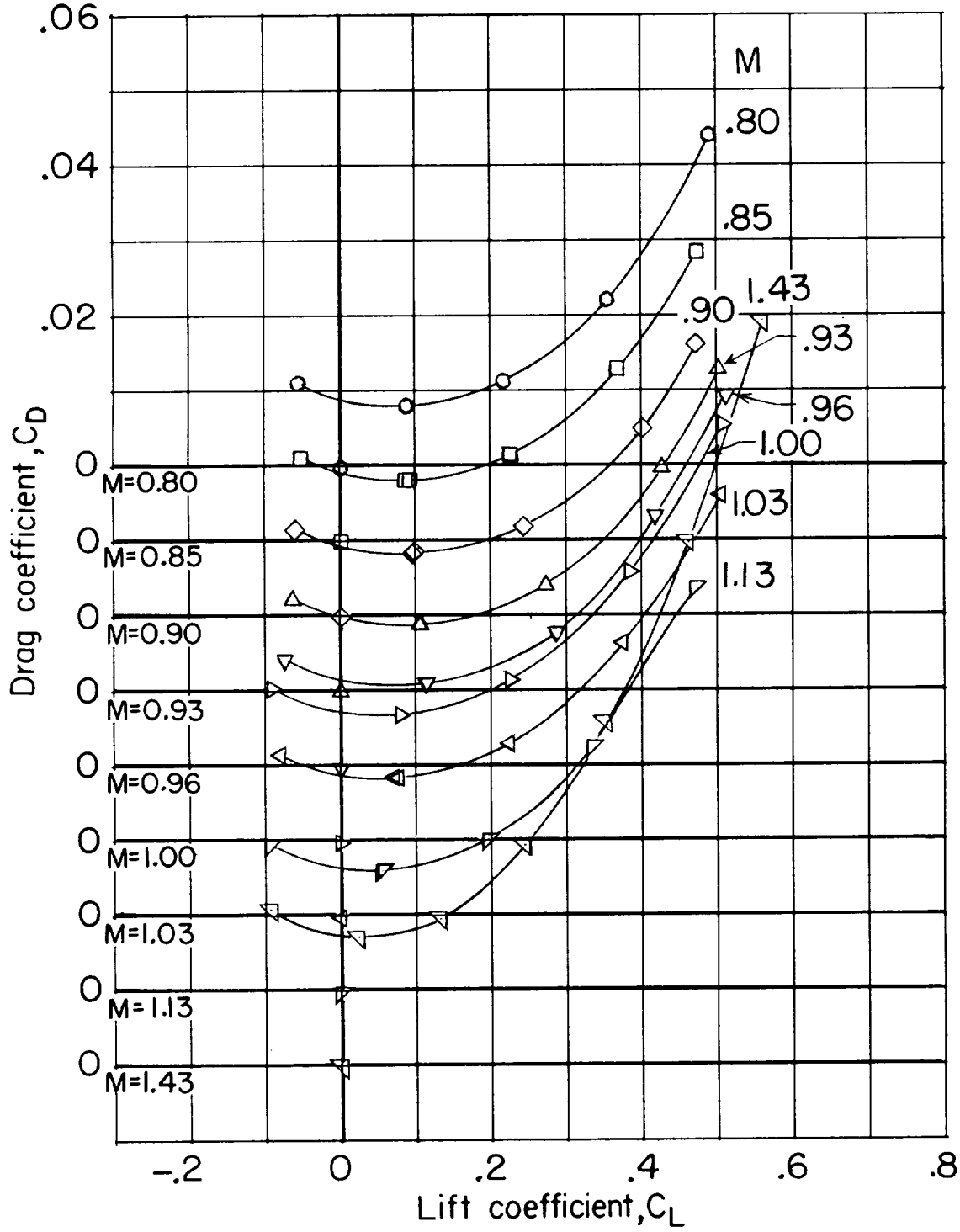

(g) C_D against C_L for basic wing-body combination. $i_W = 0^o$.

Figure 11.- Continued.

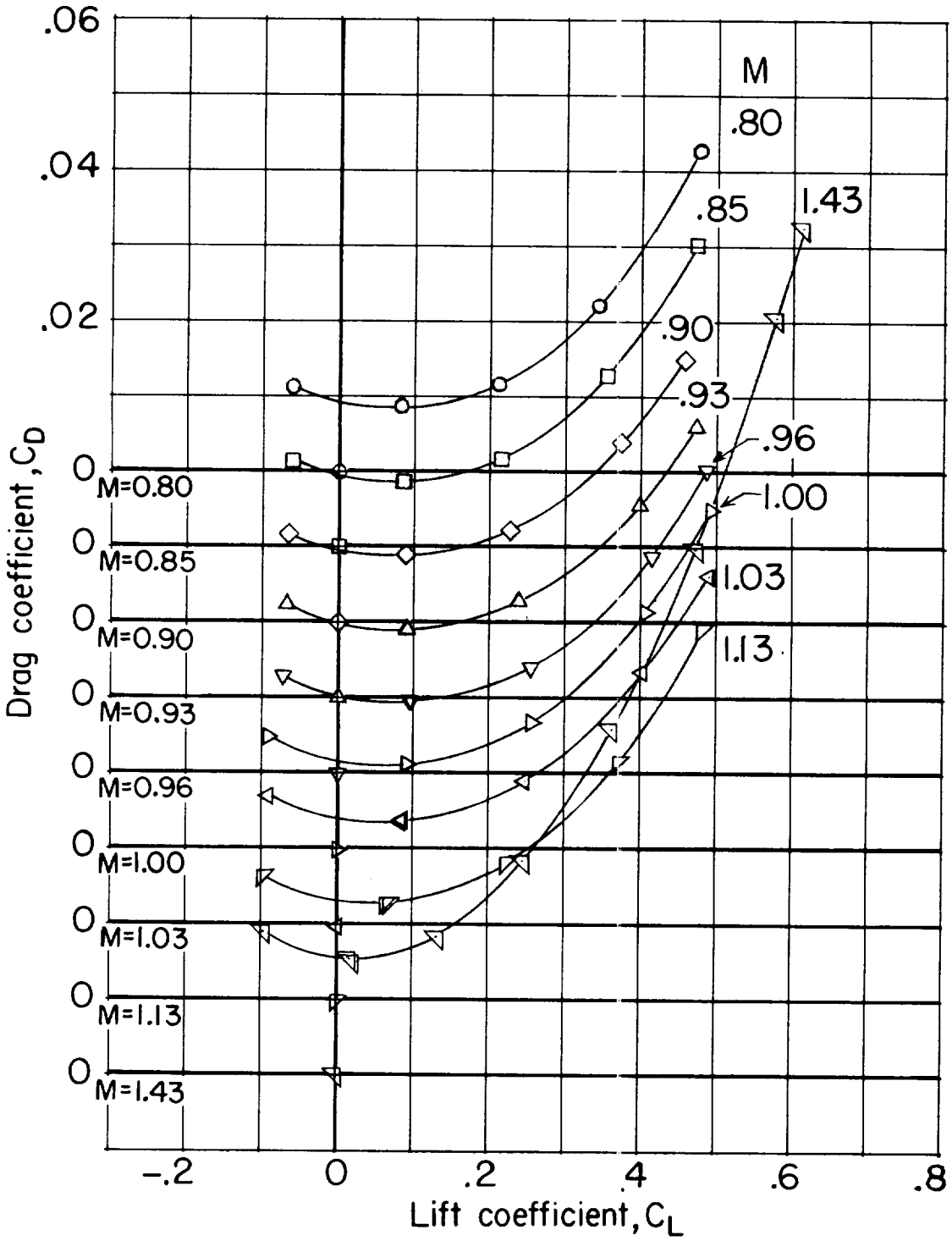

(h) C_D against C_L for M = 1.0 wing-body combination. $i_W = 0^o$.

Figure 11.- Continued.

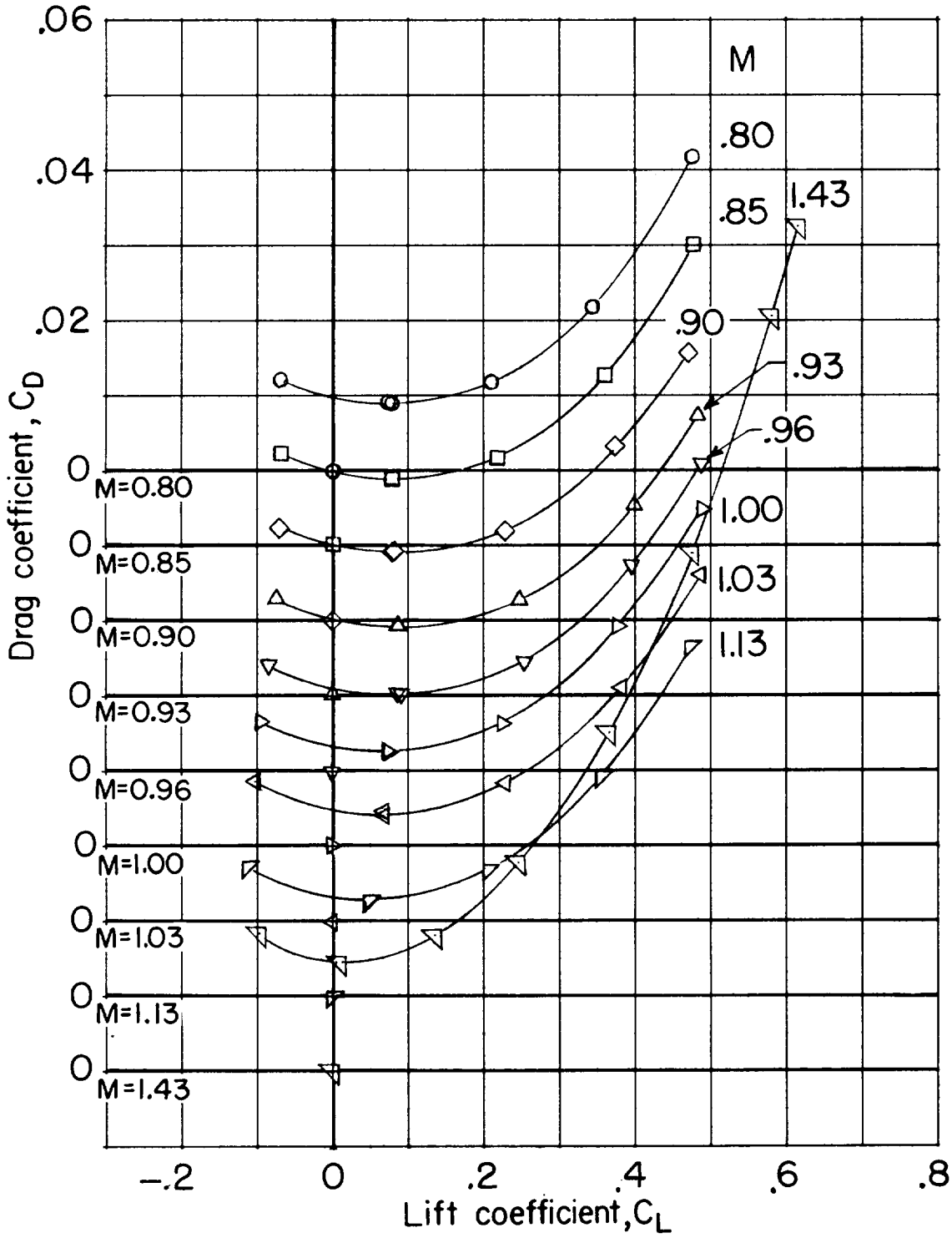

(i) C_D against C_L for M = 1.2 wing-body combination. $i_W = 0^o$.

Figure 11.- Continued.

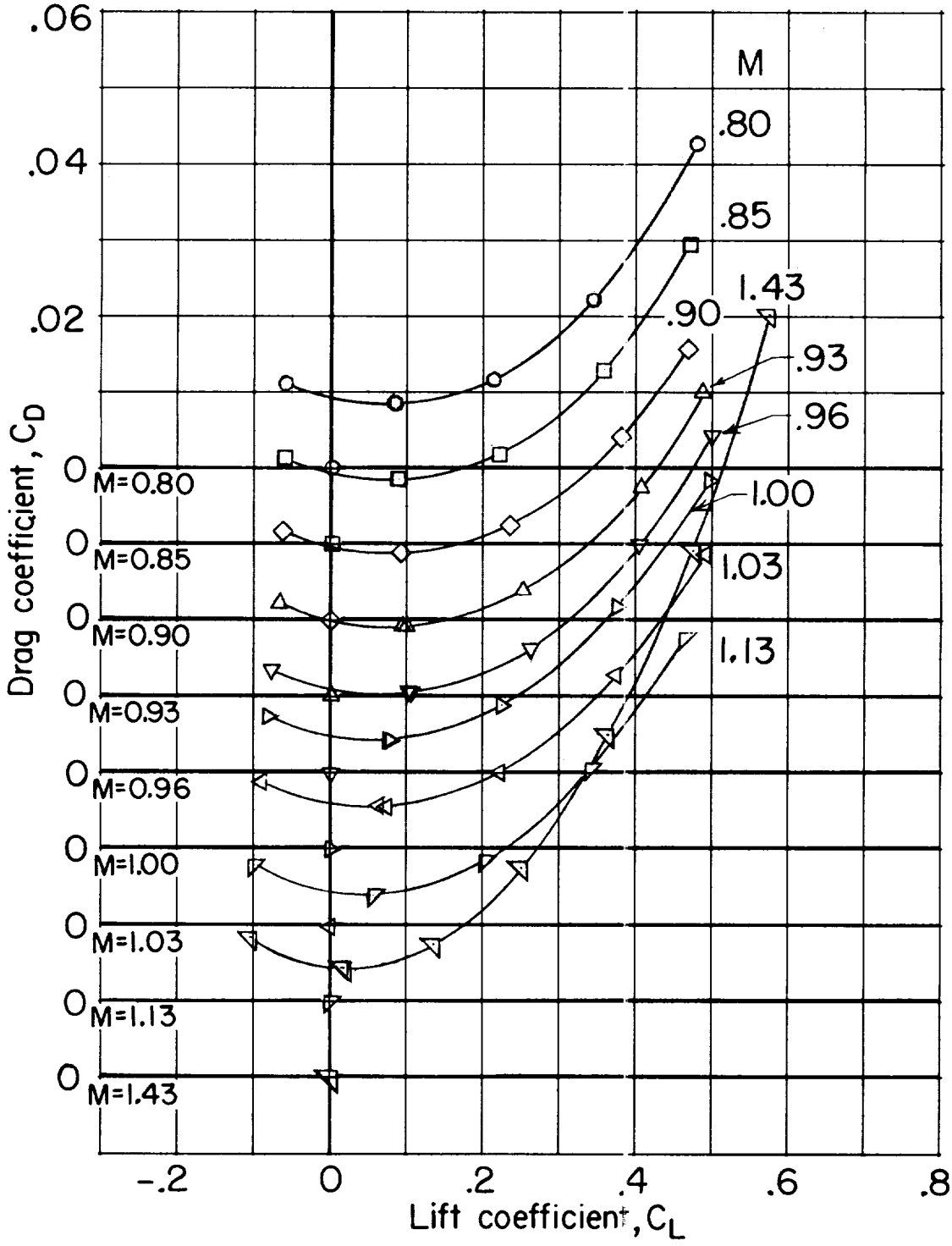

(j) C_D against C_L for M = 1.4 wing-body combination. $i_W = 0^\circ$.

Figure 11.- Continued.

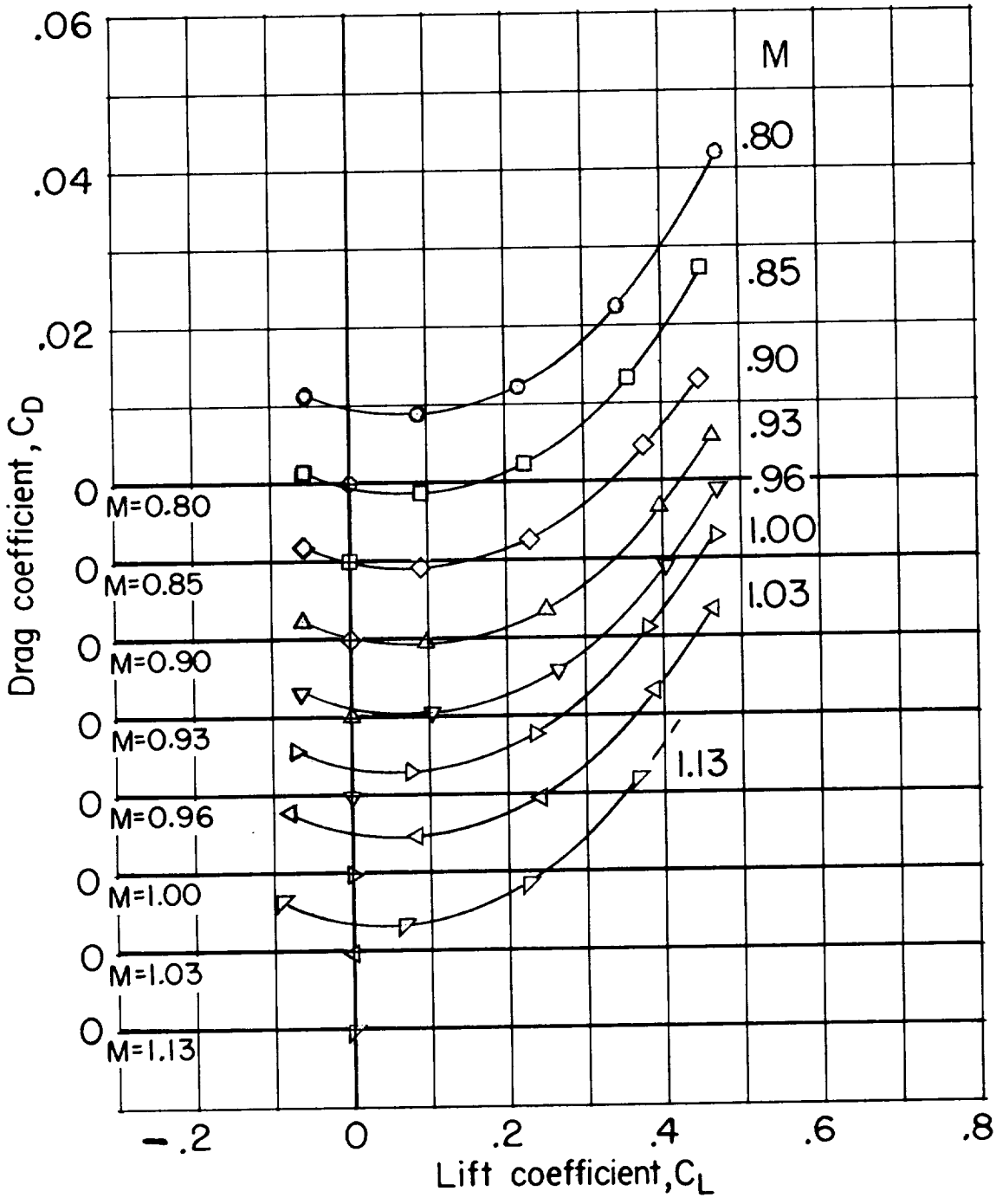

(k) C_D against C_L for M = 1.2 wing-body combination. $i_W = -2^\circ$. Dashed line indicates extrapolation of data.

Figure 11.- Continued.

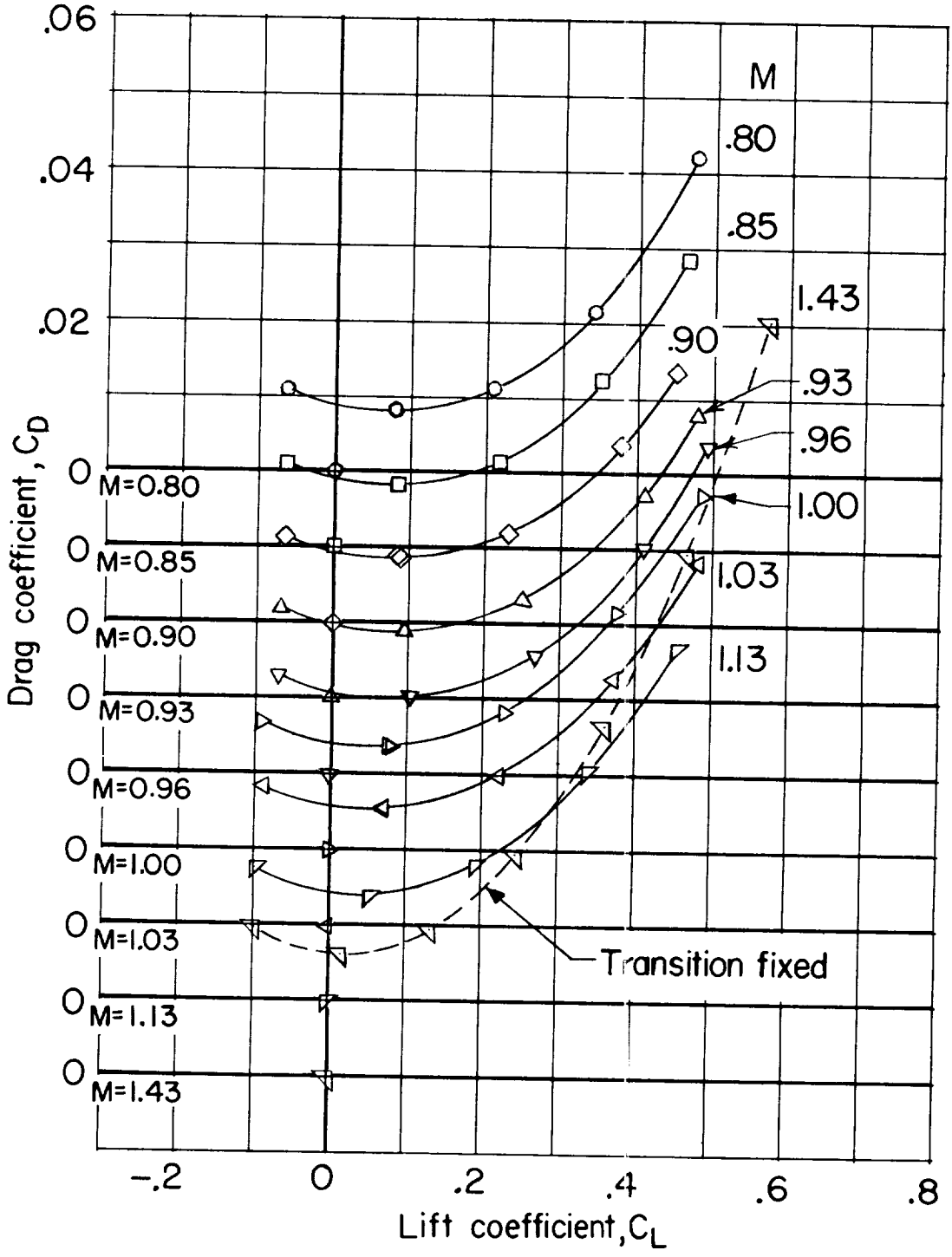

(l) C_D against C_L for M = 1.4 revised wing-body combination. $i_W = 0^o$.

Figure 11.- Continued.

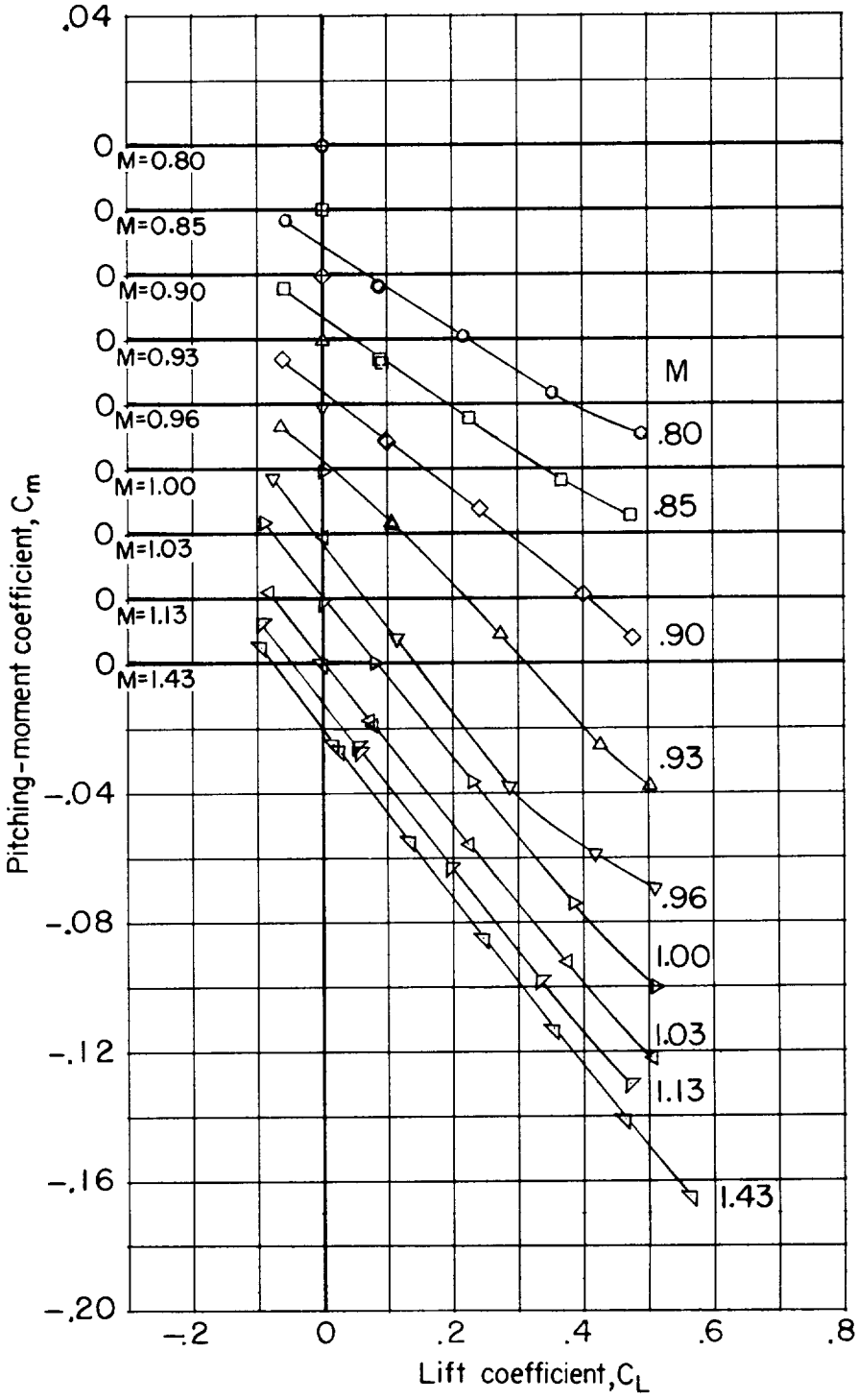

(m) C_m against C_L for basic wing-body combination. $i_W = 0^\circ$.

Figure 11.- Continued.

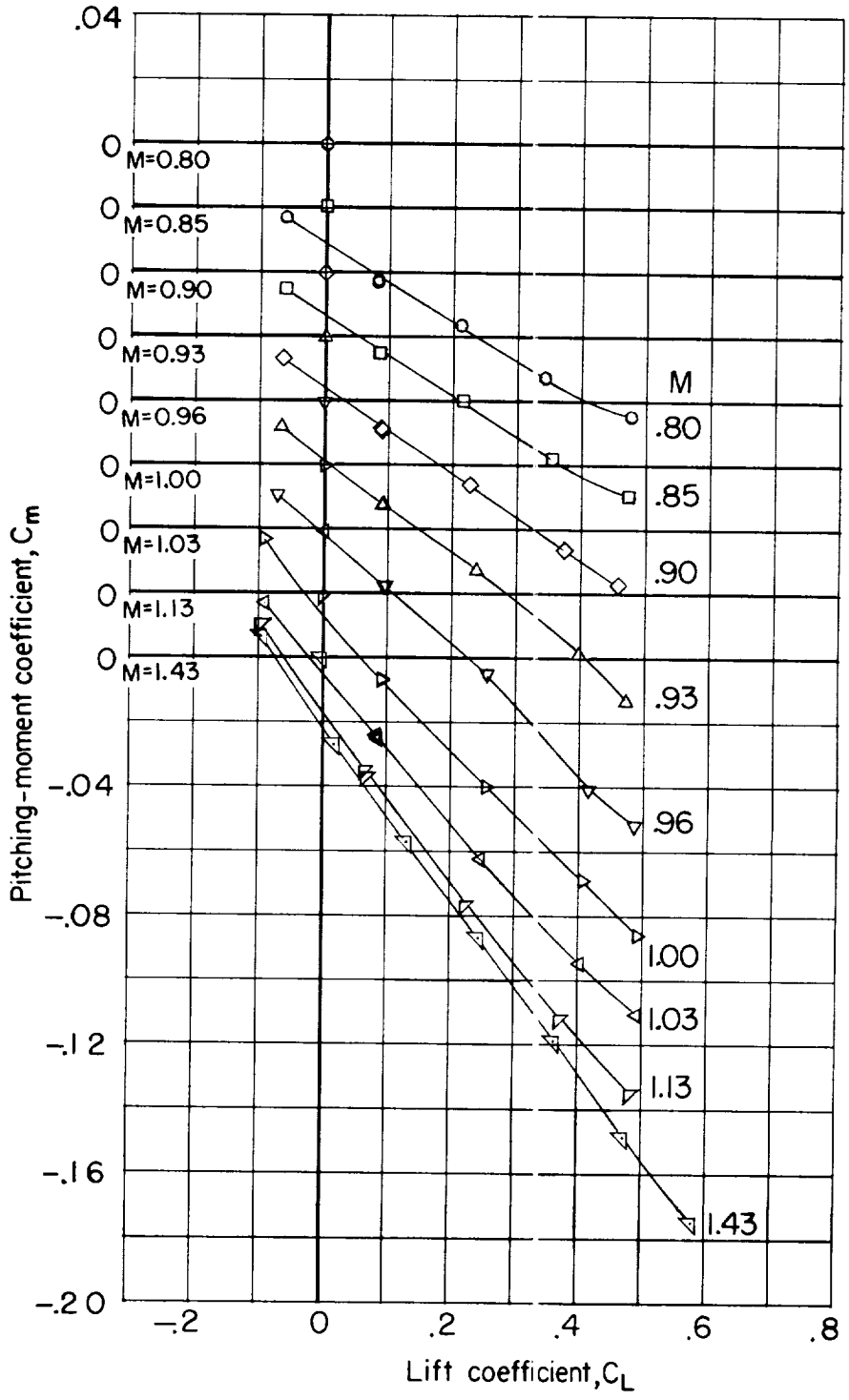

(n) C_m against C_L for M = 1.0 wing-body combination. $i_W = 0^o$.

Figure 11.- Continued.

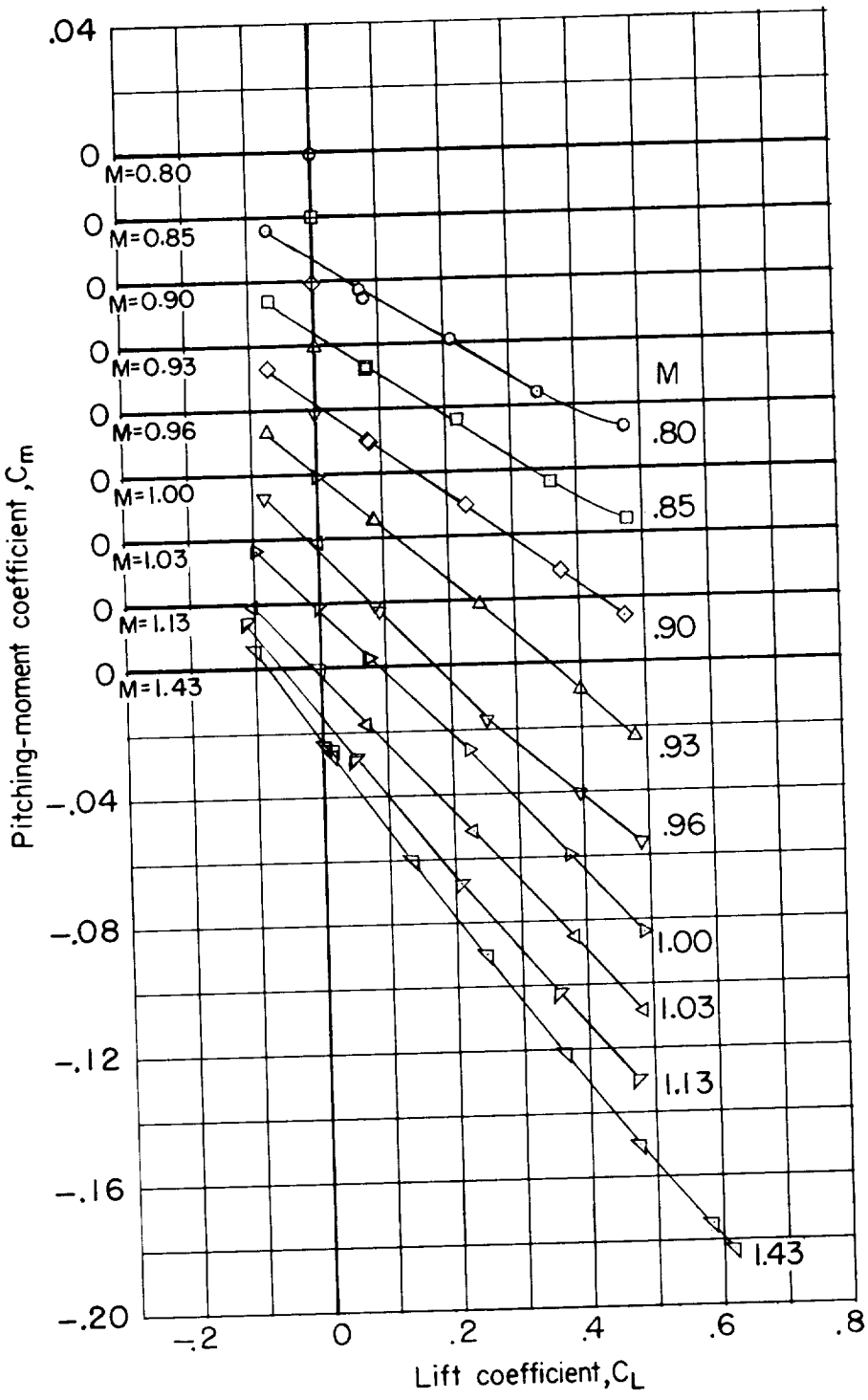

(o) C_m against C_L for M = 1.2 wing-body combination. $i_W = 0^\circ$.

Figure 11.- Continued.

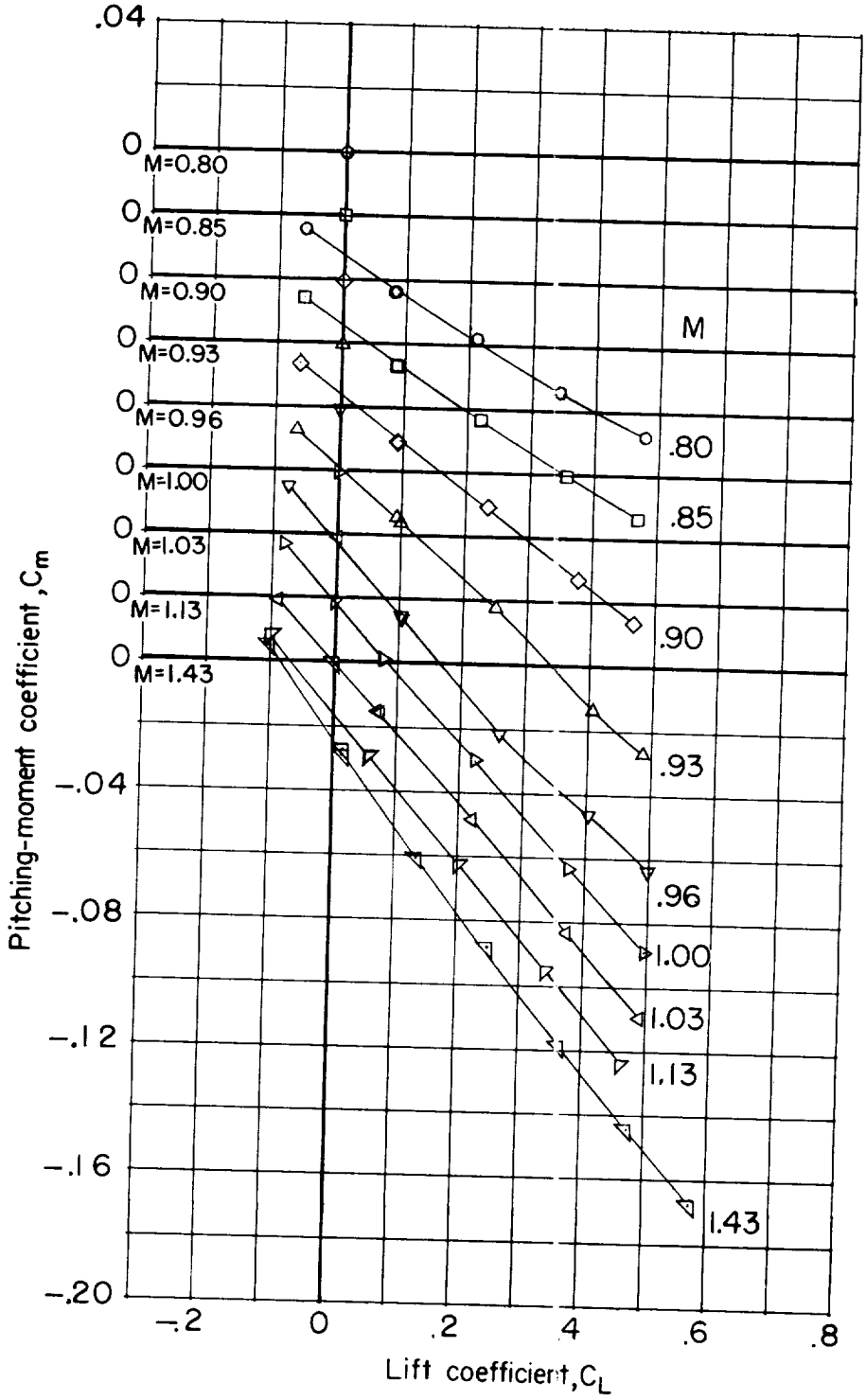

(p) C_m against C_L for $M = 1.4$ wing-body combination. $i_W = 0^\circ$.

Figure 11.- Continued.

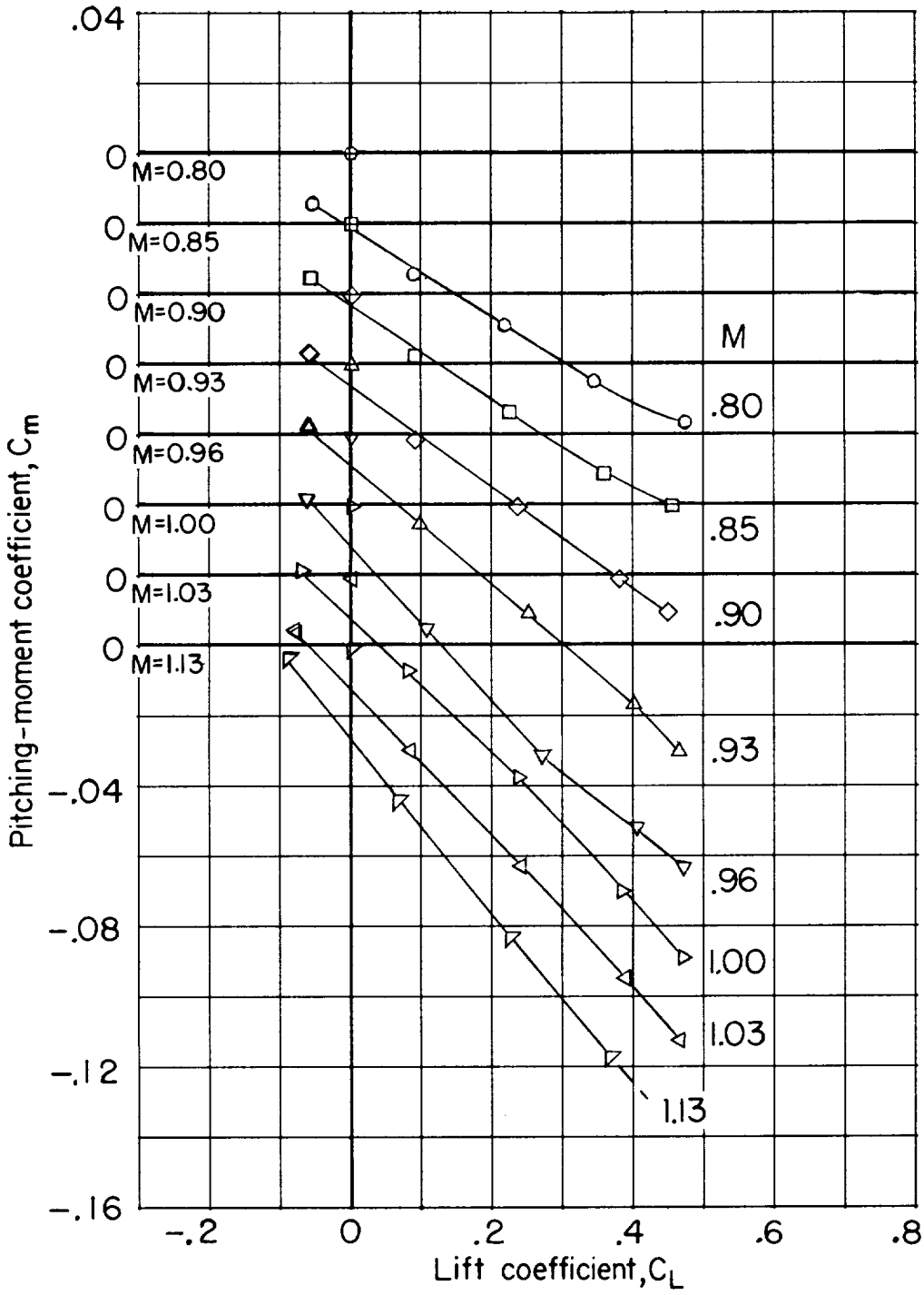

(q) C_m against C_L for M = 1.2 wing-body combination. $i_W = -2^o$. Dashed line indicates extrapolation of data.

Figure 11.- Continued.

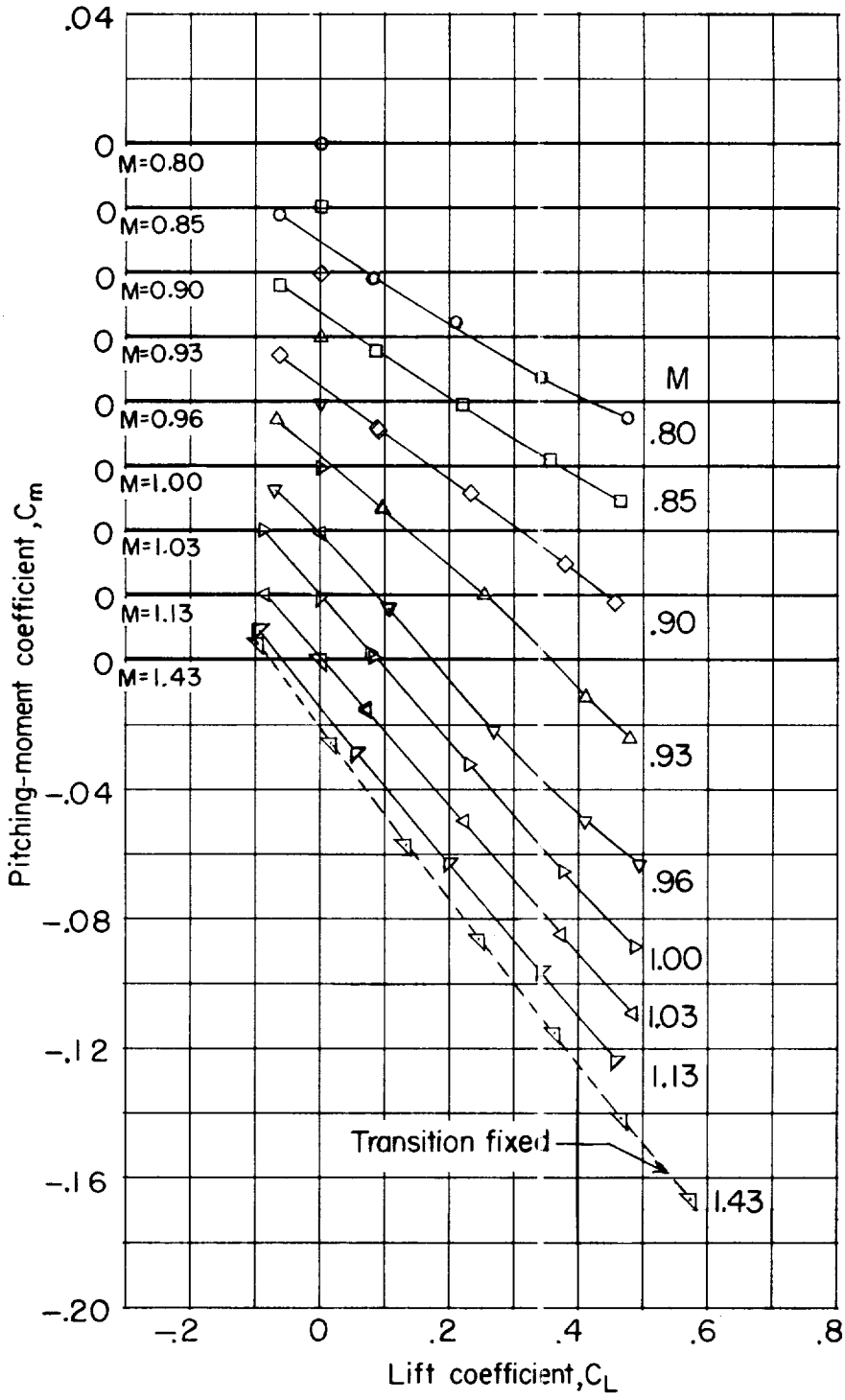

(r) C_m against C_L for $M = 1.4$ revised wing-body combination. $i_W = 0^\circ$.

Figure 11.- Concluded.

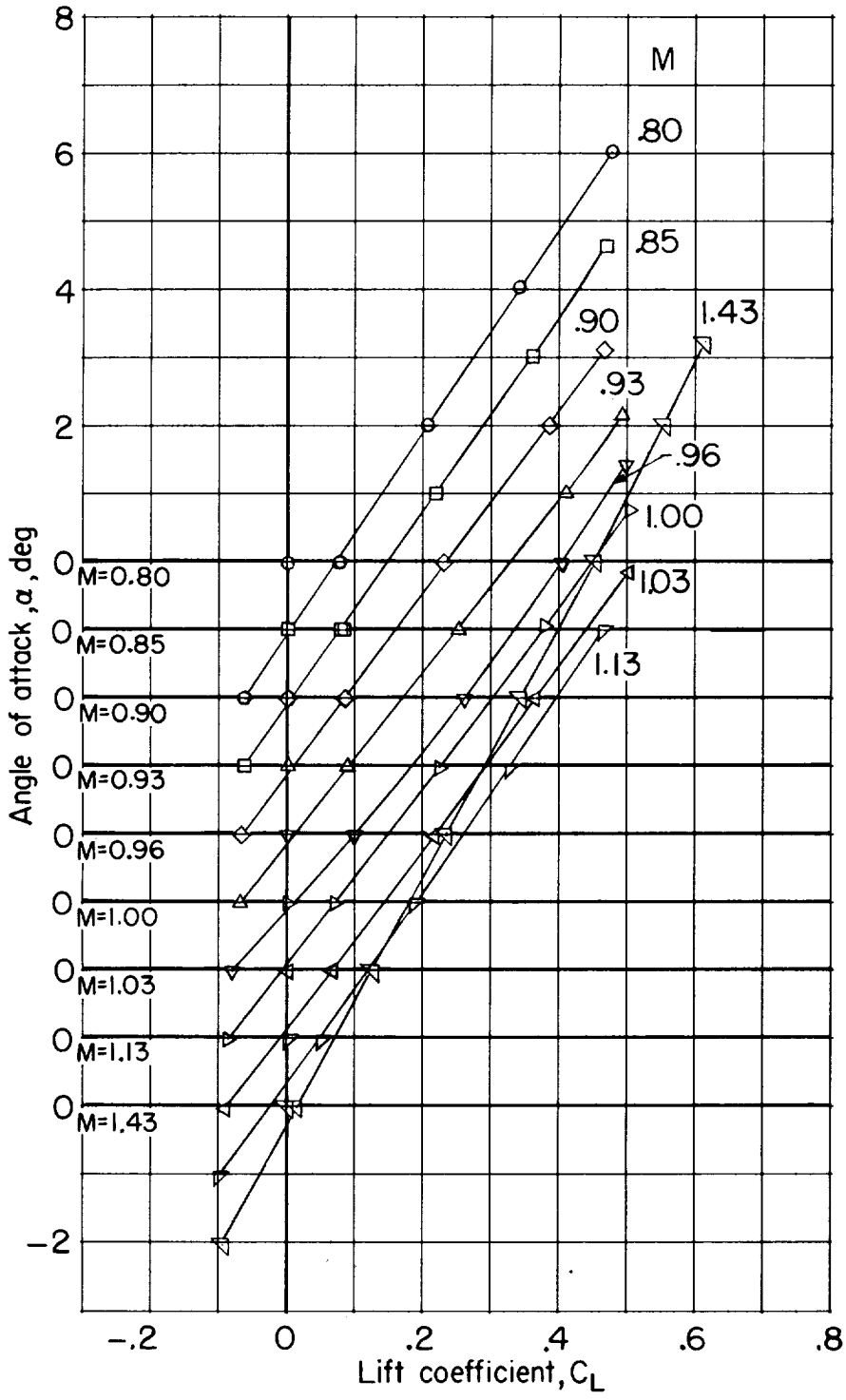

(a) α against C_L for basic wing-body combination. $i_W = 0^\circ$.

Figure 12.- Basic aerodynamic characteristics of the various wing-body combinations with transition fixed.

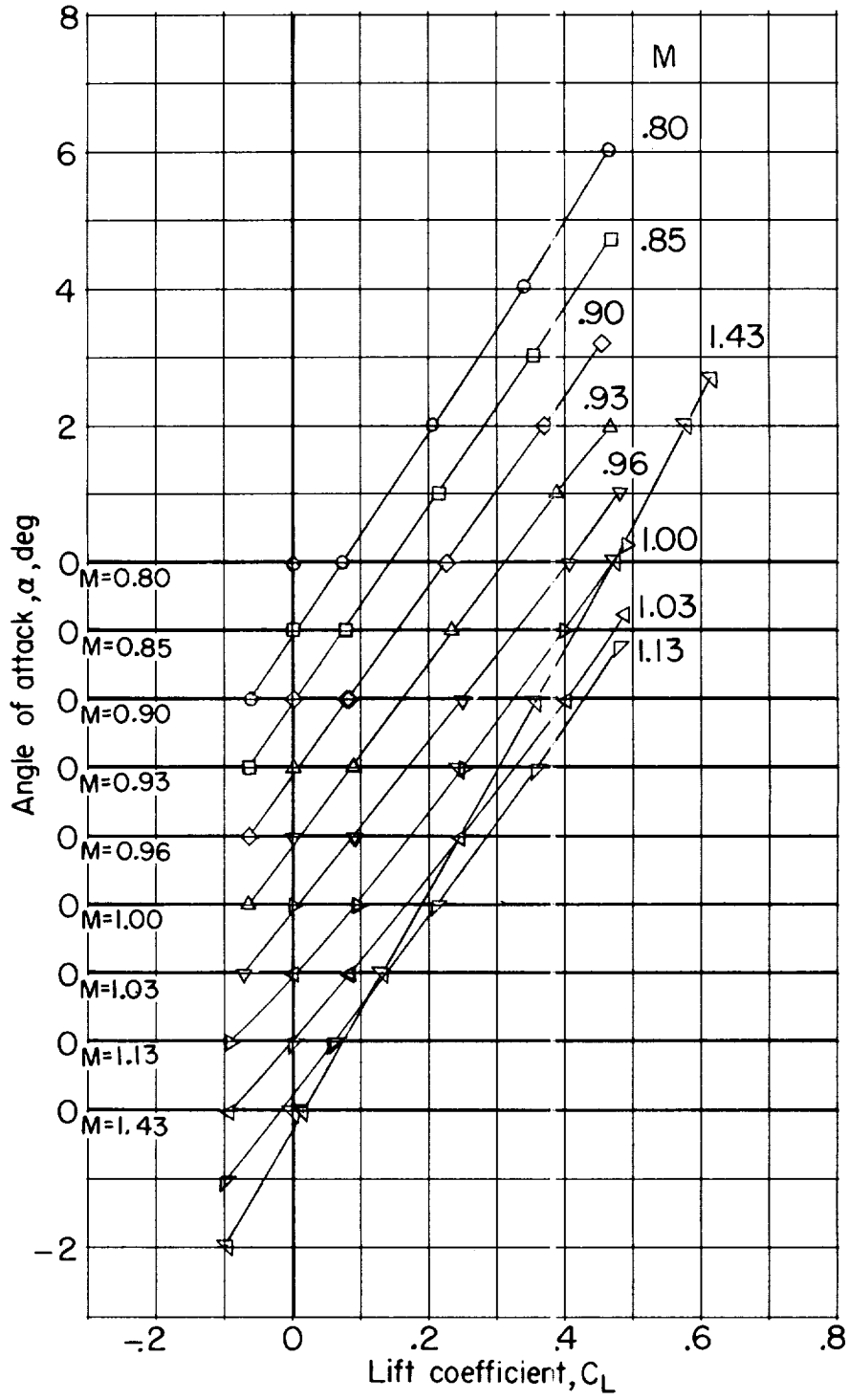

(b) α against C_L for M = 1.0 wing-body combinations. $i_W = 0^o$.

Figure 12.- Continued.

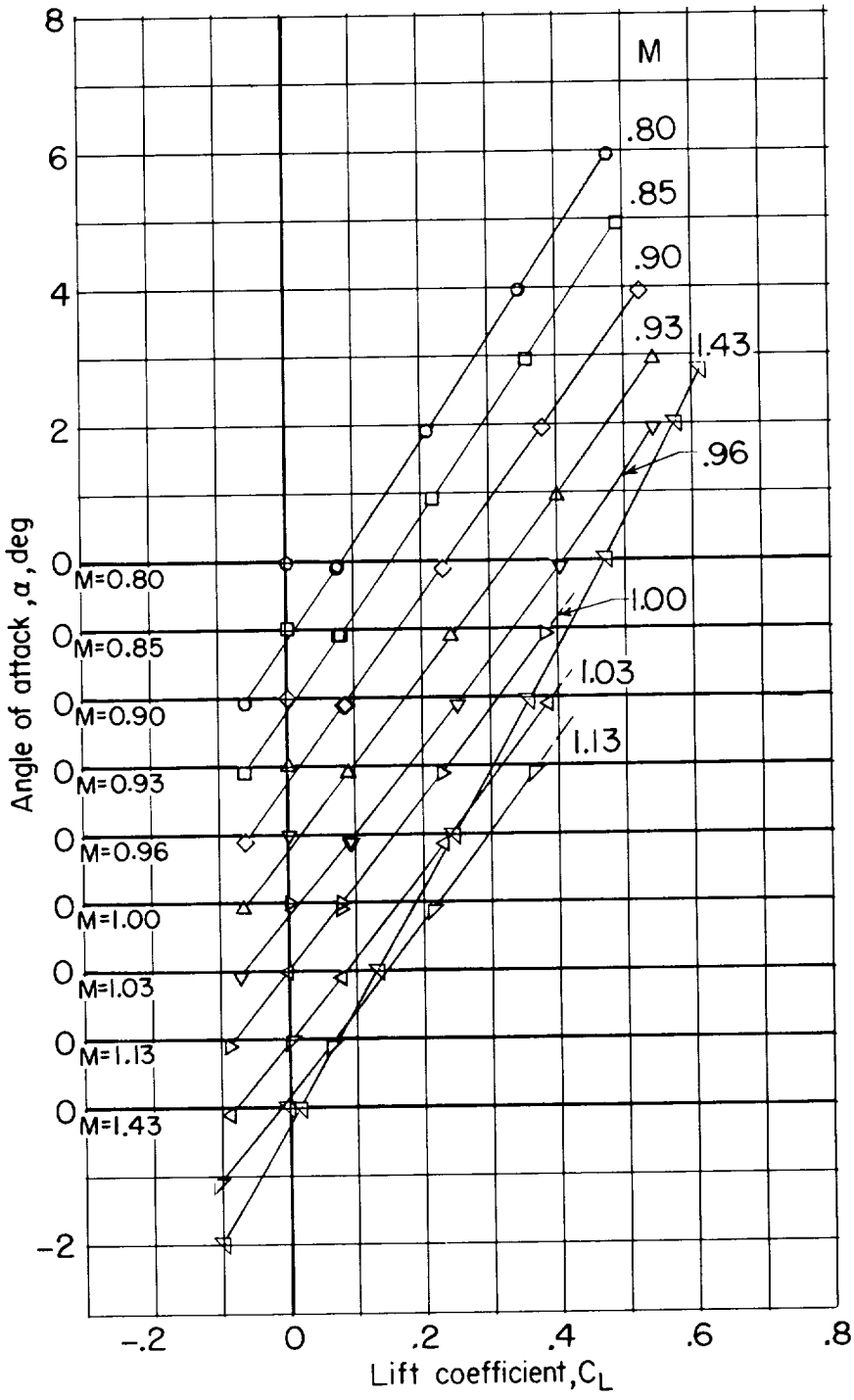

(c) α against C_L for M = 1.2 wing-body combination. $i_W = 0^\circ$. Dashed lines indicate extrapolation of data.

Figure 12.- Continued.

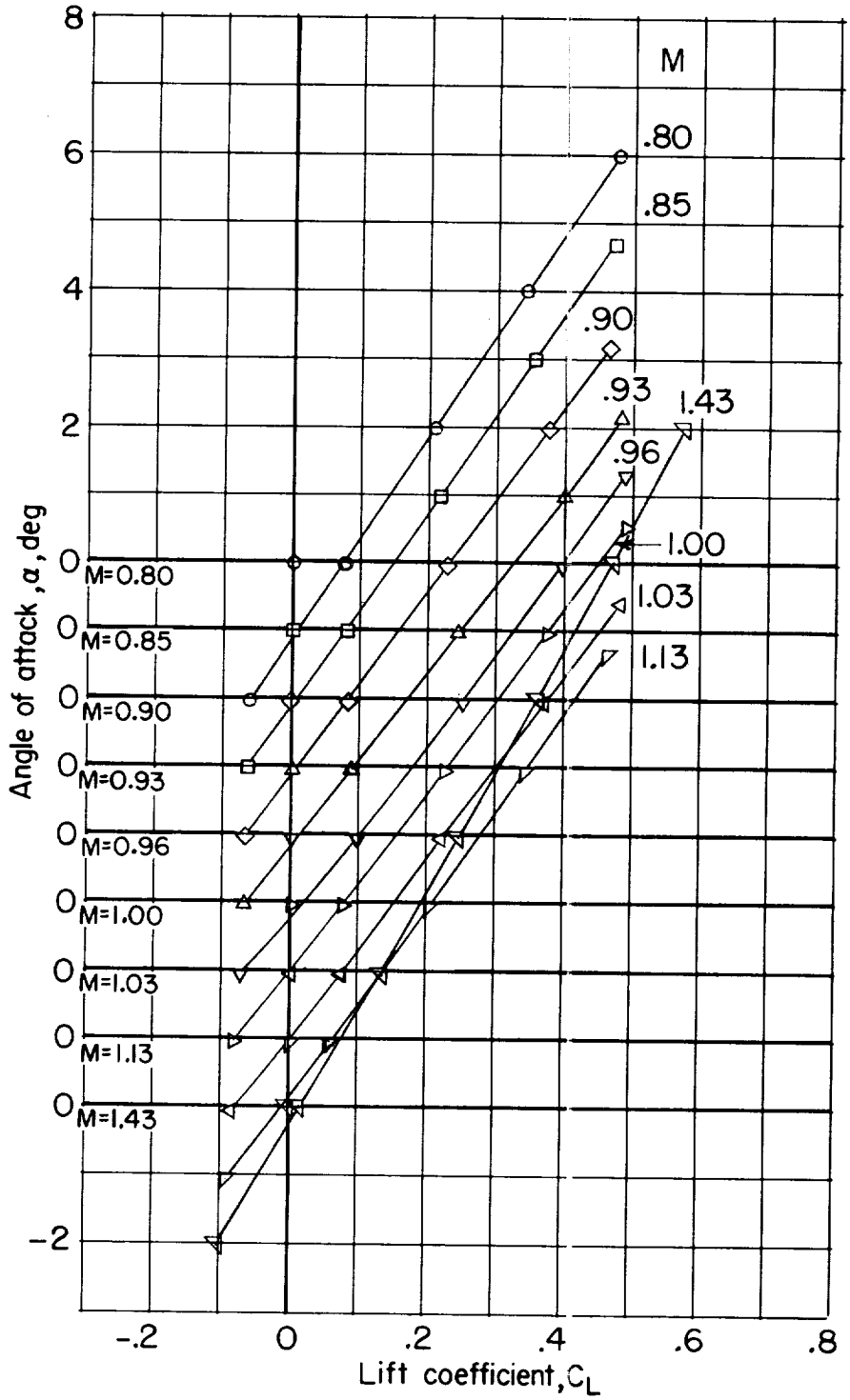

(d) α against C_L for M = 1.4 wing-body combination. $i_W = 0^o$.

Figure 12.- Continued.

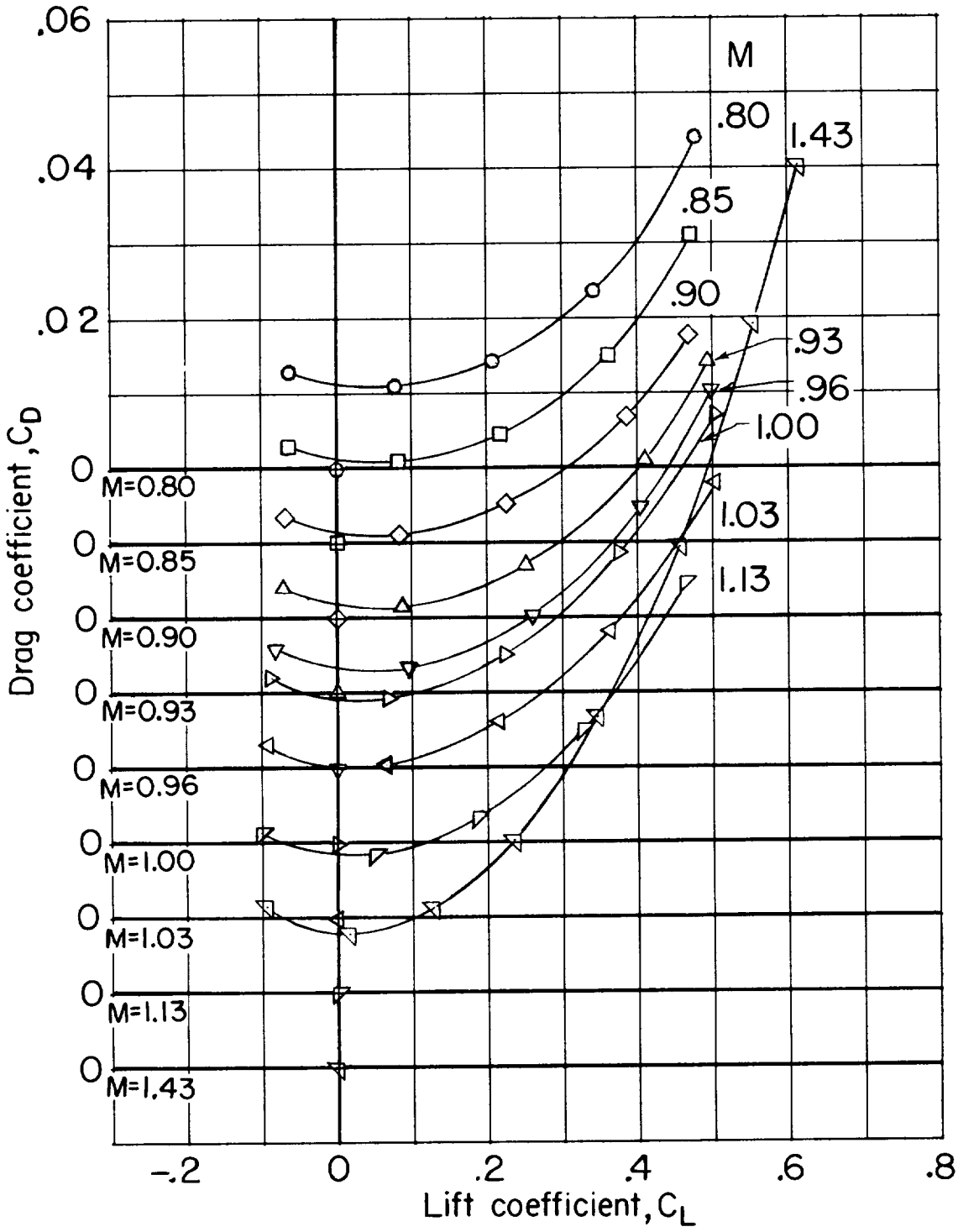

(e) C_D against C_L for basic wing-body combination. $i_W = 0^\circ$.

Figure 12.- Continued.

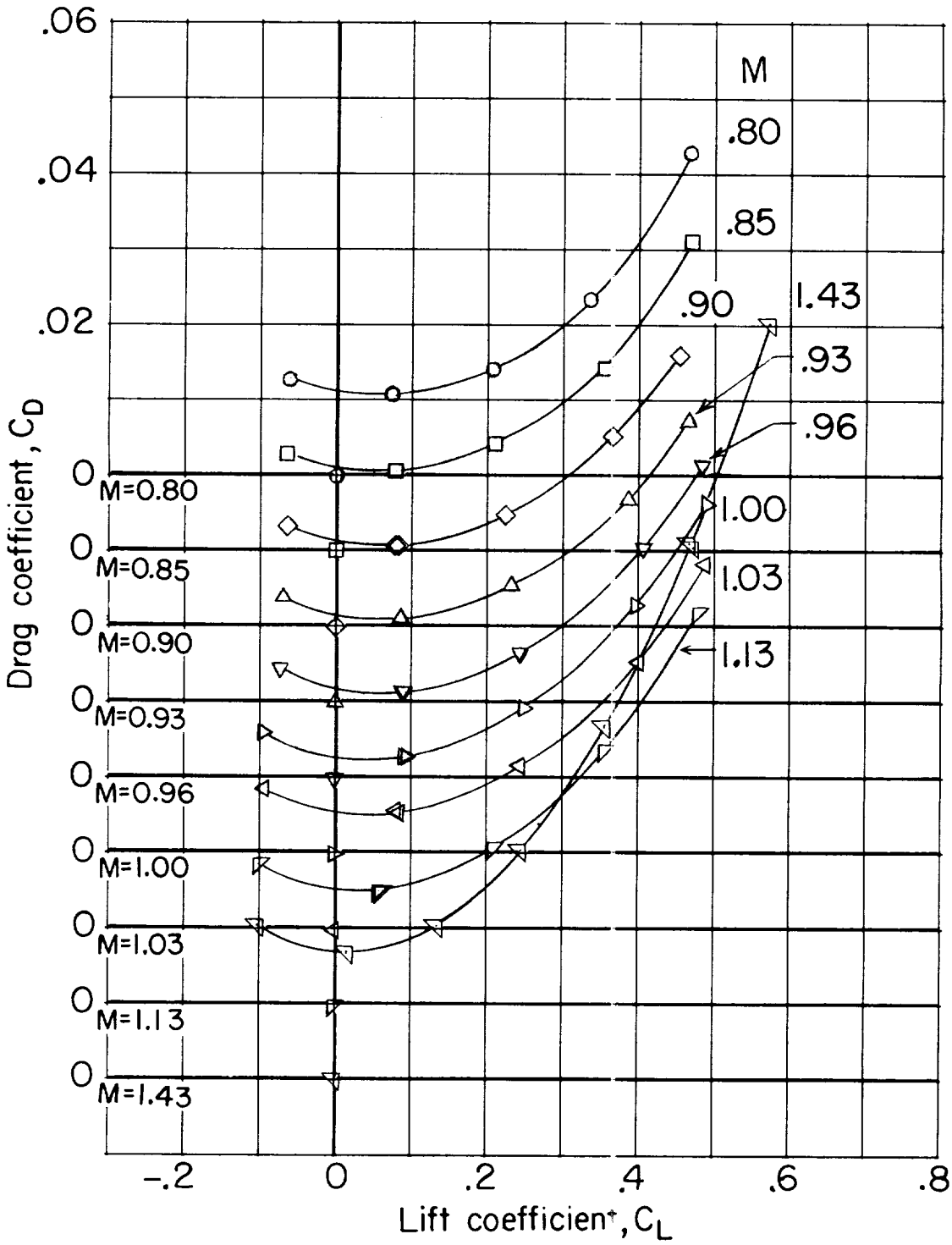

(f) C_D against C_L for M = 1.0 wing-body combination. $i_W = 0^\circ$.

Figure 12.- Continued.

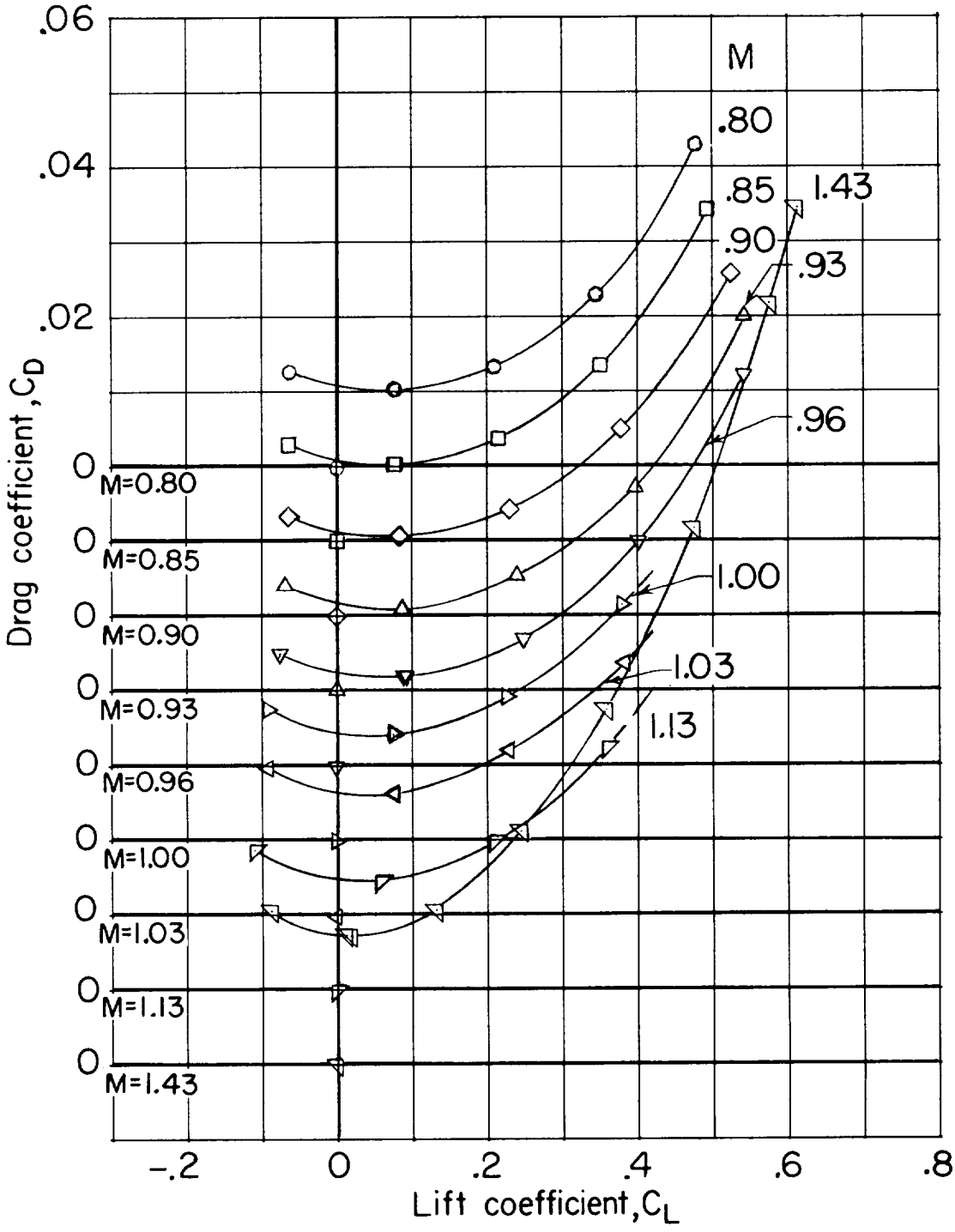

(g) C_D against C_L for M = 1.2 wing-body combination. $i_W = 0^\circ$. Dashed lines indicate extrapolation of data.

Figure 12.- Continued.

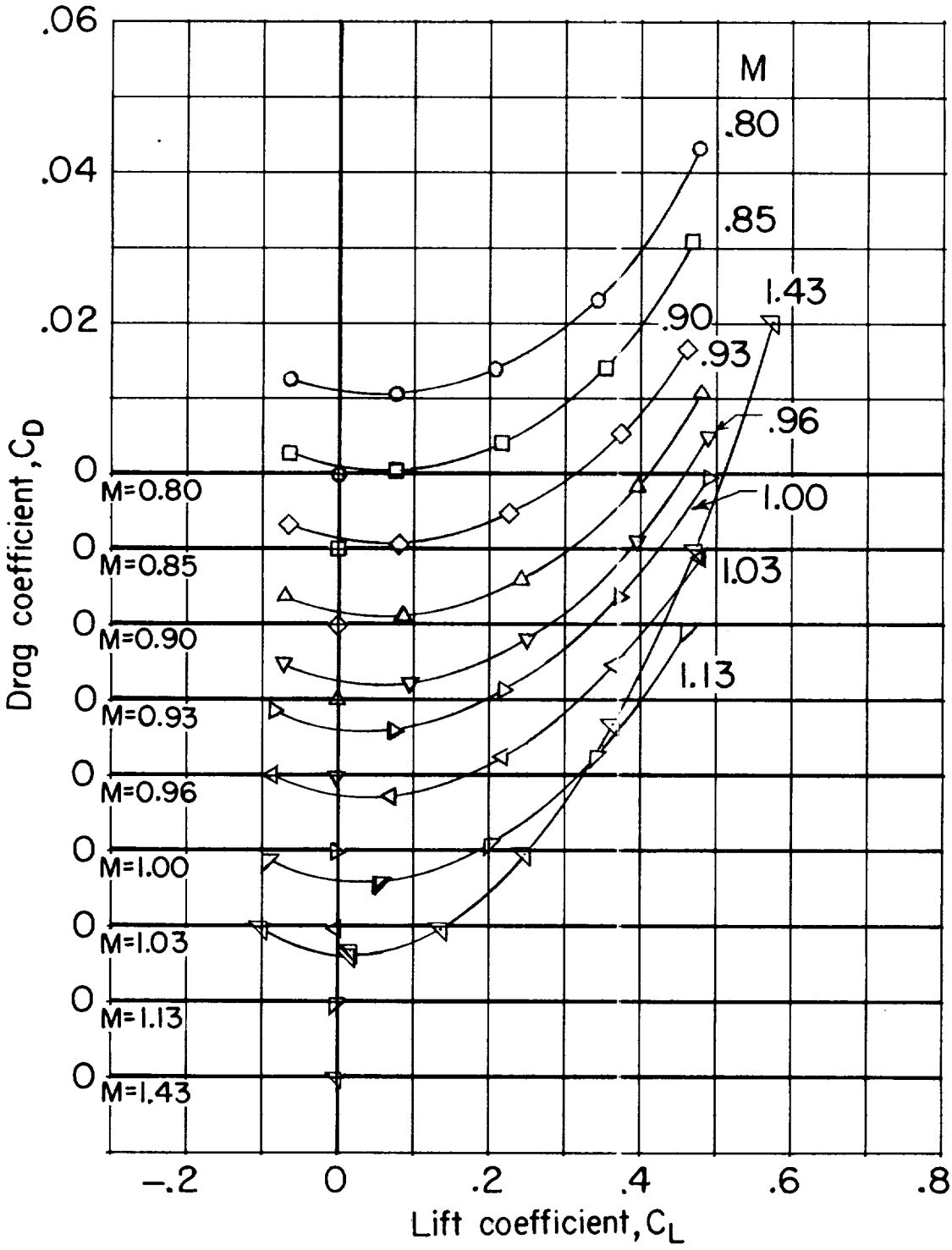

(h) C_D against C_L for M = 1.4 wing-body combination. $i_W = 0^\circ$.

Figure 12.- Continued.

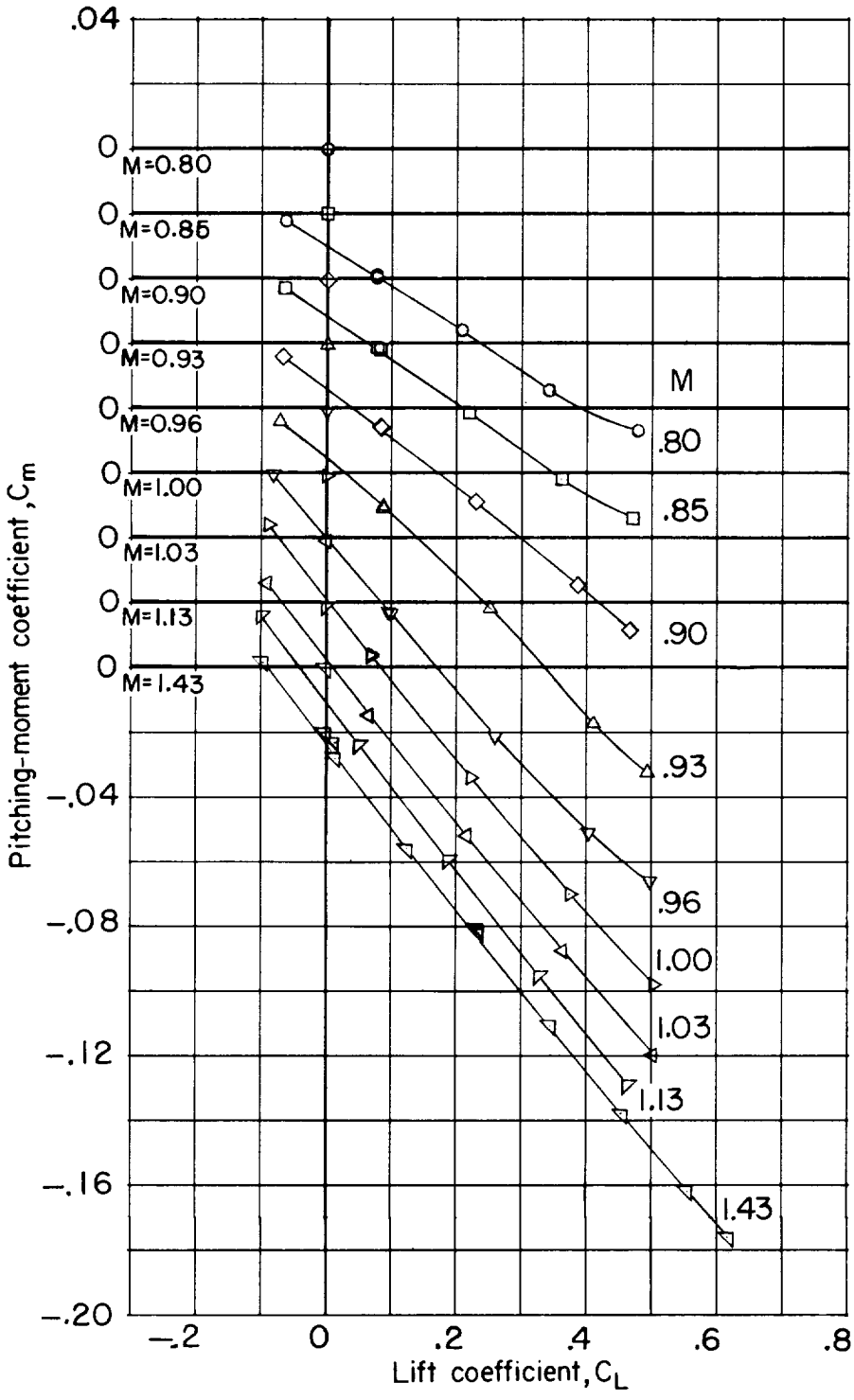

(i) C_m against C_L for basic wing-body combination. $i_W = 0^\circ$.

Figure 12.- Continued.

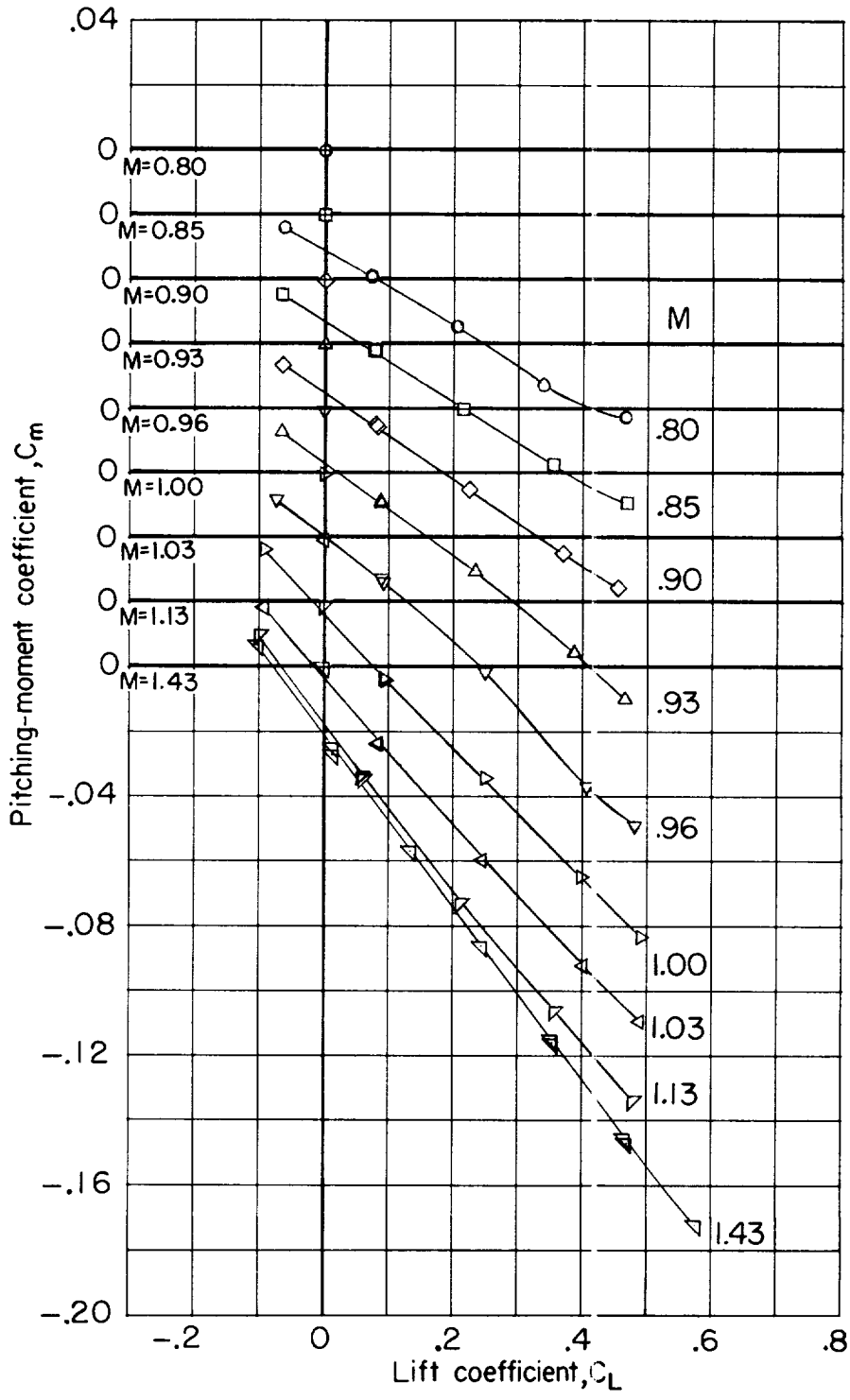

(j) C_m against C_L for M = 1.0 wing-body combination. $i_W = 0^o$.

Figure 12.- Continued.

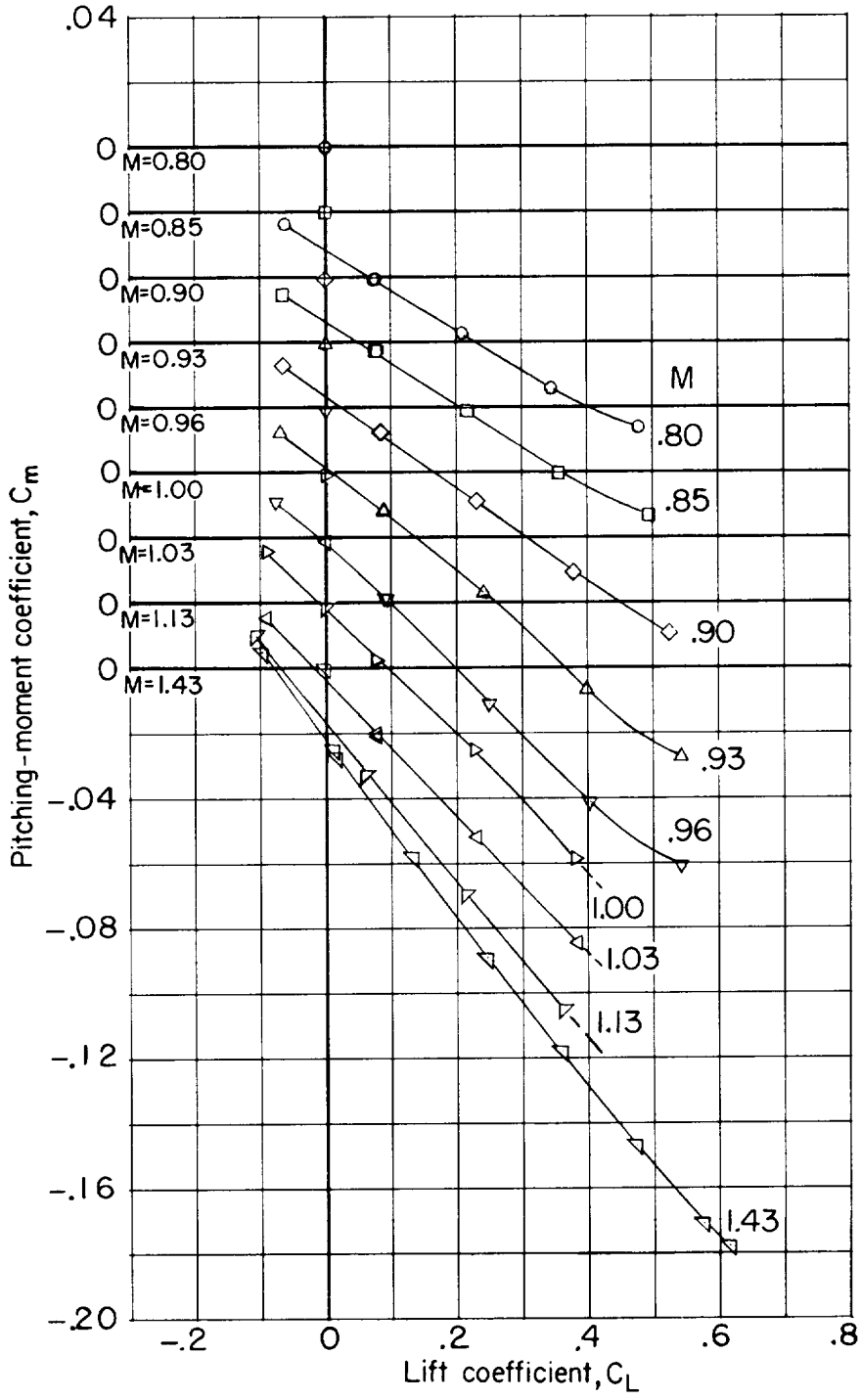

(k) C_m against C_L for M = 1.2 wing-body combination. $i_W = 0^o$. Dashed lines indicate extrapolation of data.

Figure 12.- Continued.

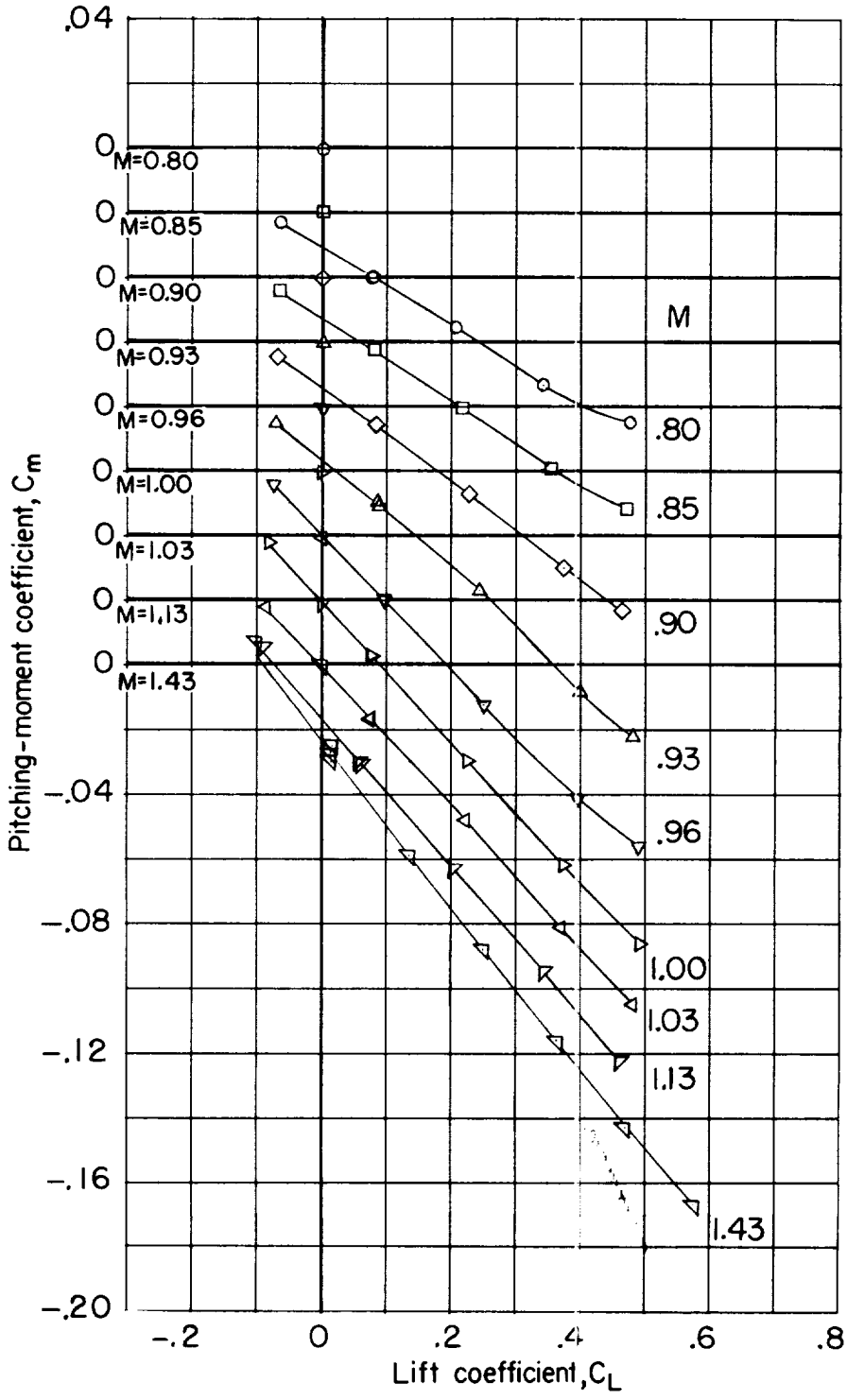

(l) C_m against C_L for M = 1.4 wing-body combination. $i_W = 0^o$.

Figure 12.- Concluded.

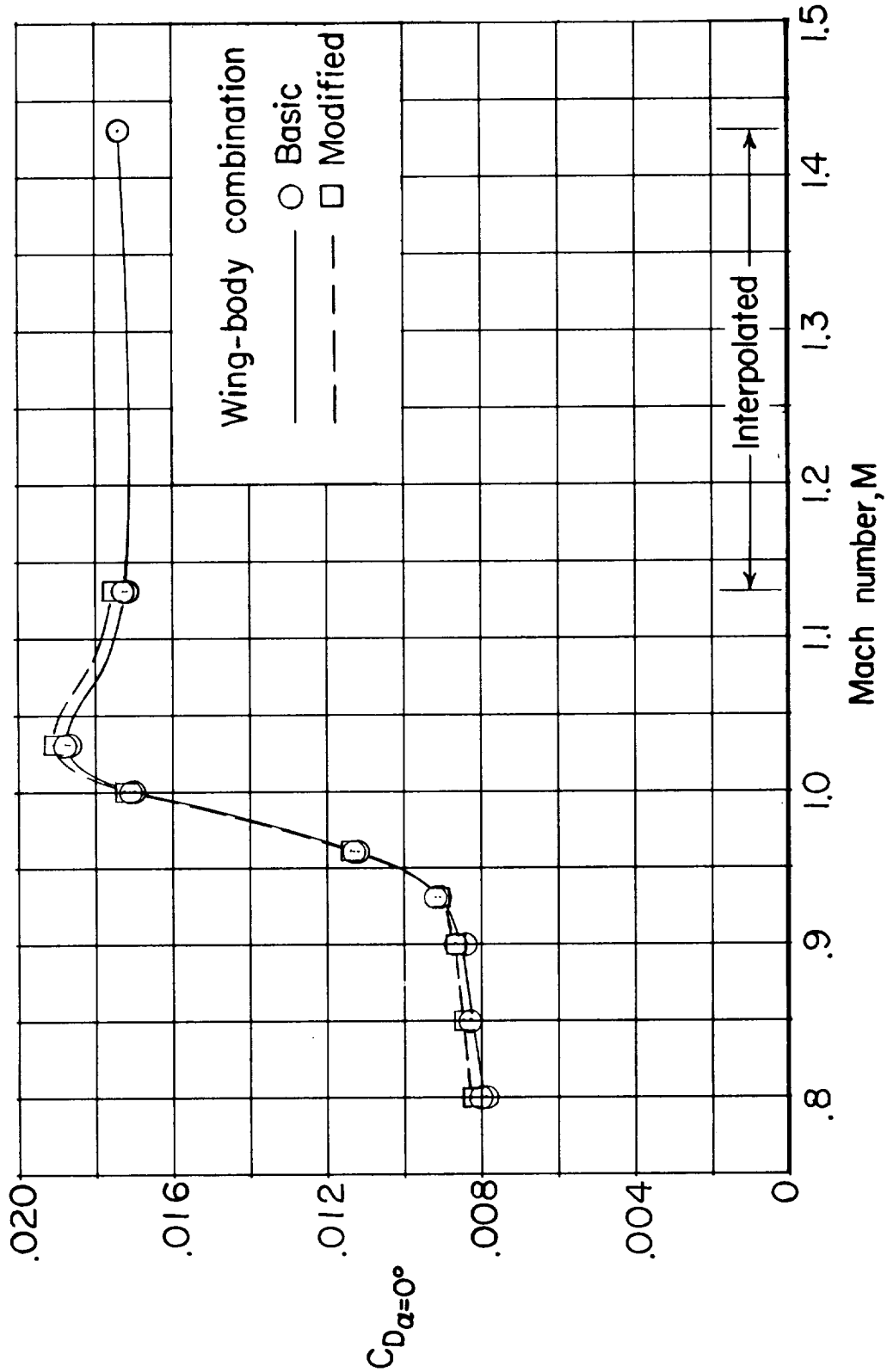

Figure 13.- Drag characteristics of 45° sweptback wing in combination with basic and modified bodies. $\alpha = 0°$.

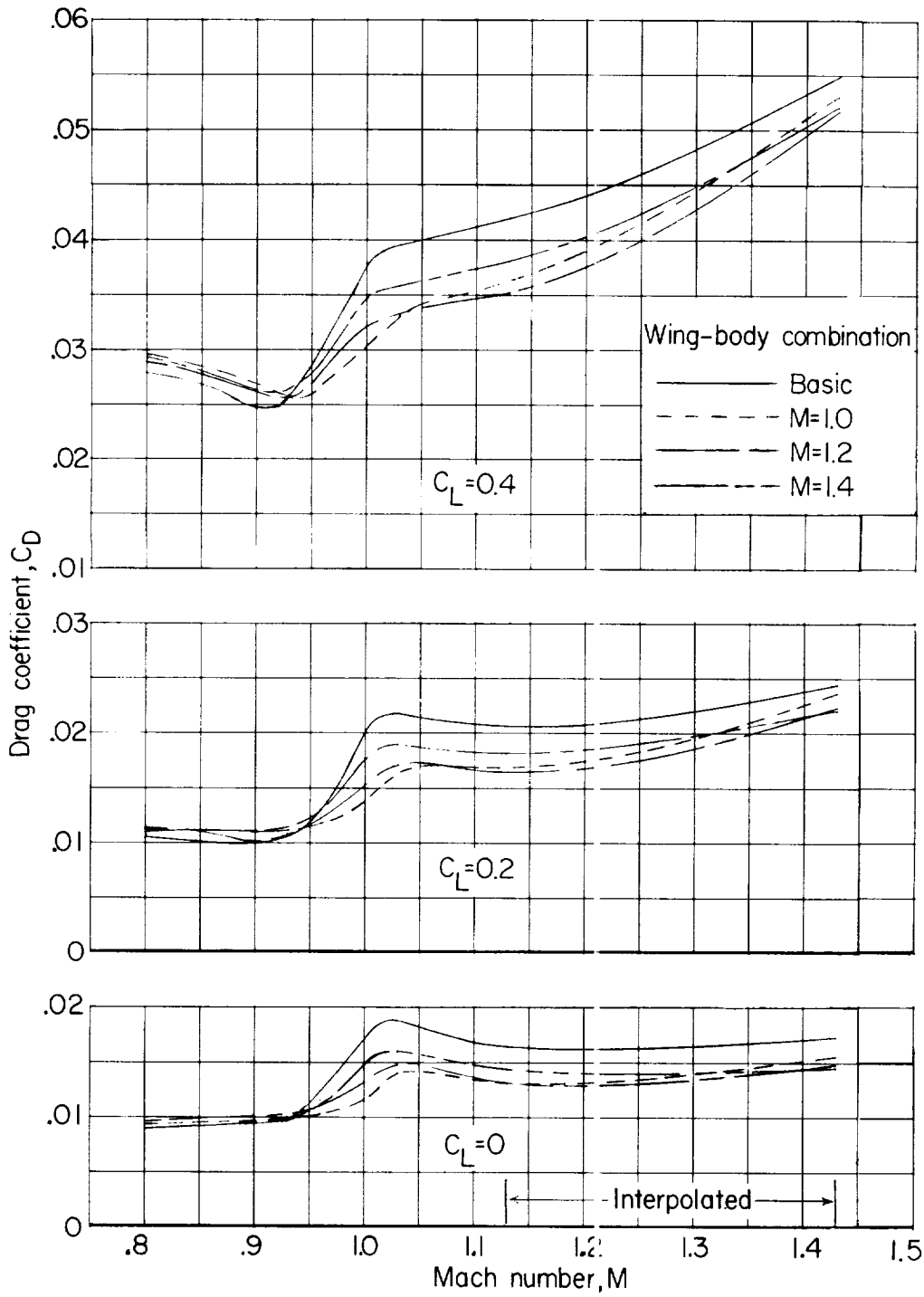

Figure 14.- Drag characteristics of 45° sweptback wing in combination with basic and indented bodies. C_L = 0, 0.2, and 0.4.

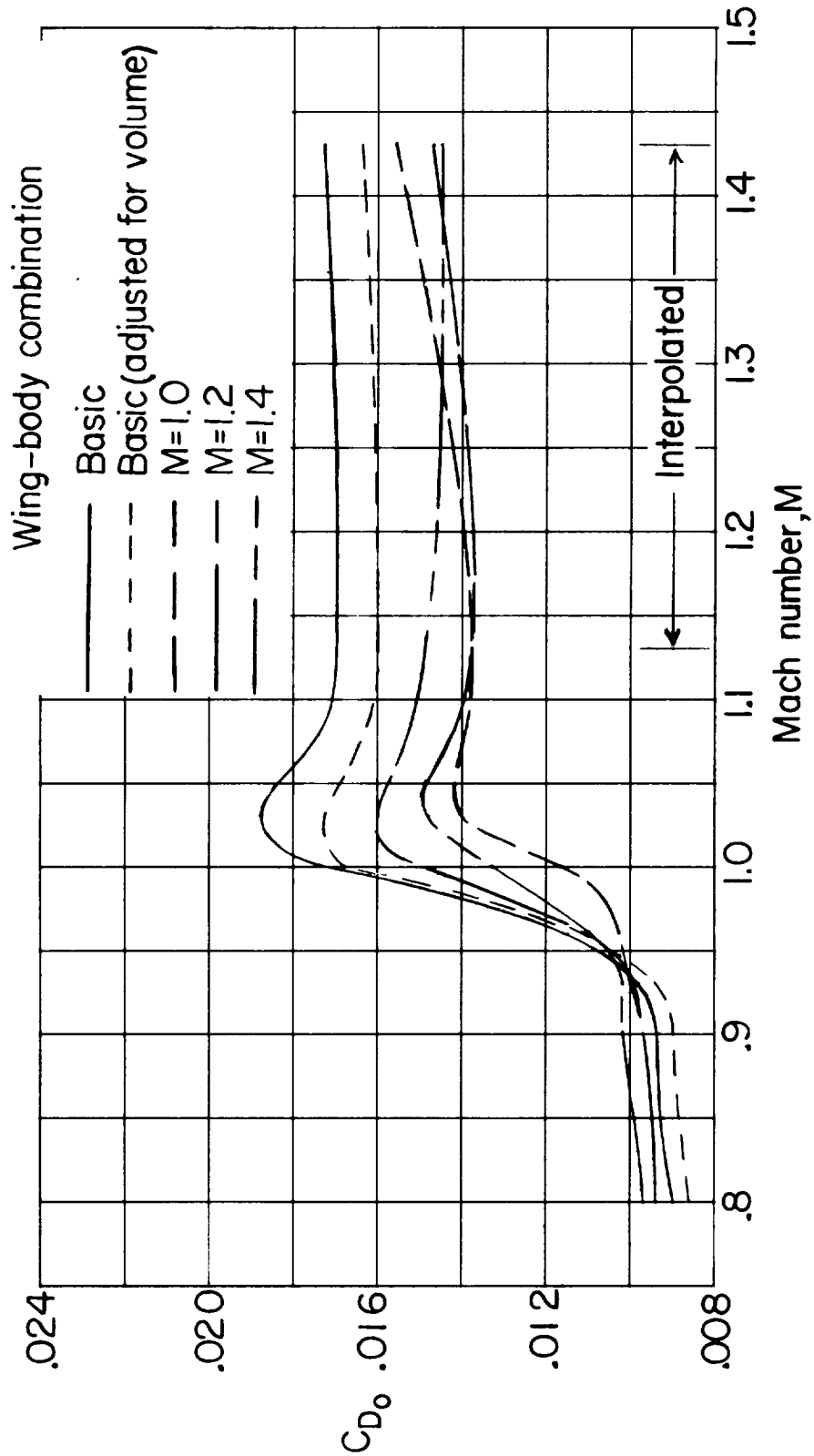

Figure 15.- Drag characteristics of 45° sweptback wing in combination with basic and indented bodies adjusted for tunnel boundary reflection interference. $C_L = 0$.

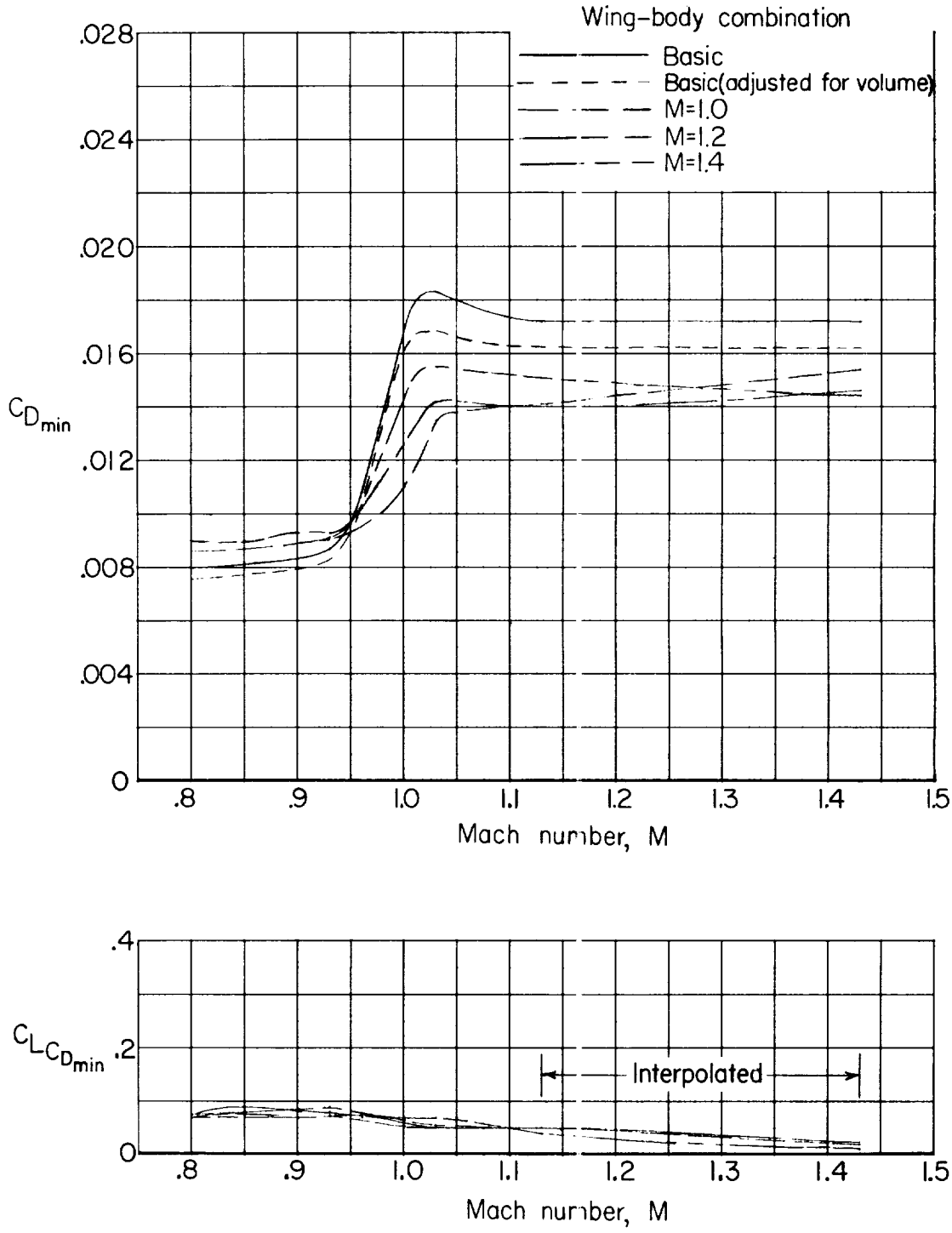

Figure 16.- Minimum-drag characteristics and lift coefficient for minimum drag of 45° sweptback wing in combination with basic and indented bodies.

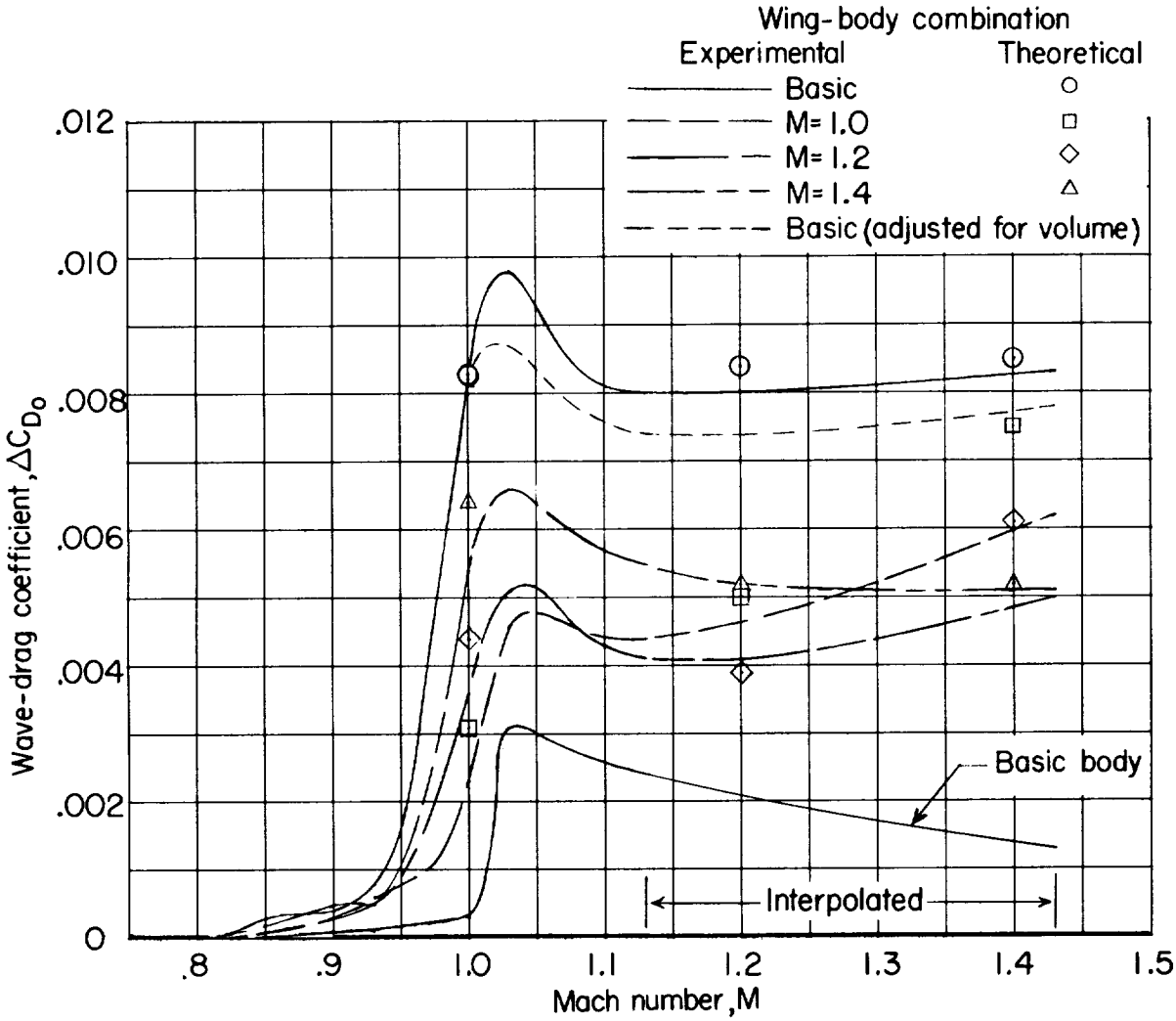

Figure 17.- Wave-drag characteristics of basic body and 45° sweptback wing in combination with basic and indented bodies. $C_L = 0$.

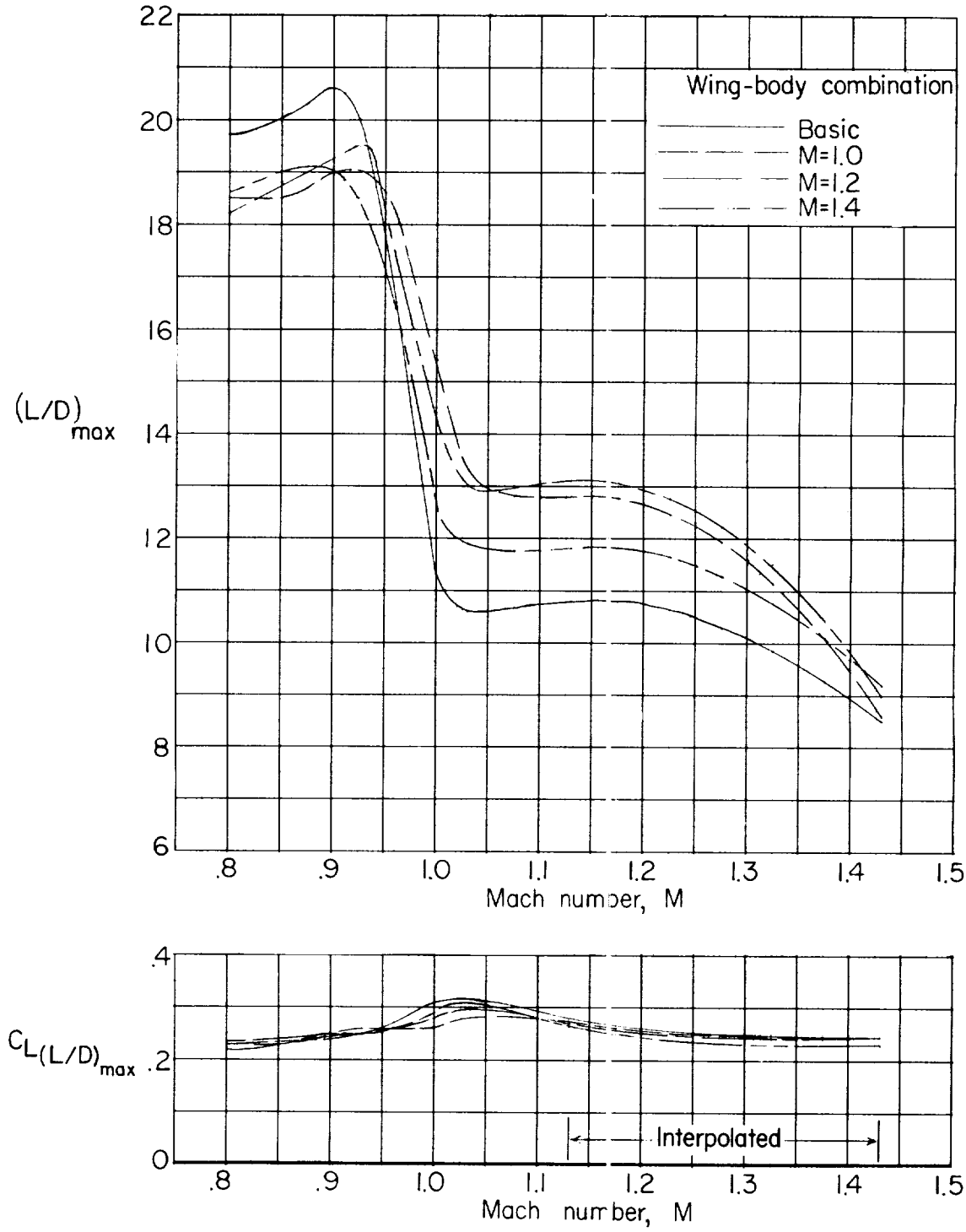

Figure 18.- Maximum lift-drag ratio characteristics and lift coefficient for maximum lift-drag ratio for 45° sweptback wing in combination with basic and indented bodies.

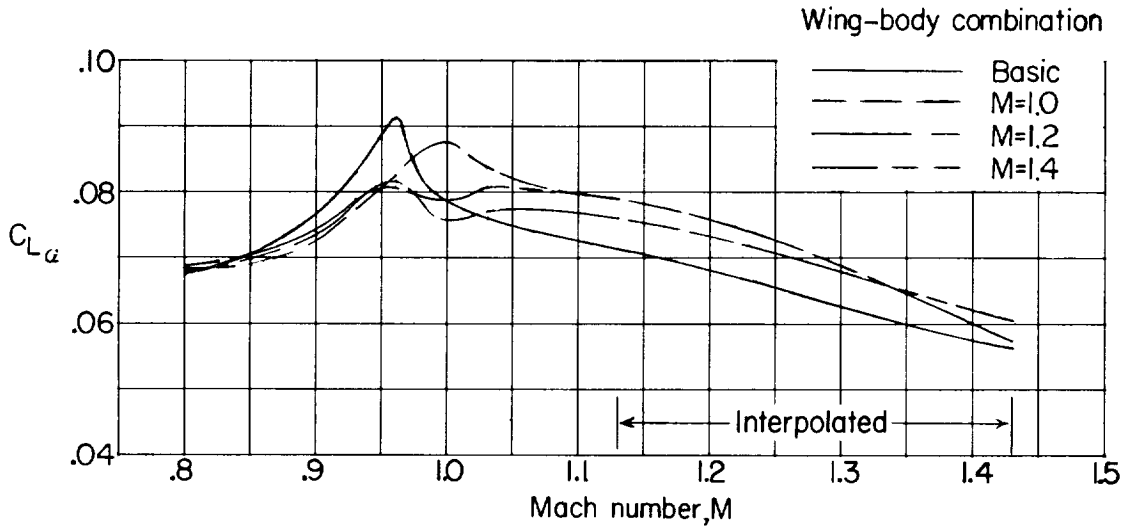

Figure 19.- Average lift-curve-slope characteristics of the 45° swept-back wing in combination with the basic and indented bodies. C_L = -0.05 to 0.3.

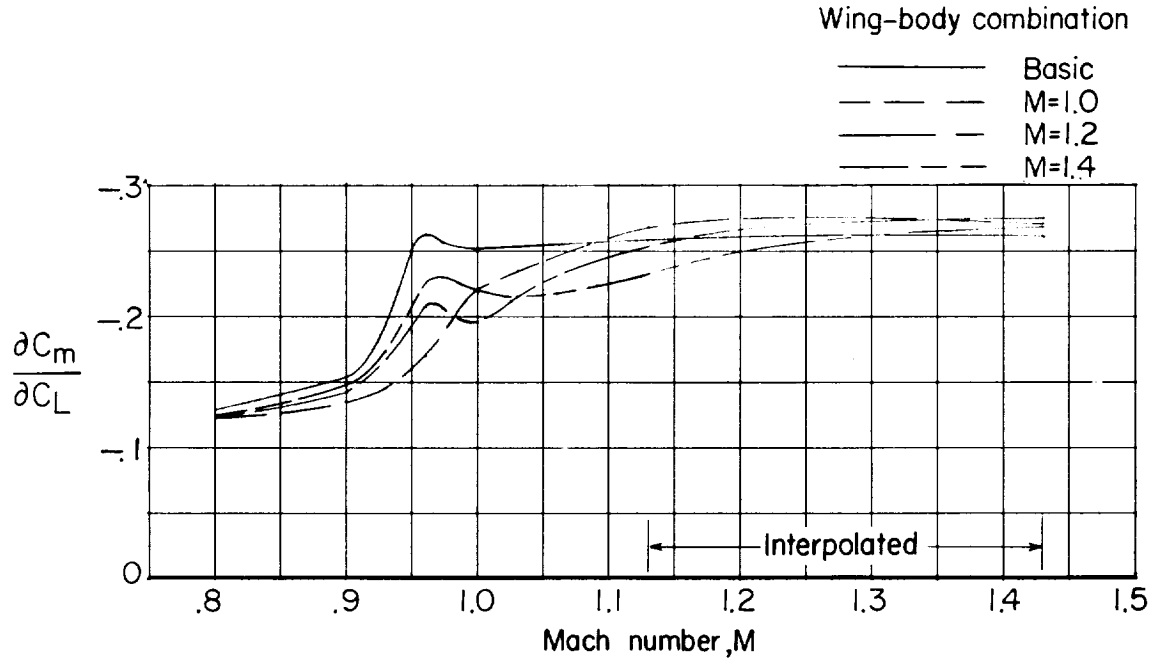

Figure 20.- Stability characteristics of the 45° sweptback wing in combination with the basic and indented bodies. C_L = -0.05 to 0.3.

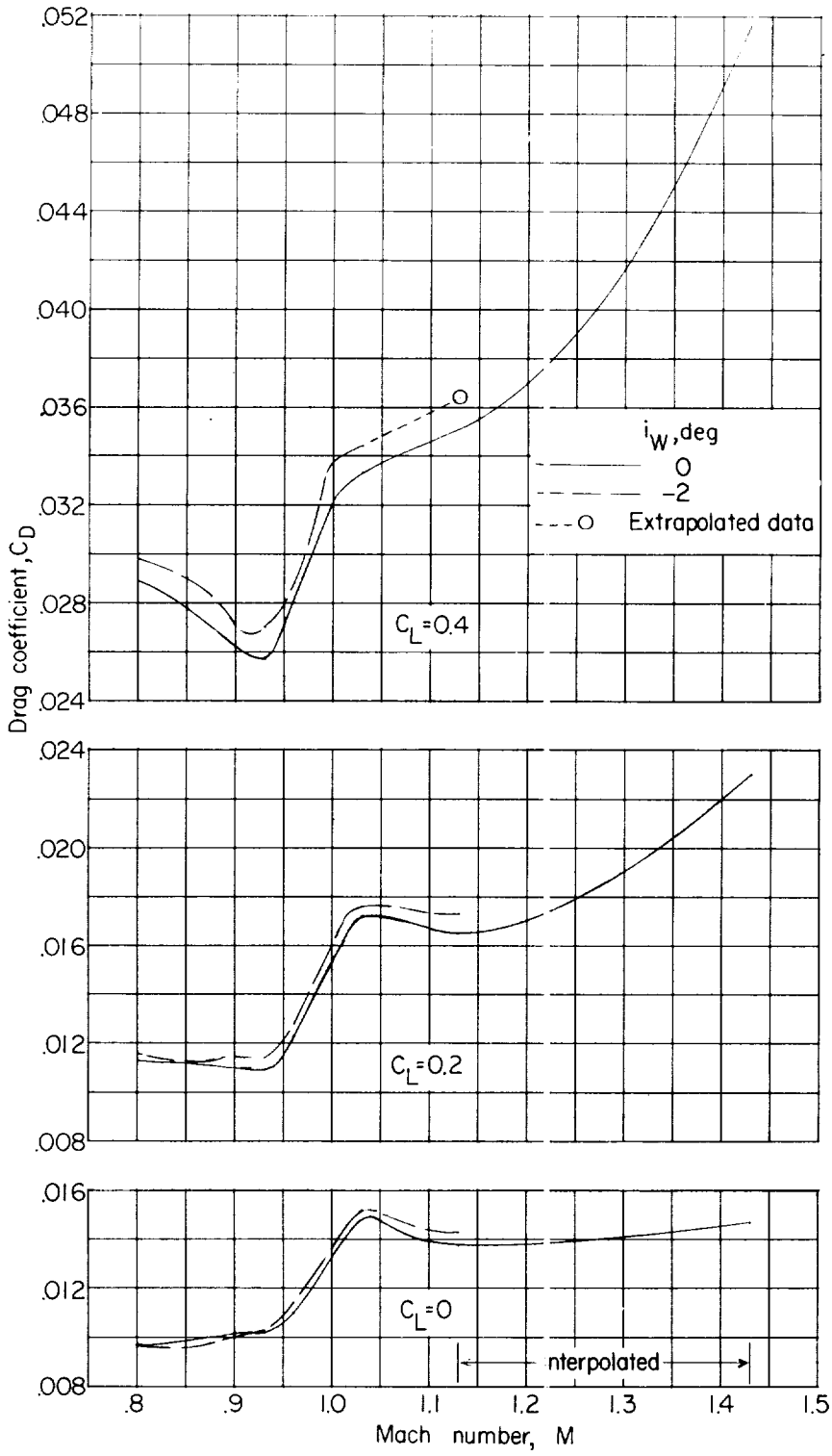

Figure 21.- Drag characteristics of 45° sweptback wing in combination with M = 1.2 body. i_W = 0° and -2°; C_L = 0, 0.2, and 0.4.

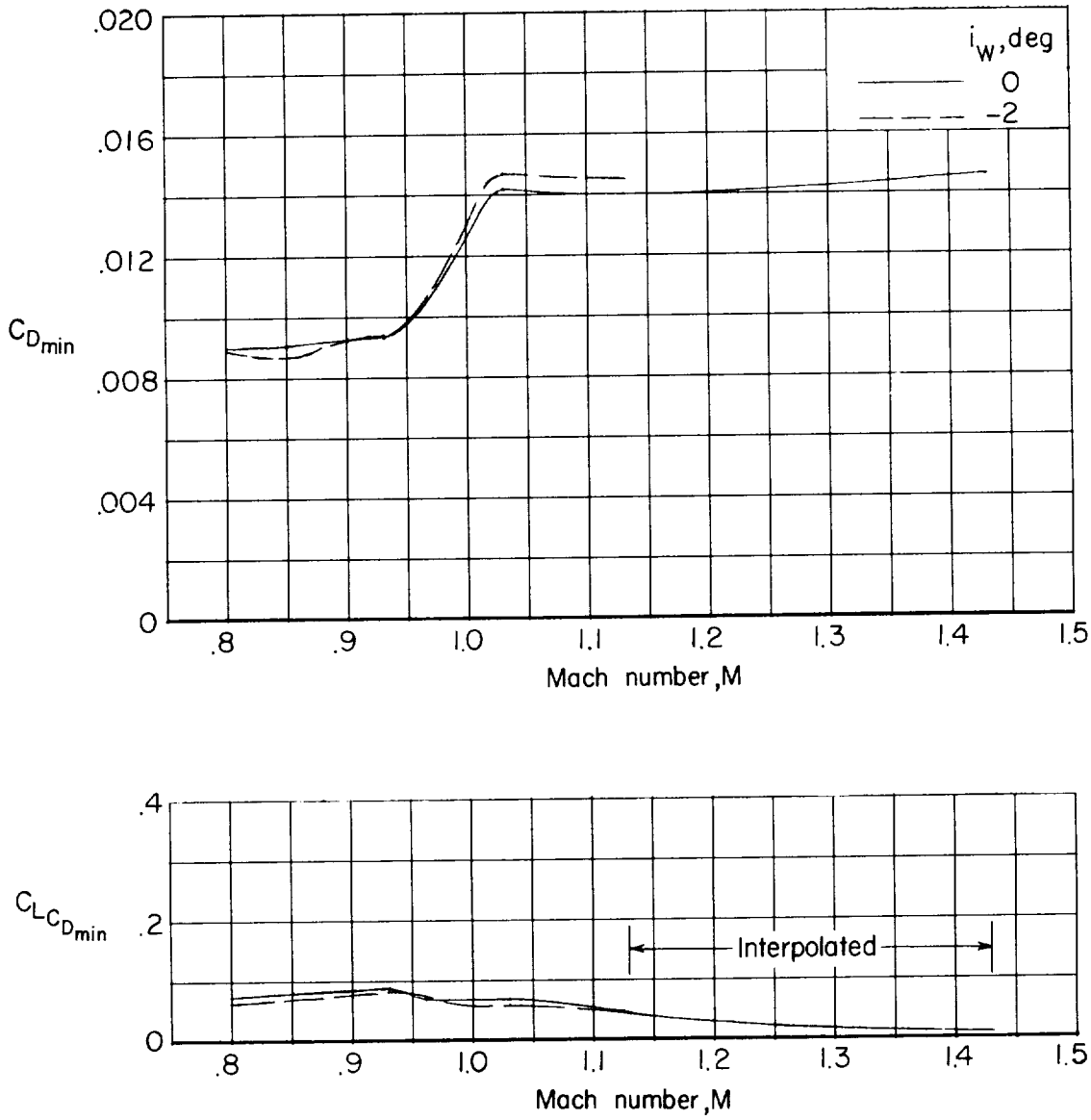

Figure 22.- Minimum drag characteristics and lift coefficient for minimum drag of 45° sweptback wing in combination with M = 1.2 body. i_W = 0° and -2°.

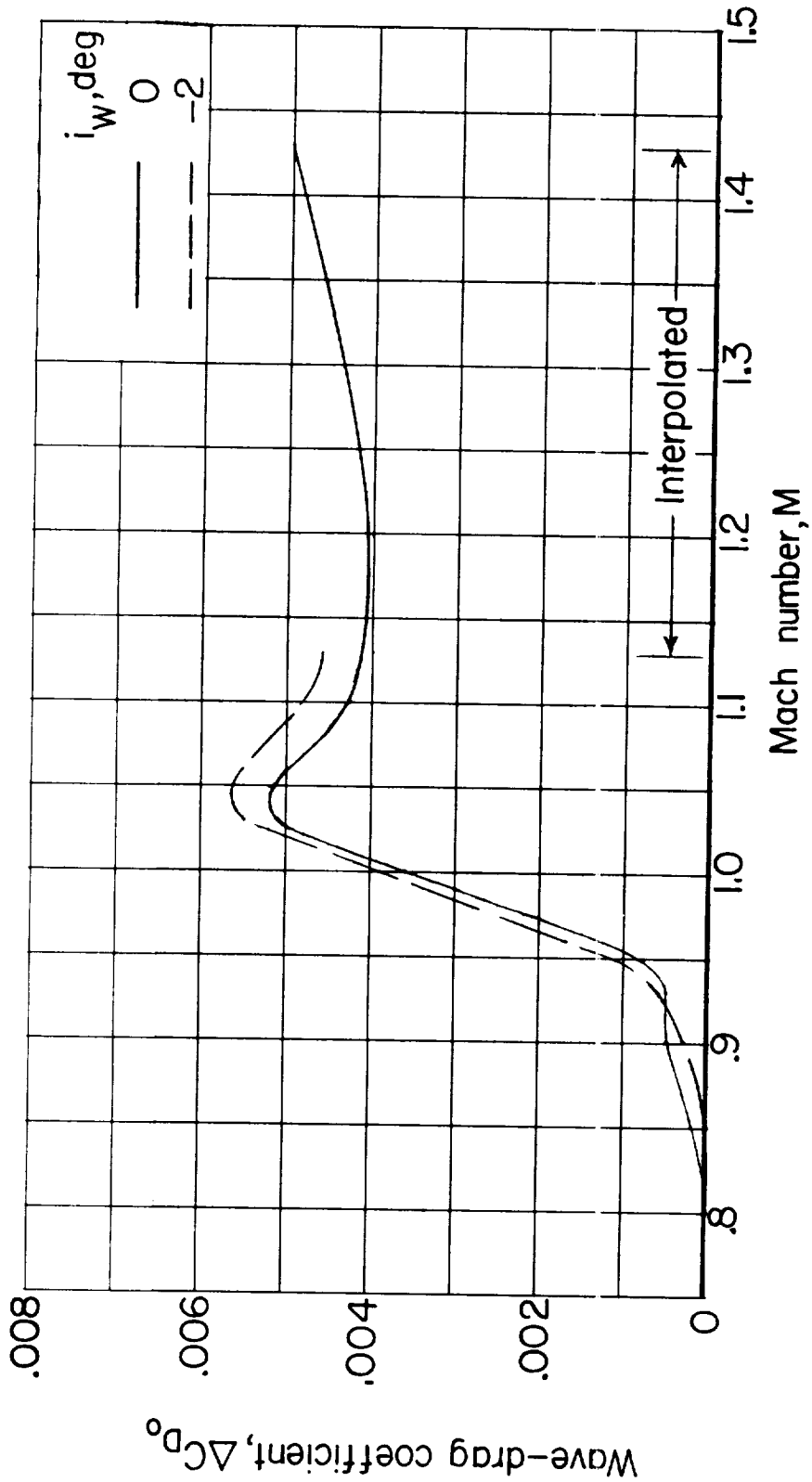

Figure 23.- Wave-drag characteristics of 45° sweptback wing in combination with M = 1.2 body. $i_W = 0^\circ$ and -2°; $C_L = 0$.

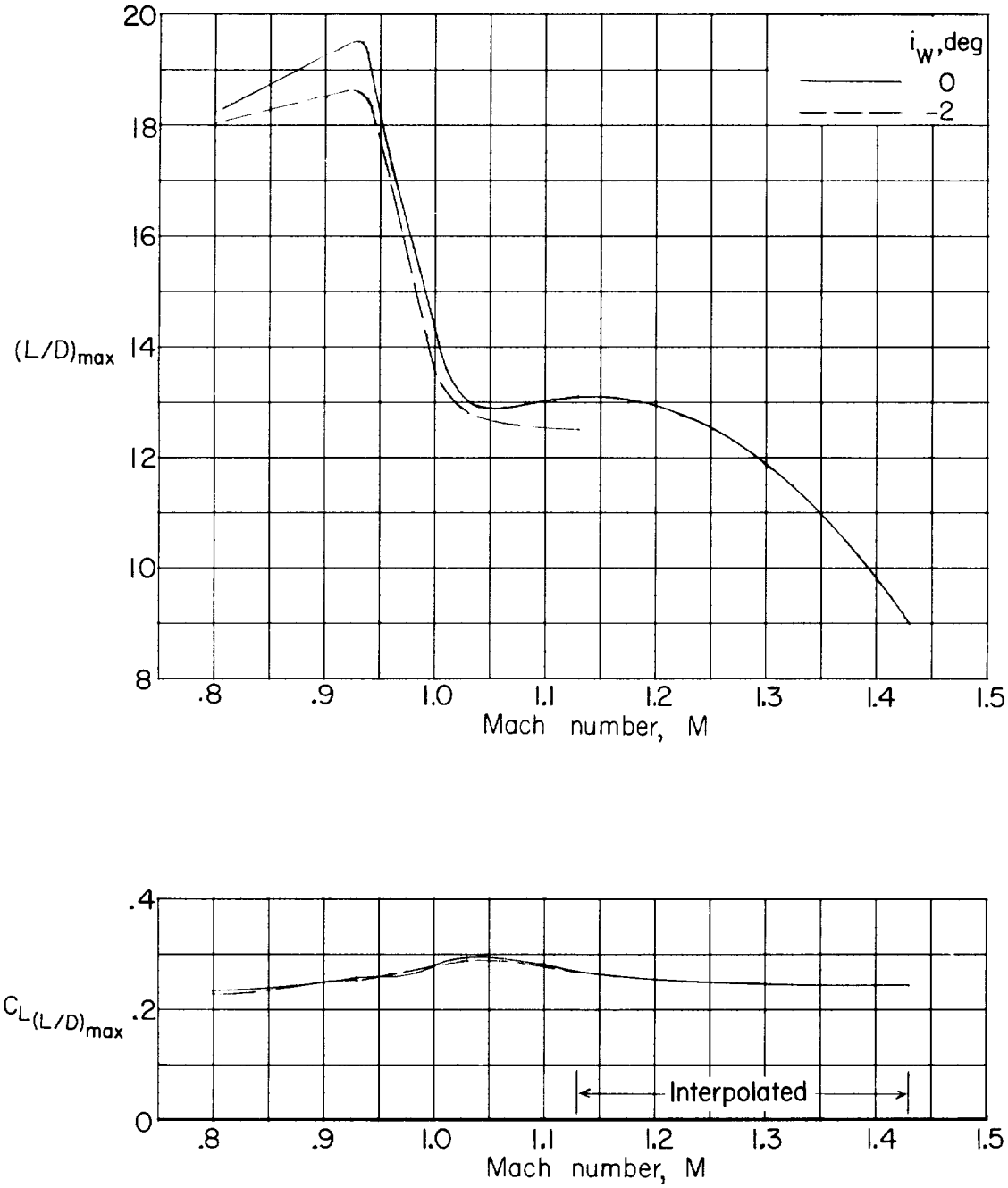

Figure 24.- Maximum lift-drag ratio characteristics and lift coefficient for maximum lift-drag ratio for 45° sweptback wing in combination with M = 1.2 body. i_W = 0° and -2°.

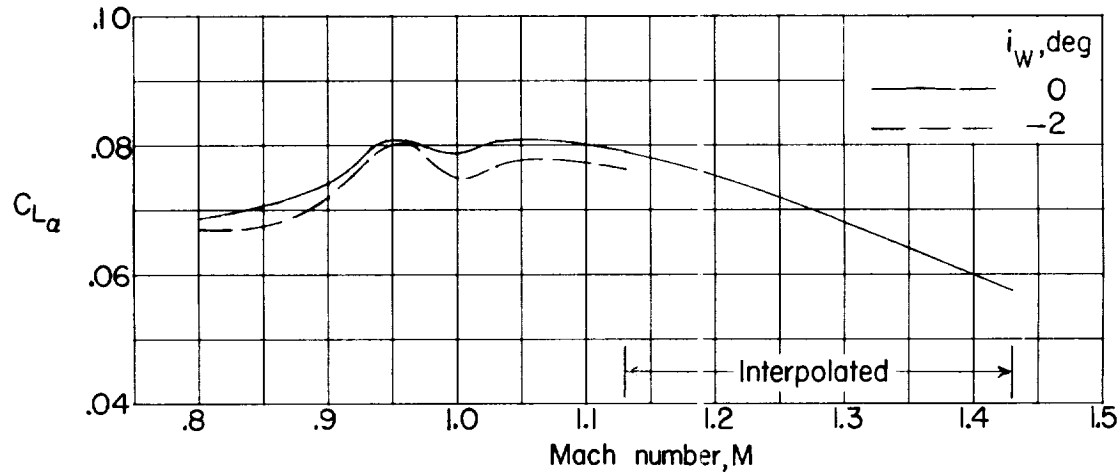

Figure 25.- Average lift-curve-slope characteristics of the 45° sweptback wing in combination with the M = 1.2 body. i_W = 0° and -2°; C_L = -0.05 to 0.3.

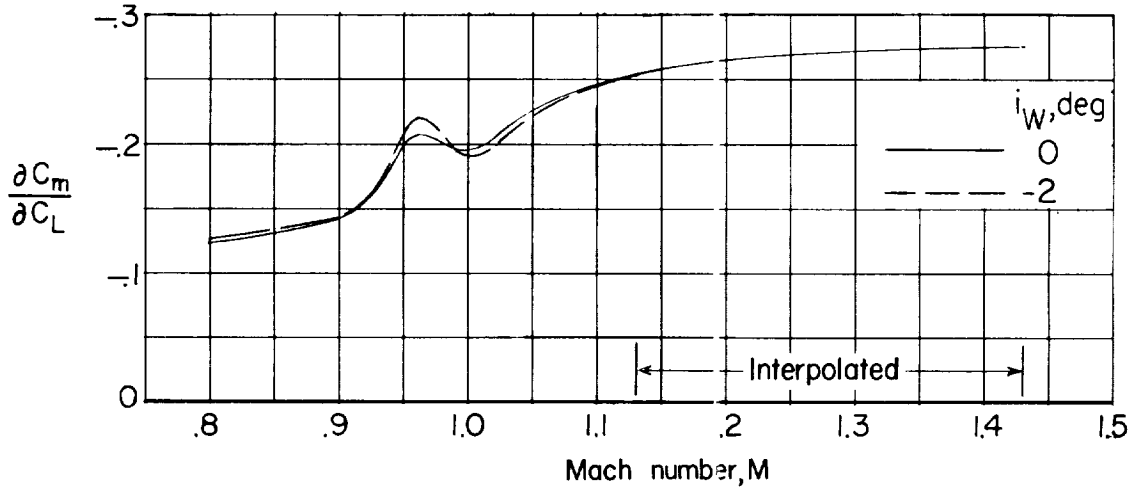

Figure 26.- Stability characteristics of the 45° sweptback wing in combination with the M = 1.2 body. i_W = 0° and -2°; C_L = -0.05 to 0.3.

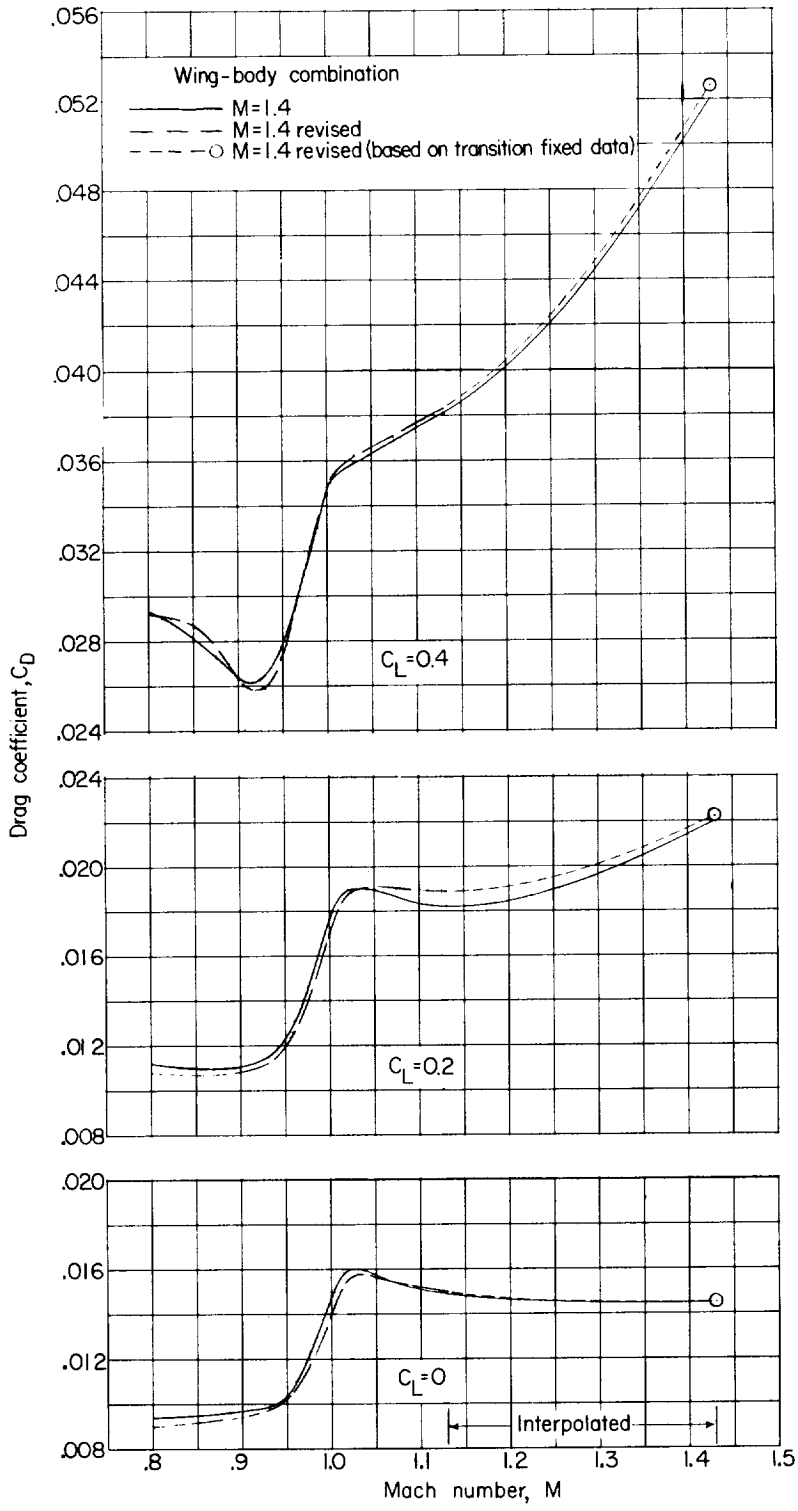

Figure 27.- Drag characteristics of 45° sweptback wing in combination with M = 1.4 and M = 1.4 revised bodies. C_L = 0, 0.2, and 0.4.

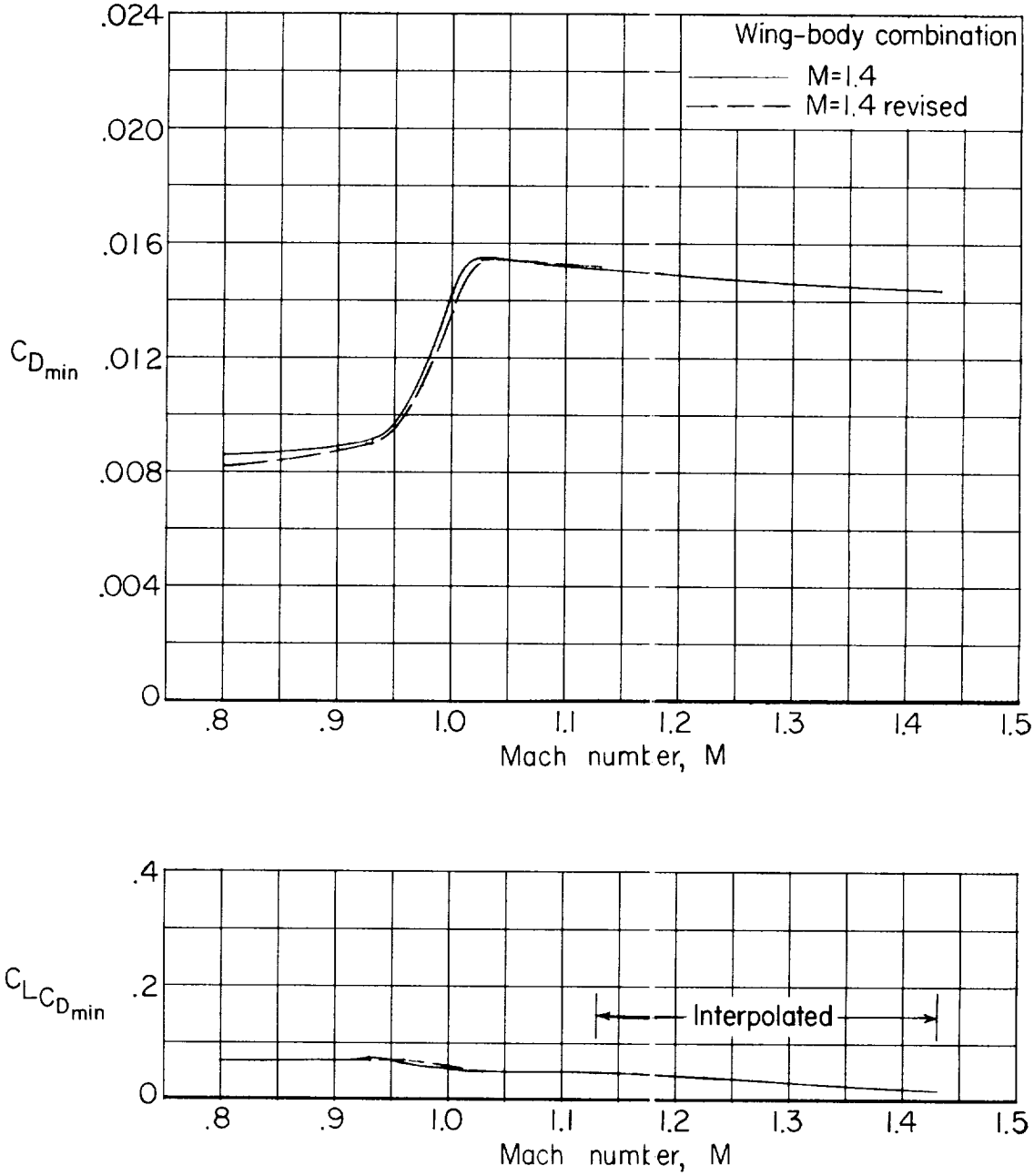

Figure 28.- Minimum drag characteristics and lift coefficient for minimum drag of 45° sweptback wing in combination with M = 1.4 and M = 1.4 revised bodies.

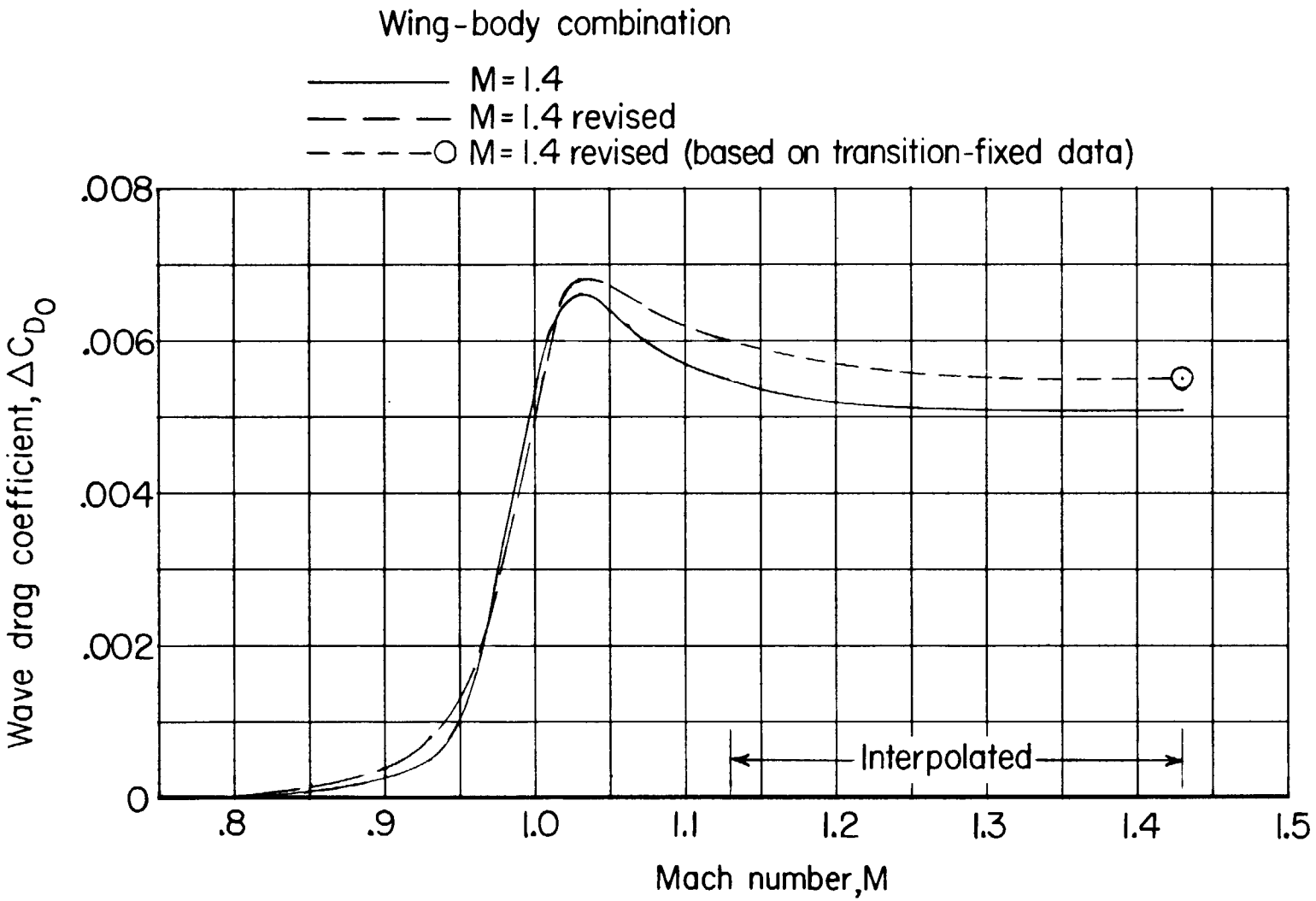

Figure 29.- Wave drag characteristics of 45° sweptback wing in combination with M = 1.4 and M = 1.4 revised bodies. C_L = 0.

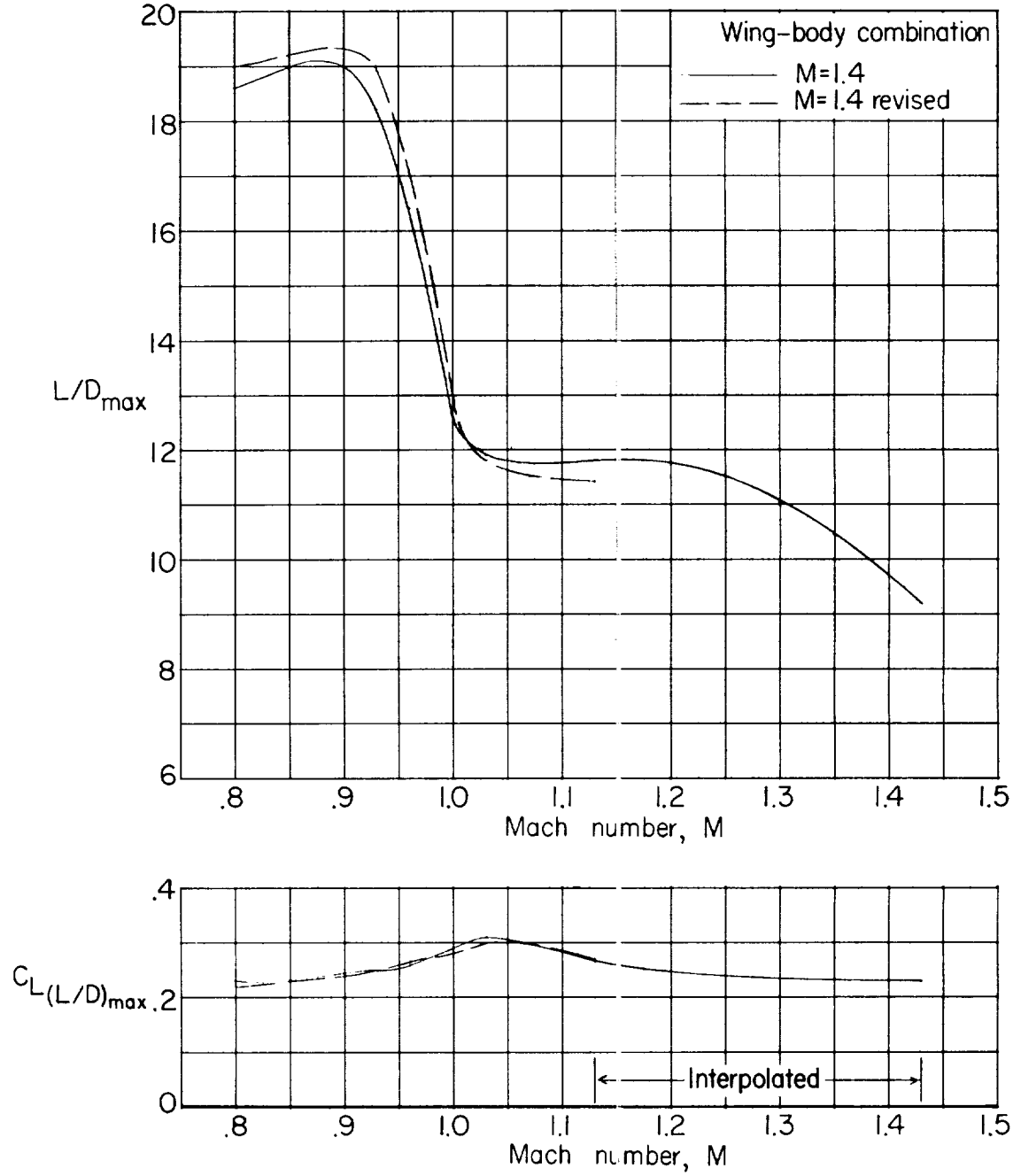

Figure 30.- Maximum lift-drag ratio characteristics and lift coefficient for maximum lift-drag ratio for 45° sweptback wing in combination with M = 1.4 and M = 1.4 revised bodies.

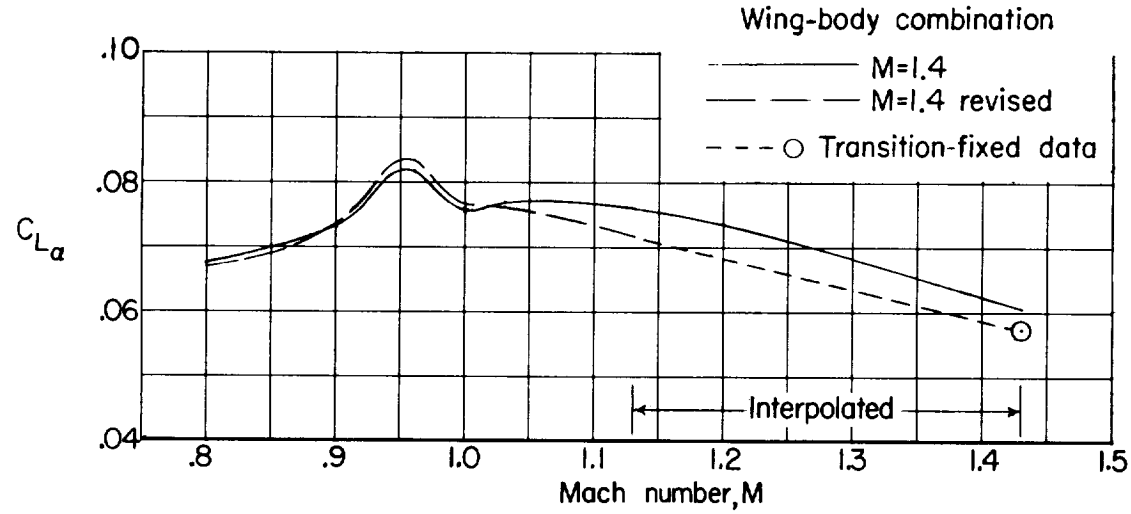

Figure 31.- Average lift-curve-slope characteristics of the 45° sweptback wing in combination with the M = 1.4 and M = 1.4 revised bodies. C_L = -0.05 to 0.3.

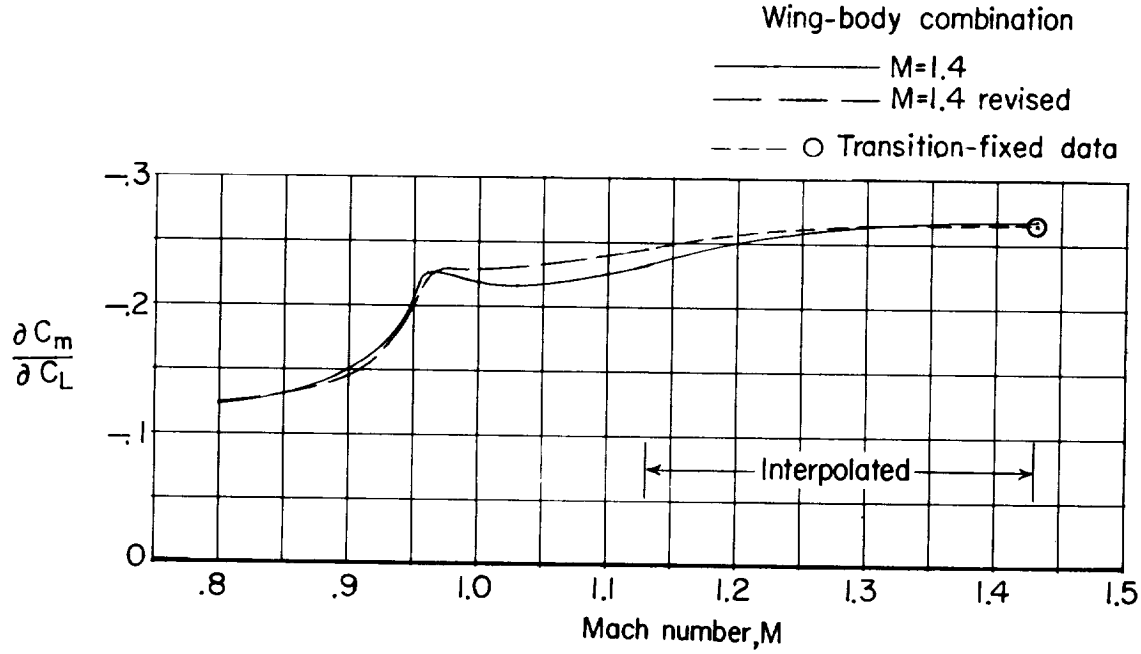

Figure 32.- Stability characteristics of the 45° sweptback wing in combination with M = 1.4 and M = 1.4 revised bodies. C_L = -0.05 to 0.3.

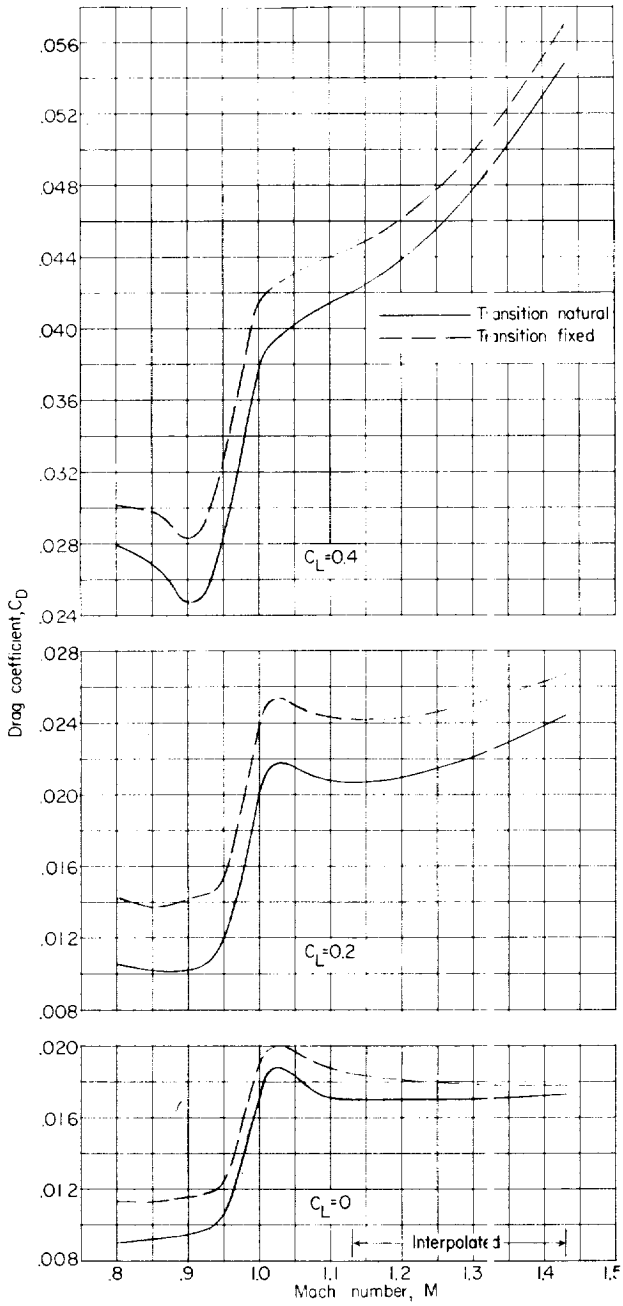

(a) Basic wing-body combination.

Figure 33.- Drag characteristics of 45° sweptback wing in combination with basic and indented bodies with transition natural and fixed on wing and bodies. C_L = 0, 0.2, and 0.4.

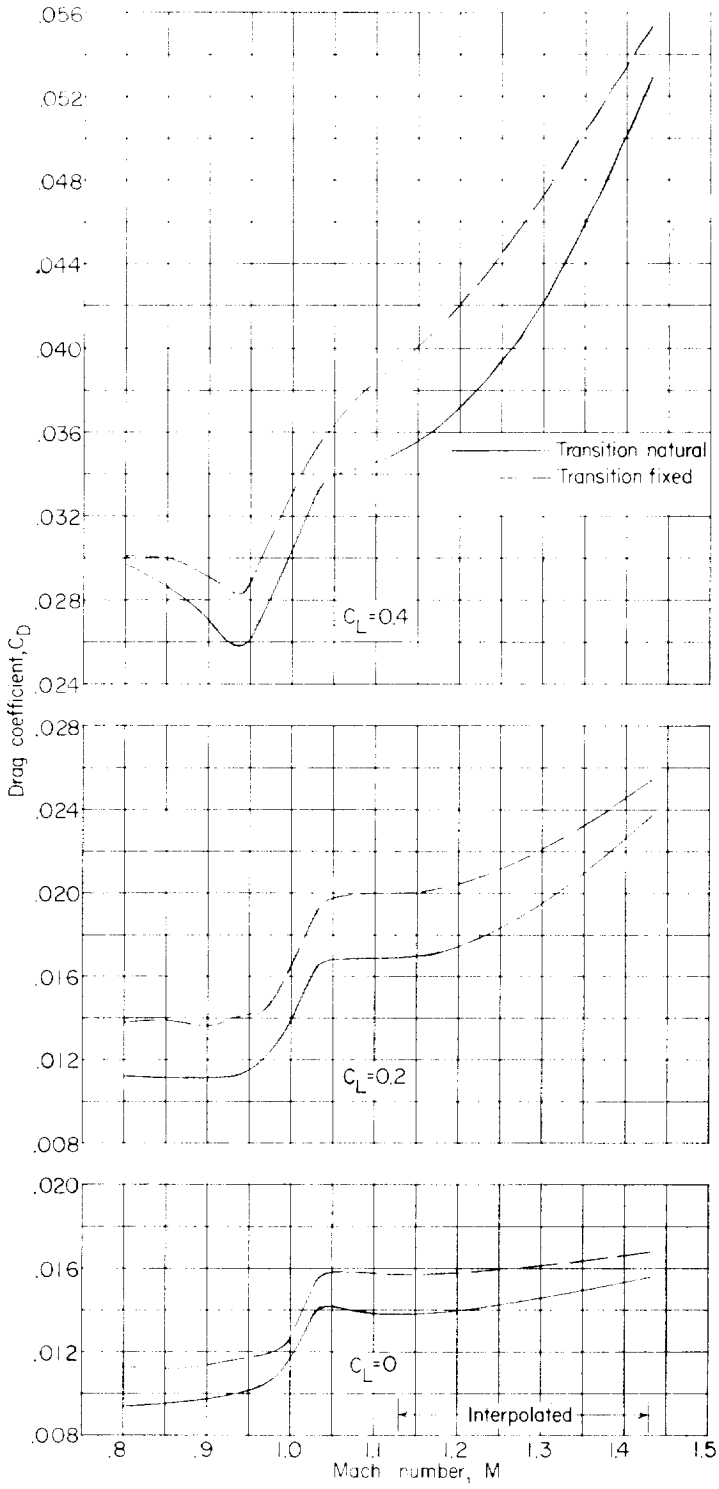

(b) M = 1.0 wing-body combination.

Figure 33.- Continued.

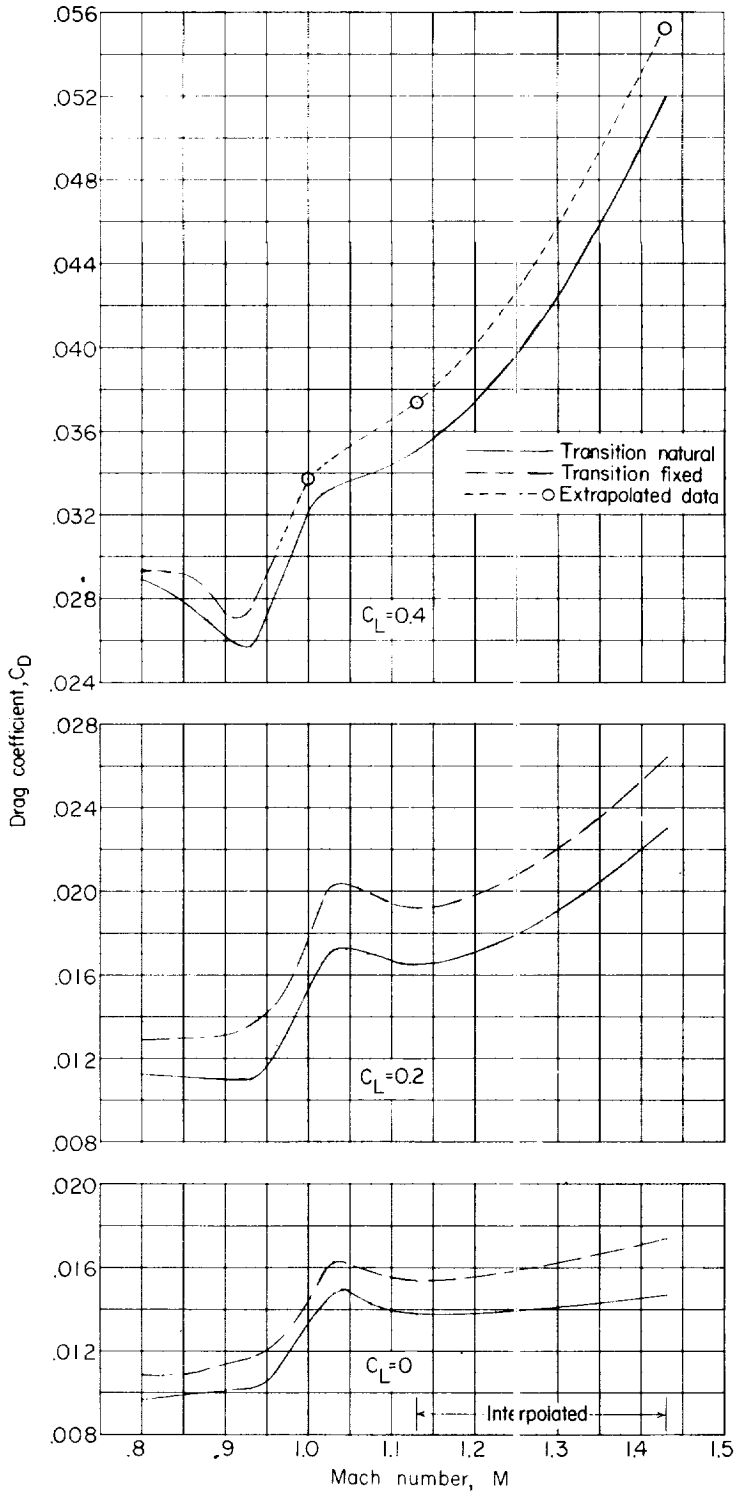

(c) M = 1.2 wing-body combination.

Figure 33.- Continued.

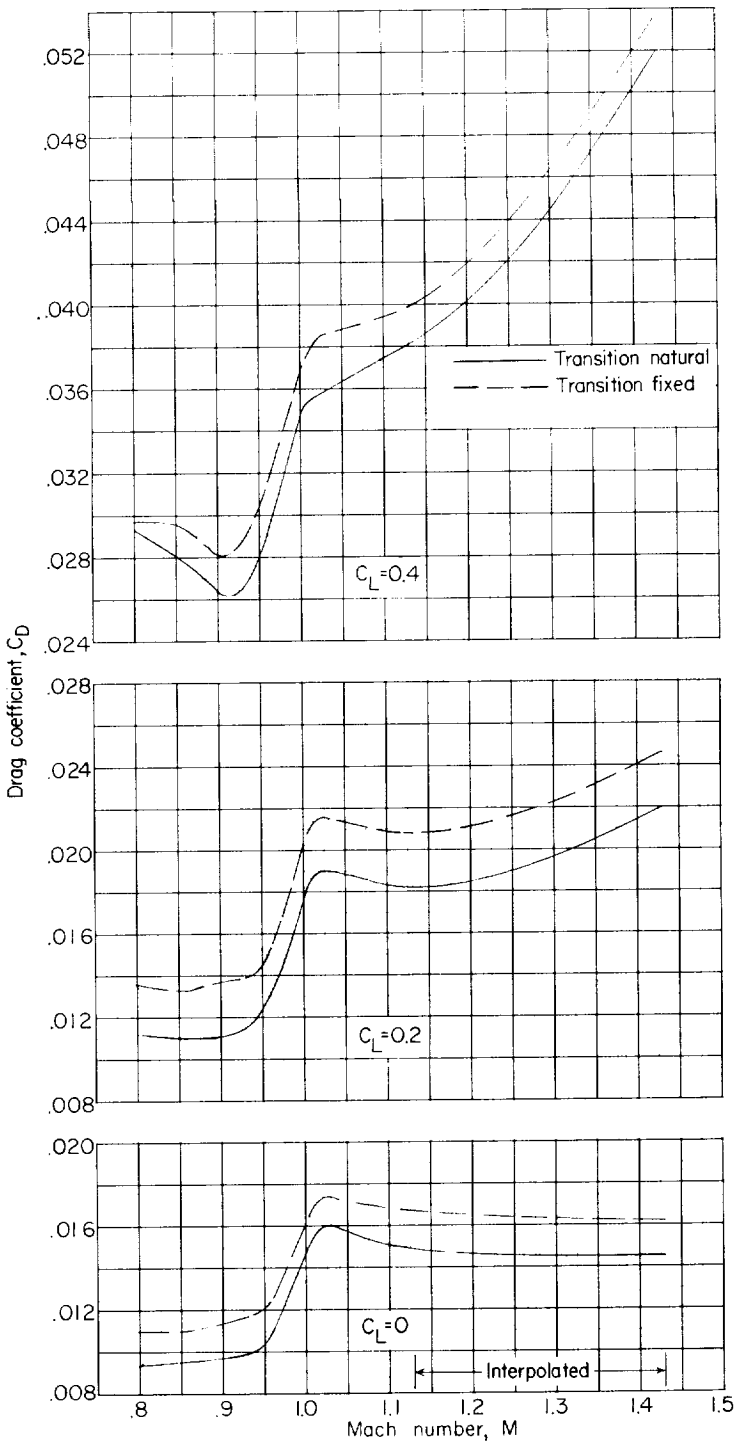

(d) M = 1.4 wing-body combination.

Figure 33.- Concluded.

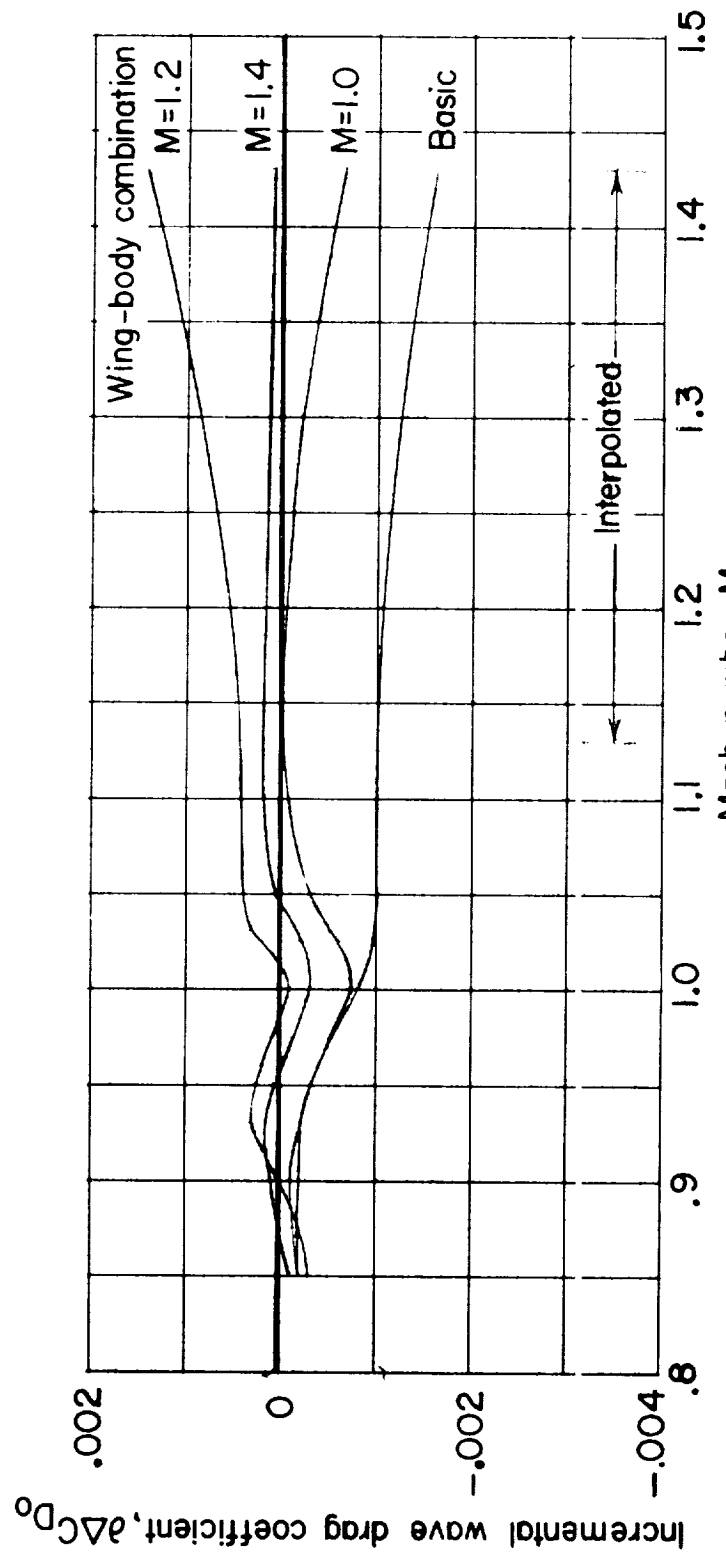

Figure 34.- The effect of transition on the wave drag characteristics of the 45° sweptback wing in combination with the basic and indented bodies. $C_L = 0$.

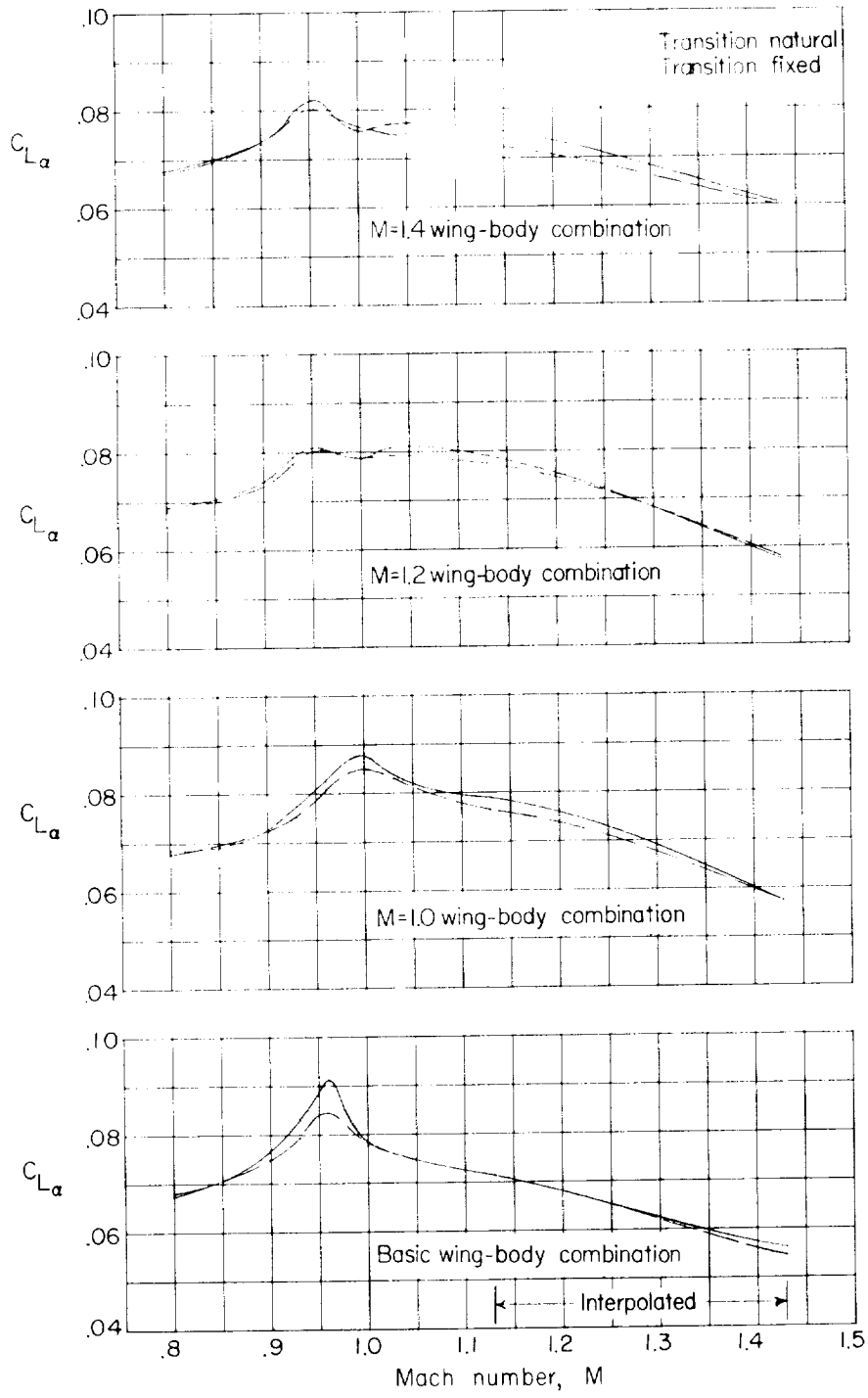

Figure 35.- Average lift-curve-slope characteristics of the 45° swept-back wing in combination with the basic and indented bodies with natural transition and fixed transition on the wing and bodies. C_L = -0.05 to 0.3.

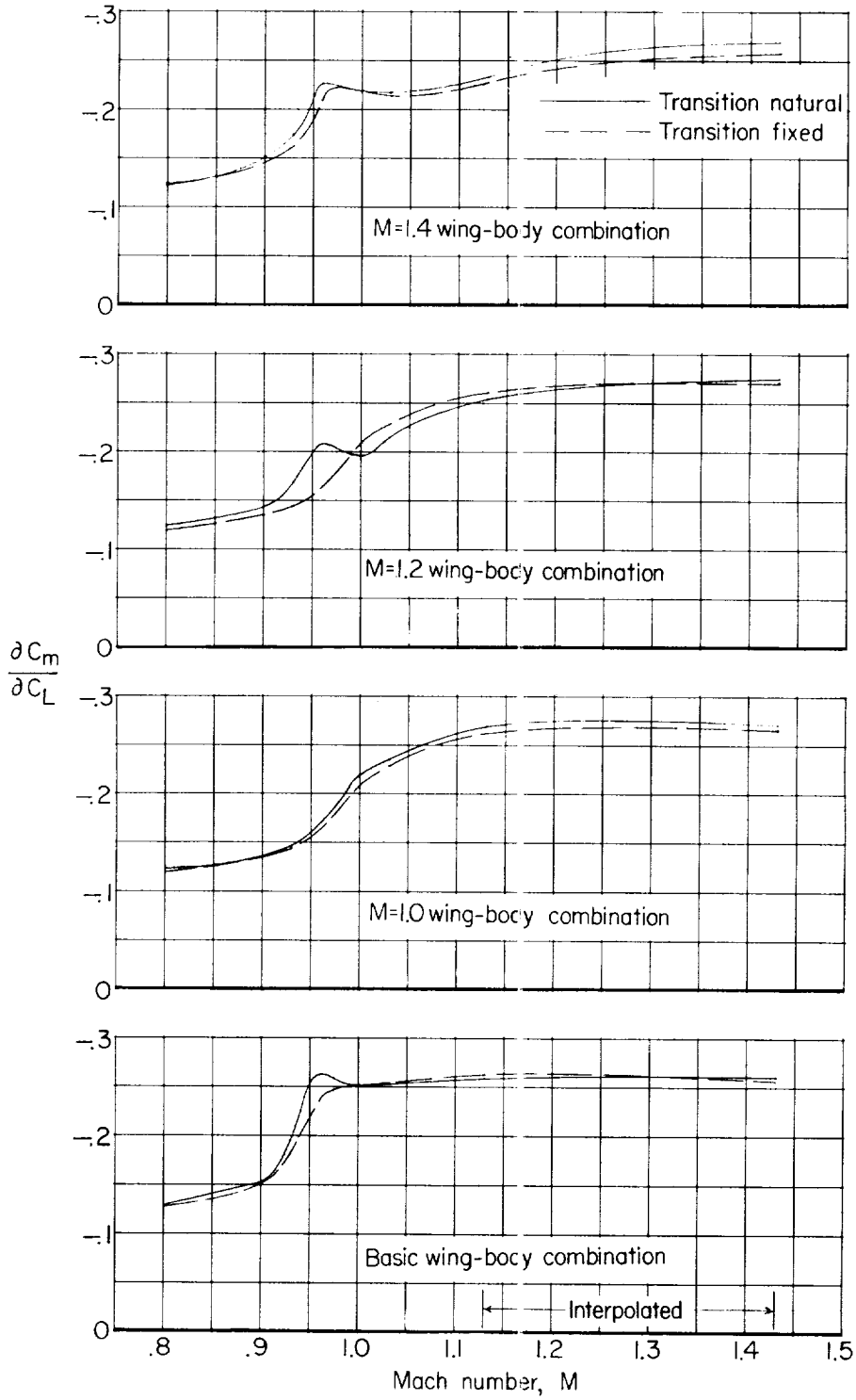

Figure 36.- Stability characteristics of the 45° sweptback wing in combination with the basic and indented bodies with transition natural and fixed on the wing and bodies. C_L = -0.05 to 0.3.

NASA-Langley, 1961 L-1698